IJCE

Printed by
Diagnosis Engineering & Technology Corp., Japan

International Journal of Comprehensive Engineering

ISSN 2186-2680
Volume 1, Number 1, December 2012

IJCE

Published by
International Association of Comprehensive Engineering (IACE)

http://www.iace-journal.org/

Honorary Editors

Toshio TOYOTA , Japan Institute of Condition Diagnosis Technology, Japan

Jinji GAO, Academician of the Chinese Academy of Engineering (CAE)

Hisayoshi MATSUYAMA, Vice-president The Society of Plant Engineers Japan

Editor-In-Chief

Peng CHEN
Mie University, 1577 Kurimamachiya-cho,Tsu-shi, Mie-ken, 514-8507 Japan
E-mail : chen@bio.mie-u.ac.jp

Associate Editors

Zhengjia HE, Xi'an Jiaotong University, China
E-mail: hzj@mail.xjtu.edu.cn

Maria Q. FENG, University of California, USA
E-mail: mfeng@uci.edu

Tadao KAWAI, Osaka City University, Japan
E-mail: kawai@mech.eng.osaka-cu.ac.jp

Susumu OKUMURA, University of Shiga Prefecture, Japan
E-mail: okumura.s@usp.ac.jp

Lei Li, Faculty of Science and Engineering Hosei University, Japan
E-mail:lilei@k.hosei.ac.jp

Huaqing WANG, Beijing University of Chemical Technology, China
E-mail: hqwang@mail.buct.edu.cn

Editorial Board

Changzheng CHEN, Shenyang University of Technology, China

Jin CHEN, Shanghai Jiaotong University, China

Fulei CHU, Tsinghua University, China

Zhiqian DONG, China development investment company

Lixin GAO, Beijing University of Technology, China

Jie HAN, Zhengzhou University, China

Min HU, Agent Director, China Plant Engineering Editorial office

Niaoqing HU, National University of Defense Technology, China

Jianping HU, Jiangsu University, China

Lixin LU, Jiangnan University, China

Ke LI, Jiangnan University, China

Hanping MAO, Jiangsu University, China

Zhongxing Li, Jiangsu University, China

Arata MASUDA, Kyoto Institute of Technology, Japan

Tetsuro MITOMA, Mitsui Chemicals, Inc., Japan

Hiromitsu OHTA, National Fisheries University, Japan

Yelian MIAO, Nanjing University of Technology, China

R.R.Pechon, Agriculture,Bohol Agricultural Promotion Center,Philippines

Zhongyong PAN, Jiangsu University, China

Yimin. SHAO, Chongqing University, China

Noriaki SATONAGA, Showa Denko K.K., Japan

Yukio WATANABE, TOSHIBA CORPORATION, Japan

Toshiaki WAKABAYASHI, Kagawa University, Japan

Taiyong WANG, Tianjin University, China

Shiming WANG, Shanghai Ocean University, China

Hongtao XUE, Mie University, Japan

Xiaoli XU, Beijing Information Science and Technology University, China

Mitsushi YAMASHITA, Mie University, Japan

Ruqiang YAN, School of Instrument Science and Engineering, China

Yanyang ZI, Xi'an Jiaotong University, China

Chongsheng YUAN, DIAZYME Corporation, USA

Secretariat Board

Email : ijce@nifty.com

(Head) **Hao SUN,** Jiangnan University, China
Email : sunhao@jiangnan.edu.cn

Ke LI, Jiangnan University, China

Feng WANG, Beijing University of Chemical Technology, China

Hongtao XUE, Mie University, Japan

Haiyang JIANG, MieUniversity, Japan

International Journal of Comprehensive Engineering (IJCE)

International Journal of Comprehensive Engineering (IJCE) is an international interdisciplinary journal that integrates publication from aspects of research on engineering science. This journal provides a medium of communication among engineers and scientists who have engaged in research and development concerning the fields of comprehensive engineering, while maintaining a healthy balance between fundamental and experimental topics. Now, the journal has three separate fields, the scopes of which are Part A: Maintenance Engineering; Part B: Intelligent Engineering; Part C: Engineering in Agriculture, Ocean and Light Industry shown in flows, and other specialized fields will also be updated in the near future.

Part A: Maintenance Engineering

Executive editors：

Prof. Dr. Yanyang ZI
Xi'an Jiaotong University, China
E-mail: ziyy@mail.xjtu.edu.cn

Associate Prof. Dr. Hiromitsu OHTA
National Fisheries University, Japan
E-mail: ohta@fish-u.ac.jp

Prof. Dr. Huaqing WANG
Beijing University of Chemical Technology, China
E-mail: hqwang@mail.buct.edu.cn

Topics of interest for submission on the field of maintenance engineering include, but are not limited to:
Condition Diagnosis Engineering and Technology; Sensing Technology; Maintenance Management; Fault Tolerant System; Fault Self-Recovery Engineering; E-Maintenance; Signal Processing; Risk, Health and Safety Management; Structural Health Monitoring; Information and Communication Technology; Data and Information Fusion; Reliability/Quality; Maintenance Robot; Data Quality and Acquisition; Human Factors; Education and Training; Risk Based Engineering; Others on Maintenance.

Part B: Intelligent Engineering

Executive editors：

Prof. Dr. Huaqing WANG
Beijing University of Chemical Technology, China
E-mail: hqwang@mail.buct.edu.cn

Associate Prof. Dr. Arata MASUDA
Kyoto Institute of Technology, Japan
E-mail: masuda@kit.ac.jp

Associate Prof. Dr. Ke LI
Jiangnan University, China
E-mail: like@jiangnan.edu.cn

Topics of interest for submission on the field of intelligent engineering include, but are not limited to:
Application of Artificial Intelligence in Engineering; Intelligent Design, Modeling, Planning and Control for Applied Engineering; Intelligent Robot System; Intelligent Fault Diagnosis; Intelligent Signal Processing for Applied Engineering; Others on Intelligent Engineering.

Part C: Engineering in Agriculture, Ocean and Light Industry

Executive editors (Agriculture):

Prof. Dr. Hanping MAO
Jiangsu University, China
E-mail: maohp@ujs.edu.cn

Prof. Dr. Jianping HU
Jiangsu University, China
E-mail: hujp@ujs.edu.cn

Executive editor (Ocean):

Prof. Dr. Shiming WANG
Shanghai Ocean University, China
E-mail: smwang@shou.edu.cn

Executive editor (Light Industry):

Prof. Dr. Lixin LU
Jiangnan University, China
E-mail: lulx@jiangnan.edu.cn

Topics of interest for submission on the field of engineering in agriculture, ocean and light industry include, but are not limited to:
Agriculture Engineering: Agricultural Equipment and Mechanical Engineering; Agricultural Bioenvironmental Engineering; Agricultural Renewable Energy Engineering; Agricultural Produce Processing Engineering; Agricultural Information and Electrical Technologies; Others on Agricultural Engineering.
Ocean Engineering: New Ocean Energy; Ocean Maintenance Technology; Ocean Monitoring Technology; Ocean Diagnosis Method; Ocean Experimental Development; Professional Sensor Technology; Observational and Computational Tools Others on Ocean Engineering.
Light Industry Engineering: Agri-food Products Processing/Packaging Technology and Equipment; Comprehensive Utilization of Resource; Preservation; Storage and Packaging of Agri-food Products; Innovative IT Applications in Agri-food Chain; Sensing, Testing, Automation and Internet of Things Technologies; Green Environmental Protection; Energy Saving Technologies; Others on Light Industry.

Manuscript Submission

Manuscripts should be submitted online at http://www.iace-journal.org/ by registering and logging in to the website of the IJCE. Once you have registered, please click the “Submit Manuscript” to go to the submission from. Please use the MS Word template file to prepare your manuscript. Manuscript prepared in MS Word must be converted into a single file before submission. The Microsoft Word template file can be downloaded from the website of the IJCE.

Submission Declaration

The submission, such as articles, reviews, technical report etc., to the IJCE means these facts that the work described has not been published previously, that it is not under consideration for publication elsewhere, that its publication is approved by all authors and tacitly or explicitly by the responsible authorities where the work was carried out, and that, if accepted, it will not be published elsewhere including electronically in the same form, in English or in any other language, without the written consent of the copyright-holder.

Copyright

Authors will be asked to complete a "Copyright Transfer Statement", when submitting the manuscript. Acceptance of the agreement will ensure the widest possible dissemination of information. Permission of the publisher is required for resale or distribution outside the institution and for all other derivative works, including compilations and translations. The "Copyright Transfer Statement" can be downloaded from the website of the IJCE as follows:
http://www.iace-journal.org/views/Copyright_Transfer_Statement.pdf.

Review Policy

The following types of contribution to the IJCE are peer-reviewed: Articles, Reviews and Technical Reports. The articles accepted for publishing in the IJCE include regular paper and letter, which will be decided by editors according the reviewing results. All forms of published correction may also be peer-reviewed at the discretion of the editors. Other contributed types to the IJCE, particularly if they present technical information, may be peer-reviewed at the discretion of the editors. For any general questions and comments about the peer-review process, the journal or its editorial policies that are not mentioned here, please contact us using the email: ijce@nifty.com. Questions about a specific submitted manuscript should be directed to the executive editor who is handling the manuscript.

International Journal of Comprehensive Engineering (IJCE)

Volume 1, Number 1, December 2012 (ISSN 2186-2680)

1 Peng Chen
Prefatory Note

2 Toshio Toyota
Greetings to the Publishing of the First Issue of IJCE

5 Jinji Gao
Development of Engineering Science and Missions of Modern Engineers and Science Workers
--For the first issue of IJCE --

11 Hisayoshi Matuyama
Congratulations on the First Issue of International Journal of Comprehensive Engineering (IJCE)

********** Part A：Maintenance Engineering **********

14 Ruqiang Yan and Robert X. Gao
Performance Evaluation of Complex-valued Wavelet Basis on Vibration Analysis for Bearing Defect Diagnosis

21 Hiromitsu Ohta , Keiji Sasada , Shintaro Shiota and Satoru Ezoe
New Condition Monitoring Method of Rotary Machine Elements under the Other Operating Machineries Located Close Range -- Extraction of Fault Components Based on Proposed Multiplex Elements AR Model--

32 Bing Li , Hongrui Cao and Zhengjia He
Numerical and Experimental Research on Pitch Mechanism of Gun with Clearances

38 Wei Hao, Lidong He, Wanfu Han and Jian Chang
Experimental Research on Vibration Control of High-rise Petrochemical Equipment with Lumped-mass Tuned Mass Damper

44 Hongfang Yuan, Changdui Zhu, Xi Cao, Huaqing Wang, Wenbin Liu and Jianfeng Yang
A Selection Method of Vibration Signal Feature Based on Mutual Information and Distance Measurement

********** Part B：Intelligent Engineering **********

51 Bo Ma , Kun Feng and Yujie Xi
The Research of Intelligent Diagnosis Expert System on Pumps Group

60 Shouqi Yuan, Lingdi Tang, Erhui Liu and Yue Tang
Numerical Calculation of Transient Characteristics in Centrifugal Pump Speed Regulation process based on CEL language

******** Part C：Engineering in Agriculture, Ocean Industry and Light Industry ********

67 Zhongyong Pan , Taotao Wu, Junjie Li and Yanjun Li
Mechanism of Characteristic Instability and its Suppression in Mixed Flow Pump

74 Xiudong Shi , Weiwei Zhao and Wanchun Fan
Study on Autofrettage Design of Composite Natural Gas Vehicle Cylinder

80 Zhanhua Dong , Lixin Lu , Zhigang Liu , Yali Tang and Jun Wang
Migration of Lead, Cobalt, Nickel and Zinc from Ceramic Glazes by Acid Food Simulants

Copyright © 2012 DET Corp., Japan All Rights Reserved
International Journal of Comprehensive Engineering
1(1), 1, 2012
Doi: 10.14270/IJCE2012.1.1.1

ISSN 2186-2680
e-ISSN 2186-2656
www.iace-journal.org

Prefatory Note

Peng Chen

Editor-in-Chief, International Journal of Comprehensive Engineering
Professor, Faculty of Bioresources, Mie University

Director, Research Center of Security Technology for Industry and Social Infrastructure, Mie University
1577 Kurimamachiya-cho, Tsu-shi, Mie-ken, 514-8507, Japan

Corresponding author:chen@bio.mie-u.ac.jp

Received: Sept. 10,2012 / Accepted: Sept. 12,2012 / Published: Dec. 15,2012

The inaugural issue of the International Journal of Comprehensive Engineering (IJCE) is published under the guidance and support of every person involved. On behalf of the editorial committee, I am deeply grateful to everyone associated with IJCE. Upon the issuance of our first issue, we received precious congratulations from Dr. Toshio TYOYTA, Prof. Jinji GAO, and Dr. Hisayoshi MATSUYAMA - high-profile international academic authorities-, and I would like to express my cordial gratitude to them.

IJCE is an international interdisciplinary journal that integrates publication from all aspects of research on engineering science. This journal provides a medium of communication among engineers and scientists who have engaged in research and development concerning the fields of comprehensive engineering, while maintaining a healthy balance between fundamental and experimental topics.

Although we have set five specialized fields, namely, maintenance engineering, intelligent engineering, engineering in agriculture, ocean industry, and light industry, we sincerely attempt to accept and publish papers from other specialized fields. We are now looking forward to receiving submissions of academic or technical papers from each engineering field, in particular from the five abovementioned fields.

To maintain IJCE as a high-level scientific and technical journal and to serve the authors wholeheartedly, we will especially try our best in the following items:

1. Establishing a fair and reasonable peer review system that focuses on the executive editors;
2. Performing the peer review process, responding to authors and publishing each accepted paper as soon as possible;
3. Positively advertising IJCE for increased visibility and for indexing by many academic databases and search engines worldwide.

We will continually strive for the development of IJCE and authors under the guidance and cooperation of the participants.

Editor-In-Chief Peng Chen

December 2012

Copyright © 2012 DET Corp., Japan All Rights Reserved
International Journal of Comprehensive Engineering
1(1), 2-4, 2012
Doi: 10.14270/IJCE2012.1.1.2

ISSN 2186-2680
e-ISSN 2186-2656
www.iace-journal.org

Greetings to the Publishing of the First Issue of IJCE

Toyota Toshio

President researcher of Japan CDT Lab,
Emeritus Professor of Kyushu Institute of Technology
IJCE Honorary Editor

[#] Corresponding author: ijce-journal@live.jp

Received: May 31,2012 / Accepted: Sept. 12,2012 / Published: Dec. 15,2012

Congratulations on the publishing of the first issue of International Journal of Comprehensive Engineering (IJCE).

International Journal of Comprehensive Engineering (IJCE) contains three important fields: equipment management and maintenance engineering (Part A), intelligent engineering (Part B), engineering in agriculture, ocean and light industry (Part C), which are more complicated and rapid-developing recently in the world.

What's worth noticing is that the journal also plays an important role in Engineering in Agriculture, Ocean and Light Industry, which are the key sectors in the recent and future social and economic development.

Hopefully the research papers, reviews and technical reports published in this journal will provide valuable academic and technological information to researchers and engineers in these engineering fields.

At last, I firmly believe that JICE will be a worldly essential and famous academic journal in the above fields.

International Journal of Comprehensive Engineering 創刊への祝辞

豊田利夫

日本診断工学研究所所長
九州工業大学 名誉教授
IJCE 顧問

International Journal of Comprehensive Engineering(IJCE)の創刊おめでとうございます。

最近複雑化した生産プラントの設備管理と設備保全、ICT 技術の進歩および農林水産工学と軽工業の発展に対応するための必須技術要素である３分野、すなわち Part A :Maintenance Engineering、Part B：Intelligent Engineering、Part C：Engineering in Agriculture, Ocean and Light Industry を重点取扱い技術分野とされている点はすぐれた企画だと思います。

特に、今後の社会、経済発展にとって益々重要になる技術分野である Engineering in Agriculture, Ocean and Light Industry をも取り上げられた点も高く評価可能です。

今後、この３分野での研究論文や解説文、報告書など、本分野の研究者のみでなく現場の保全技術者にとっても大変有益な学術・技術誌に発展すると期待します。

JICE が全世界の本分野の技術者や学者にとって必須で有効な国際学術誌として発展されることを確信し、創刊の祝辞とさせて頂きます。

International Journal of Comprehensive Engineering 创刊祝词

丰田利夫

日本诊断工学研究所所长
九州工业大学　名誉教授
IJCE 顾问

首先祝贺 International Journal of Comprehensive Engineering(IJCE)创刊号的出版发行！

International Journal of Comprehensive Engineering(IJCE)包含了关于近年来越来越复杂化的生产设备管理与维修工程、快速发展的 ICT 工程以及农林水产工程与轻工业的 3 大重要领域： Maintenance Engineering (Part A)、Intelligent Engineering (Part B)、Engineering in Agriculture, Ocean and Light Industry (Part C)。

特别是本杂志设置了对今后的社会与经济发展非常重要的 Engineering in Agriculture,Ocean and Light Industry 领域之处值得注目。

希望本杂志今后在以上 3 个领域的研究论文、展望与解说以及技术报告等不仅给研究人员与学者，也给技术人员与工程师提供非常有价值的学术与技术信息。

我确信 JICE 将在以上领域在全世界范围发展成为必不可缺的著名国际学术杂志。特此祝词。

Copyright © 2012 DET Corp., Japan All Rights Reserved
International Journal of Comprehensive Engineering
1(1), 5-10, 2012
Doi: 10.14270/IJCE2012.1.1.5

ISSN 2186-2680
e-ISSN 2186-2656
www.iace-journal.org

Development of Engineering Science and Missions of Modern Engineers and Science Workers

--For the first issue of IJCE--

Jinji Gao

Vice-president of China association of Equipment Management
Academician of Chinese Academy of Engineering
IJCE Honorary Editor

Corresponding author: ijce-journal@live.jp

Received: May 31,2012 / Accepted: Sept. 12,2012 / Published: Dec. 15,2012

Engineering science has been the powerhouse for the progress of human civilization. It is the scientific foundation of engineering practice, the bridge between natural science and engineering technology. Modern engineering science has extensive research fields and sub disciplines.

IJCE is an international multidisciplinary journal. It involves a number of fields of engineering science and serves as a communication platform for engineers and science workers of engineering-related R&D backgrounds. It will enhance the mutual communication and balanced development between fundamental research and engineering practice.

The publishing of the first issue of IJCE is a sensation in the world of engineering technology. We firmly believe that it will make great contributions to engineers and science workers who are important creators of new productivity and pioneers of new industries.

1. Engineers and science workers are bridges between science and production development

Engineers are the intermediaries connecting science and production. They should possess the innovative power to solve practical problems. Especially when a production problem is new and there does not exist a solution in reference books, engineers need to develop methods and management rules that base on science to drive the advancement of production and technology.

2. Engineers and science workers are bridges between science and social development

In today's industrial society, engineering technology system has become the guarantee and support for social existence and development, such as the service of non-material production like transportation, telecommunication and medical care. The system also controls the stability of social production, such as the control on natural disaster, production accident, disease, environment, resources, and urban planning. By relying on this system, science achievements are improving the outlook of social production, and engineers are becoming a widening bridge that joins human science, behavior science and social science.

3. Engineers and science workers are bridges between science and high-tech industrialization.

Massive capitals, equipment and tangible assets are crucial to traditional industries. In high-tech industry, however, the investment of knowledge, intelligence and intangible assets plays a key role. To some extent, advantages of the industry and values of the products are determined by each worker's experience, knowledge and innovativeness. That is to say, winners are those who quickly master knowledge and apply it to the organization of the production process. Therefore, engineers' responsibilities are to build a bridge between science and high-tech industrialization.

4. Engineers and science workers are bridges between engineering and natural science.

The research of science in the 16th and 17th centuries focused purely on nature, but the scientific research has gone beyond the scope of nature after the 18th century, incorporating the entire objective world, the natural and the man-made. The analysis and improvement of engineering technology's research results can be parts of natural science. The famous "Control Theory of Engineering" of Qian Xuesen, a well-known Chinese scientist, is a classic example. Engineers are always working in the front line of engineering, so they should raise research topics based on engineering practices and science, flexibly combine theory and practice, and create science-based engineering theories, before making contributions to the development of the science.

Modern people increasingly rely on industries of high-degree mechanization, automation and intellectualization, thus needing highly mechanized, automotive and intellectualized engineering equipment and controlling projects. As such equipment and projects are applied in large-scale and complicated systems, its research cannot be as simple as Newton's observation of the falling apple to discover gravity. Instead, it requires modernized research equipment and testing methods, computers and advanced software, as well as concerted efforts from specialists from various disciplines. This leads to the development of many new areas of engineering science, such as maintenance engineering and intelligence engineering. The communication and corporation between contemporary engineering technology societies is very important. We hope IJCE can continually work towards this goal.

A one-thousand-mile journey starts from the first step. We firmly believe that IJCE will contribute its due part to the development of engineering technology, social economy and natural science.

May 2012, Beijing

工学の発展および現代の工学技術者と工学研究者の使命

－ 国際総工学雑誌（IJCE）創刊号への祝辞 －

高金吉

中国設備管理協会 副会長
中国工学アカデミー会員（中国工程院 院士）
IJCE 顧問

工学に関する科学技術は人類文明の発展と進歩に対して常に牽引力の役割を果たしている。工学は様々な工業実践に関する科学技術の基礎であり、自然科学と工業技術の架け橋である。現代工学には幅広い研究領域と学問分野がある。

国際総合工学雑誌（IJCE）は国際的な多分野学術誌であり、工学の広領域に及び、工学に関する研究と開発に従事する技術者（エンジニア）と研究者（学者）に技術・学術交流のためのプラットフォームを提供し、工学に関する基礎研究と現場実践との相互融合および平衡発展を促進しようとしている。

国際総合工学雑誌（IJCE）の創刊号が読者の皆さんにお目にかかることは工学技術分野において喜ぶべき重大な出来事である。私は国際総合工学雑誌（IJCE）がエンジニアらと研究者ら、すなわち、新生産力の創造者らと新産業領域の開拓者らに対して有益な貢献を果たすと確信している。

１．エンジニアと研究者は科学発展と生産発展の架け橋

エンジニアは科学と生産との仲介者であり、科学と生産との繋ぎの役割を果たしている。エンジニアには技術革新能力および創造的な問題解決能力を有することが望まれる。エンジニアは特に専門書に解答や前例がない生産問題に直面しているときには、科学を基礎にして生産に適した新技術と新管理方法を創出し、生産の発展と技術の進歩を促進すべきである。

２．エンジニアと研究者は科学進歩と生産進歩の架け橋

現代の工業社会の中で、工学的な技術システムは社会の生存と発展を保障・支持しているものであり、例えば運送、通信、医療などは非物質生産のサービス、 時に社会の生産秩序と安定の維持、自然災害、生産事故および疾病の抑制、環境と資源の保全、都市の計画と管理等々である。科学的な研究成果がこのシステムを通して社会生産の変貌を遂げさせ、エンジニアは次第に人文科学、行動科学および社会科学への架け橋に拡大していく。

３．エンジニアと研究者は科学とハイテク産業化の架け橋

伝統的な産業においては大量の資金、設備、有形資産が決定的効果を発揮しようとするのに対して、ハイテク産業においては知識、知力、無形資産が生産発展の決定的要因となる。産業の優位性と製品の価値の決定的な要因は一定の程度の上ですべての従業員の経験、知識と革新性にあるといえる。つまり

先に知識を掌握し、そして生産過程に成功に応用した者は勝者となる。エンジニアの職責は科学とハイテク産業化の架け橋になることである。

４．エンジニアと研究者は工学と自然科学の架け橋

十六、十七世紀の自然科学は純粋な自然界を研究していたが、十八世紀末以降、自然科学の研究の範囲は自然界を超え、全ての客観的な世界：自然と人工物を含む。工業科学技術の成果は再分析、再昇華によって自然科学の一部になる。中国の著名な科学者の銭学森先生が創出した「Engineering Cybernetics」は典型的な例である。エンジニアは長期にわたり生産現場で働いて、現場実践から共通性のある研究課題を引き出す必要があり、理論と 実践との有機的な結 に力を入れ、科学根拠のある工学理論を創出して昇華させることにより自然科学の発展に貢献することが望まれる。

現代人はますます高度の機械化、自動化および知能化の産業を頼りにして物を創造するようになっている。よって、高度機械化・自動化・知能化された産業装備と制御プロセスに対するニーズもますます高まっている。しかし、大型複雑なシステムに応用される産業装備と制御プロセスに関する研究開発は、ニュートンがリンゴの落下観察により万有引力を発見するように簡単な事でなく、現代化の実験装置と計測手段および計算機と先進的なソフトウェアが必要であり、また多くの異分野の専門家や学術技術チームの協力と努力も必要である。これは幾つの新しい工学研究領域、たとえば保全工学や知能工学などを生み出している。

現代の国際工学分野における交流と協力が非常に重要であるので、我々は国際総合工学雑誌（IJCE）がこのために怠らない努力を続けることを期待している。国際総合工学雑誌（IJCE）は、千里の道も一歩から、責任が重大で道が遠いが、工学に関する科学技術の繁栄と発展だけでなく、社会経済の発展のために功を立てて業績を積み重ね、その上自然科学の発展のためにもあるべき貢献をすると、我々は深く信じている。

2012 年 5 月　北京にて

工程科学的发展与当代工程师和科技工作者的使命

ー为国际综工程学报(IJCE)创刊号而作

高金吉

中国设备管理协会 副会长
中国工程院 院士
IJCE 顾问

工程科学技术在推动人类文明的进步中一直起着发动机的作用。工程科学是关于工程实践的科学基础，是自然科学和工程技术的桥梁。现代工程科学具有宽广的研究领域和学科分支。

国际综合工程学报(IJCE)是国际性多学科学报，它涉及工程科学 个领域，其宗旨是为从事工程相 领域研究和开发的工程师与科技工作者提供一个交流平台，实现基础理论研究与工程实践的相互交融与平衡发展。

国际综 工程学报(IJCE)创刊号和广大读者见面了，这是值得工程科技界庆贺的大事。我们深信，国际综 工程学报(IJCE)会为工程师和科技工作者ー新生产力的重要创造者和新兴产业的积极开拓者做出应有的贡献。

1. 工程师和科技工作者是科学与生产发展的桥梁

工程师是科学与生产的中介者，实际上起着衔接科学与生产的作用。工程师要有创新能力，具备创造性解决实际问题的能力。特别是当所面临的生产问题是专业书上并无先例可循的时候，工程师以科学为基础发展出适合于生产的技术和管理手段，用于推动生产发展和技术进步。

2. 工程师和科技工作者是科学与社会进步的桥梁

在今天的工业社会中，工程技术系统成为社会生存和发展的保障和支持，如运输、通信、医疗等非物质生产的服务，同时对社会生产的有序稳定进行控制，如对自然灾害和生产事故的控制，疾病控制、环境控制、资源控制、城市规划与控制等。科学成就借助于这一系统改变着社会生产的面貌，工程师逐渐扩大到成为人文科学、行为科学和社会科学的桥梁。

3. 工程师和科技工作者是科学与高技术产业化的桥梁

传统产业是大量资金、设备、有形资产起决定性作用，高技术产业是知识、智力、无形资产的投入起决定性作用。产业的优势和产品价值的决定因素在一定程度上取决于每个工作者的经验、知识和创新性。也就是说谁先掌握知识并应用于组织生产过程，谁就是赢家。工程师的职责就是要架起科学和高技术产业化的桥梁。

4. 工程师和科技工作者是工程与自然科学的的桥梁

十六、十七世纪的自然科学上纯粹地研究自然界，而到十八世纪末以后，自然科学的研究范围超出了自然界，包括整个客观世界：自然的和人造的。工程科技的成果再加以分析，再加以提高就可能成为自然科学的一部份。中国著名科学家钱学森先生创建的“工程控制论”，就是的典型的例子。工程师长期工作在工程一线，要善于从工程实践提出共性的研究课题，善于灵活的将理论与实践相结合，创造出有科学根据的工程理论，再加以提高，为自然科学的发展做出贡献。现代人越来越依赖高度机械化、自动化和智能化的产业来创造财富，因此必然要求越来越高度机械化、自动化和智能化的工程装备与控制工程。但是工程装备与控制工程是应用于大型过程复杂系统，对它的研究不会是像牛顿观察落下来的苹果发现万有引力那么简单，而是需要现代化的实验装备和测试手段，需要计算机和先进的软件，需要有诸多学科专门人材的学术团队的共同协作和努力。这导致发展一些工程科学新的研究领域，如维修工程、智能工程等。当代国际工程科技界的交流和合作至关重要。我们希望，国际综合工程学报(IJCE)为此做出不懈的努力。

国际综合工程学报(IJCE)千里之行始于足下，任重道远，我们深信，学报不但会为工程科技的兴旺发达，为社会经济的发展建功立业，而且会为自然科学的发展做出应有的贡献。

2012 年 5 月　于北京

Copyright © 2012 DET Corp., Japan All Rights Reserved
International Journal of Comprehensive Engineering
1(1), 11-13, 2012
Doi: 10.14270/IJCE2012.1.1.11

ISSN 2186-2680
e-ISSN 2186-2656
www.iace-journal.org

Congratulations on the First Issue of International Journal of Comprehensive Engineering (IJCE)

Hisayoshi Matsuyama

Vice president of Society of Plant Engineers Japan

Emeritus Professor of Kyushu University

IJCE Honorary Editor

Corresponding author: ijce-journal@live.jp

Received: May 31,2012 / Accepted: Sept. 12,2012 / Published: Dec. 15,2012

Recent real problems become too complex to be solved by conventional engineerings which were established to solve problems of individual industries. In order to solve such real problems, it is necessary to re-organize conventional engineerings into new interdisciplinary engineerings. Though advanced researchers already started to solve complex real problems, they find difficulty in publishing their works in journals of conventional academic societies. I am sure IJCE is the best international journal on interdisciplinary engineering that can respond to their demands.

International Journal of Comprehensive Engineering 創刊への祝辞

松山久義

一般社団法人 日本設備管理学会 副会長

九州大学 名誉教授

IJCE 顧問

International Journal of Comprehensive Engineering (IJCE)の創刊，おめでとうございます。

近年，生産システムおよび社会システムが複雑化して来たため，産業別に編成された従来の工学は実問題の解決に役立たなくなって来ました。実問題を解決するためには，産業別に編成された従来の学問体系を再編した新たな学問体系を必要とします。既に多くの先進的な研究者が実問題の解決に向けて研究を進めていますが，その成果を産業別に編成された既存の学術誌に掲載するには多くの困難を伴います。実問題の解決に携わる先進的な研究者は，IJCE のような学際的な国際学術誌の登場を待ち望んでいました。IJCE の益々のご発展を祈念いたします。

International Journal of Comprehensive Engineering (IJCE)创刊祝词

松山久义

日本设备管理学会 副会長

九州大学 名誉教授

IJCE 顾问

首先祝贺 International Journal of Comprehensive Engineering (IJCE)创刊。

近年来生产系统与社会系统越来越复杂，以产业种类来划分的传统工学领域已经很难解决许多现实问题了。为了很好地解决实际问题，有必要把以产业种类来划分的传统工学体系以新学问体系进行重编。已经有许多先进的研究者为了解决现实问题进行着不懈的研究，他们的不少研究成果在有关以产业种类来划分的传统工程学术杂志上已经很难找到合适的位置。从事解决现实问题的先进研究者们早就期望着像 IJCE 这样的国际学术杂志的诞生。

最后祝 IJCE 不断发展。

Copyright © 2012 DET Corp., Japan All Rights Reserved
International Journal of Comprehensive Engineering
Part A, 1(1), 14-20, 2012
Doi: 10.14270/IJCE2012.1.1.a14
Regular paper

ISSN 2186-2680
e-ISSN 2186-2656
www.iace-journal.org

Performance Evaluation of Complex-valued Wavelet Basis on Vibration Analysis for Bearing Defect Diagnosis

Ruqiang Yan [1, #] and Robert X. Gao [2]

[1] School of Instrument Science and Engineering, Southeast University, Nanjing, 210096, China
[2] Department of Mechanical Engineering, University of Connecticut, Storrs, CT 06269, USA

[#] Corresponding author: ruqiang@seu.edu.cn; Tel.: +86-135-8405-4760; Fax: +86-25-8379-4158

Abstract: This paper presents a quantitative approach to evaluating the performance of complex-valued wavelet basis on vibration analysis of rolling bearings, using the cross-correlation measure. As a statistical tool for quantifying the relationship between two time series, cross-correlation analysis characterizes the performance of different wavelet bases in analyzing non-stationary time series, such as vibration signals. Theoretical foundation of using cross-correlation measure for evaluating wavelet basis is described, and experimental study has verified that the cross-correlation measure provides quantitative guidance to selecting wavelet basis for improved performance in defect diagnosis of rolling bearings.

Keywords: Wavelet Transform, Wavelet Basis, Cross-correlation Measure, Defect Diagnosis.

Received: May 11,2012 / Accepted: Sept. 12,2012 / Published: Dec. 15,2012

1. Introduction

As a mathematical tool, signal transformation, which maps a signal from one domain into another to better reveal the information hidden within the original signal, has been widely explored for improved monitoring of the health states of machine systems. Of various signal transformation techniques, wavelet transform has been increasingly investigated, due to its multi-scale decomposition characteristics and capability in handling non-stationarity of signals [1-3]. This is realized by scaling (stretching or squeezing) a wavelet basis and then correlating it with the signal being analyzed through a time-shift operation. The result of the operation is that characteristic signature that matches the scaled wavelet will be extracted out of the original signal. Since 1990's, the application of wavelets to defect diagnosis of machine systems has been increasingly seen world-wide [4-7], with diagnosis of rotating machines [8-12] representing an active field of research.

While such advancement has illustrated the effectiveness of wavelet transform in machine defect diagnosis, selection of wavelet basis has been traditionally practiced in an *ad hoc* manner. As an example, various wavelet bases, such as Gaussian wavelet [5], Morlet wavelet [8], Mexican hat wavelet [9], Daubechies 2 wavelet [13], and Daubechies 4 wavelet [14], have been used for bearing vibration signal analysis. The issue of wavelet basis selection has received increasing attention, and various properties of wavelets have been investigated as potential criterion for choosing wavelet basis. In a study on characterizing the topology of engineered surfaces [15], symmetry has been used for separating the roughness, waviness and form of a surface into different frequency bands for both functional correlation and process diagnosis in manufacturing. In another study, shape matching was used for picking up proper wavelet basis for vibration signal analysis [16]. The minimum total error and time-frequency resolution were devised to evaluate different wavelet bases for impulsive parameter identification in a single-degree-of-freedom system [17]. Furthermore, the Shannon entropy of wavelet coefficients has been used as a measure for wavelet basis evaluation in lamb wave analysis [18]. Genetic algorithm has also been applied to facilitating the selection of wavelet basis for gear fault identification [19].

Equally important as the wavelet basis selection is the performance evaluation of various types of wavelets for a specific type of applications, e.g. bearing defect diagnosis. Motivated by prior research, this paper investigates a

quantitative approach to evaluating complex-valued wavelet basis for bearing vibration analysis, by considering the inter-relationship between the signal and its corresponding wavelet coefficients. After a brief introduction to the wavelet transform, the method of cross-correlation for wavelet basis evaluation is presented in Section 2. In Section 3, performance evaluation of complex-valued wavelet bases for bearing diagnosis is conducted, and the effectiveness of the cross-correlation for wavelet basis evaluation is experimentally verified. Finally, conclusions are drawn in Section 4.

2. Wavelet Transform and Wavelet Basis Evaluation

2.1 Wavelet Transform

The main idea of signal transformation is to compare the signal of interest, $x(t)$, with a set of known functions $\{\psi_n(t)\}_{n\in z}$, and measure the similarity between them. Such an operation is mathematically expressed as:

$$c_n = \int_{-\infty}^{\infty} x(t)\psi_n^*(t)dt \tag{1}$$

where (•)* stands for the complex conjugate of the function (•). Depending on the chosen functions $\{\psi_n(t)\}_{n\in z}$, the signal can be transformed into different domains. For example, when the chosen functions are sine and cosine functions, Eq. (1) represents the *Fourier* transform, and the signal is transformed into the frequency domain. The resulting coefficients c_n express the power concentration of the corresponding frequency components (i.e. the power spectral density). Similarly, when the set of functions chosen for analysis are derived from a single base function through a series of *scaling* (i.e. dilation and contraction, denoted by the parameter *s*) and *shifting* (i.e. time translation, denoted by the parameter *τ*) operations such that $\psi_{s,\tau}(t) = \frac{1}{\sqrt{s}}\psi(\frac{t-\tau}{s})$, Eq. (1) represents the *wavelet* transform, which can be generally expressed as:

$$wt(s,\tau) = \frac{1}{\sqrt{s}}\int x(t)\psi^*(\frac{t-\tau}{s})dt \tag{2}$$

Through variations of the scales (corresponding to the frequency bands, with small scales for high frequencies and large scales for low frequencies) and time shifts of the base function, or *wavelet basis*, the wavelet transform provide the ability of multi-resolution, which is effective in feature extraction for non-stationary signal analysis.

Generally, the wavelet transform can be represented in both continuous (i.e. continuous wavelet transform) and discrete forms (i.e. discrete wavelet transform). Calculation for continuous wavelet transform can be directly implemented using integral operations or by means of a series of Fourier and inverse Fourier transforms [20], in which Eq. (2) takes the form of:

$$wt(s,\tau) = F^{-1}\{WT(s,f)\} = |s|^{1/2} F^{-1}\{X(f)\bar{\Psi}(sf)\} \tag{3}$$

where $WT(s,f)$, $X(f)$ and $\bar{\Psi}(\bullet)$ are the Fourier transforms of $wt(s,t)$, $x(t)$ and $\psi^*(\bullet)$, respectively. The symbol F^{-1} denotes inverse Fourier transform. It can be seen from Eq. (3) that for a signal $x(t)$, its continuous wavelet transform at scale *s* can be considered as a band-pass filtering operation performed on that signal, where the filter's band-pass is determined and controlled by the scale parameter *s*.

2.2 Cross-Correlation for Wavelet Basis Evaluation

To ensure effective feature extraction from a signal, an appropriate wavelet basis needs to be chosen before applying wavelet transform to that signal. In essence, the wavelet transform measures the "similarity" between the signal and the wavelet basis at various scales. This is analogous to cross-correlation between two quantities, from the point of view of statistics, and as such, cross-correlation analysis provides a natural method for quantitatively evaluating the performance of different wavelet bases in signal analysis. Prior study has reported using cross-correlation to find an optimal wavelet basis for detecting and locating Partial Discharge (PD) occurred in operational transformers [21-22]. Since the coefficients of a signal's wavelet transformation characterize information of the signal, they are inherently correlated with the signal. Therefore, the relative strength of the correlation can be measured in terms of the correlation coefficient, defined as [23]:

$$\rho_{x(t)wt(s,\tau)} = \frac{C_{x(t)wt(s,\tau)}}{\sigma_{x(t)}\sigma_{wt(s,\tau)}} \tag{4}$$

where the symbols $\sigma_{x(t)}$ and $\sigma_{wt(s,\tau)}$ are the standard deviation of the signal $x(t)$ and the wavelet coefficients $wt(s,\tau)$ at a specific scale s, respectively. The symbol $C_{x(t)wt(s,\tau)}$ denotes their covariance. In digitized data acquisition, the signals $x(t)$ and $wt(s,\tau)$ are sampled as discrete values. Accordingly, the correlation coefficient is estimated from the sample data as:

$$\hat{\rho}_{x(i)wt(s,i)} = \frac{\sum_{i=1}^{N}[x(i)-\bar{x}][wt(s,i)-\overline{wt(s)}]}{\sqrt{\sum_{i=1}^{N}[x(i)-\bar{x}]^2\sum_{i=1}^{N}[wt(s,i)-\overline{wt(s)}]^2}} \tag{5}$$

where N is the number of data samples, and $\bar{x}$ and $\overline{wt(s)}$ are the mean values of $x(i)$ and $wt(s,i)$, respectively. The absolute value of the correlation coefficient is bounded by

$$0 \le \left|\hat{\rho}_{x(i)wt(s,i)}\right| \le 1 \tag{6}$$

Physically, the higher the absolute correlation coefficient value is, the greater the similarity between the two quantities will be. Since a good wavelet basis should be capable of maximizing the extraction of features from a signal of interest, it means the corresponding wavelet coefficients should show a higher correlation coefficient to the signal than those obtained by other wavelet bases. Based on this concept, a maximum cross-correlation measure can be devised as a criterion for evaluating the impact of wavelet basis on vibration analysis. The criterion can be formulated as follows:

Maximum Cross-Correlation Measure Criterion**:** *The wavelet basis that maximizes the cross correlation coefficient between the signal and the wavelet coefficients represents the most appropriate wavelet for defect-induced transient vibration extraction.*

3. Experimental Bearing Defect Diagnosis

3.1 Complex-valued Wavelet Basis Evaluation

The cross-correlation measure is first used to evaluate each wavelet basis from a group of complex-valued wavelets (The reason why we evaluate the complex-valued wavelet will be explained in section 3.2), for experimental bearing vibration analysis. These wavelet bases are then used for performing multi-scale enveloping analysis for bearing defect diagnosis [24]. Fig. 1a illustrates the waveform of a vibration signal measured from a ball bearing that contains a localized defect on its outer raceway. The sampling rate is 10 kHz. The spectrum in Fig. 1b indicates a major frequency component at around 1,840 Hz. This frequency component has been used as the reference frequency (i.e., corresponding to center frequency of a decomposition scale) for scale selection when implementing the wavelet transform.

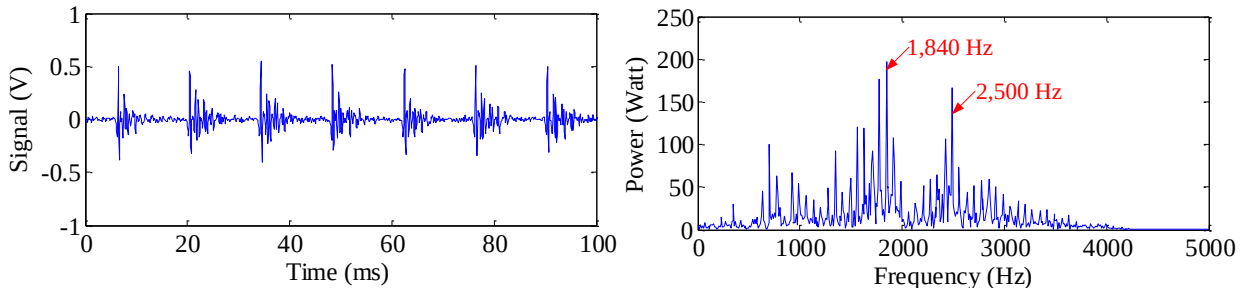

(a) waveform **(b) power spectrum.**

Fig. 1 An experimental bearing vibration signal. (a) waveform (b) power spectrum.

The cross-correlation coefficient between the bearing vibration signal and each of the five commonly used complex-valued wavelets is calculated, and the result is shown in Table 1. It is seen that the Morlet wavelet has output the highest value of correlation coefficient, indicating its appropriateness for bearing vibration analysis.

Furthermore, the energy-to-Shannon entropy ratio, which has been verified as an effective measure to guide the wavelet basis selection [25], has also been used for comparison, and the Morlet wavelet has again been identified as the most suited wavelet basis for bearing vibration analysis. A case study has then been conducted for experimental bearing defect diagnosis with the assistance of multi-scale enveloping analysis, as described below.

Table 1 Wavelet Basis Evaluation using Bearing Vibration Signal

Complex-valued Wavelet Basis	Correlation Coefficient	Energy-to-Shannon Entropy Ratio
Morlet wavelet	0.87	60.76
Gaussian wavelet	0.84	56.04
B-Spine wavelet	0.76	35.05
Shannon wavelet	0.47	12.48
Harmonic wavelet	0.53	14.50

3.2 Multi-Scale Enveloping Analysis

A common characteristic of the complex-valued wavelets evaluated above is that their imaginary parts are the Hilbert transform of their real-parts. This means that these wavelets are analytic in nature, and their moduli represent the envelopes of the wavelet coefficients. Consequently, the result of continuous wavelet transform of a signal x(t) using a complex-valued wavelet is also analytic in nature, and its modulus represents the envelope of the wavelet coefficients. Such characteristic has been leveraged when analyzing bearing vibration signals using a multi-scale enveloping analysis method [24].

The multi-scale enveloping analysis makes use of the time, scale, and frequency domain information contained in the signal in a synergistic fashion. Computationally, it first decomposes the signal into different scales by means of a complex-valued wavelet transform, as illustrated in Fig. 2. The envelope signal in each scale is then calculated from the modulus of the wavelet coefficients. Subsequently, Fourier transform is performed repetitively on the envelope signal at each scale, resulting in an "envelop spectrum" of the original signal at the various scales. The final output is a three-dimensional scale-frequency-energy map, which indicates the intensity and location of the defect-related frequency lines.

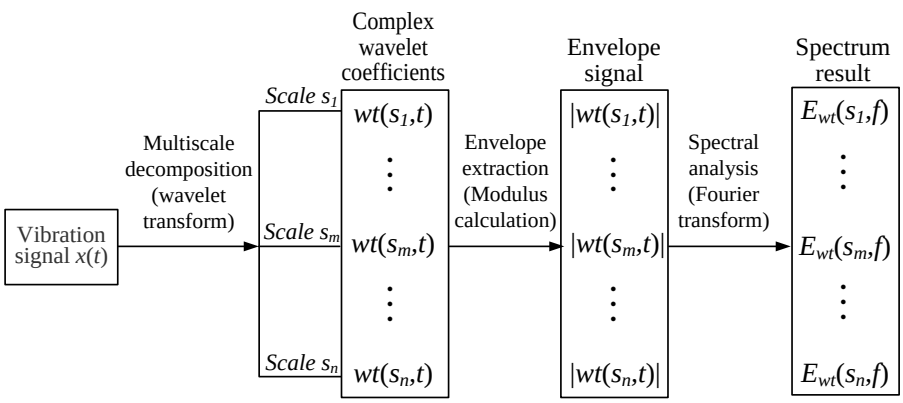

Fig. 2 The flow chart of multi-scale enveloping analysis.

3.3 Spindle-Bearing Defect Diagnosis

The case study is aimed to verify the effectiveness of the cross-correlation measure-based wavelet basis evaluation for spindle-bearing defect diagnosis. As shown in Fig. 3, a dynamic load cylinder applies impulsive forces of amplitude 13.3kN to a spindle shaft, which was preloaded at 839 N and rotating at 8,400 rpm, as a means to accelerate the structural deterioration of the spindle and establish a service life history. Fig. 4 illustrates the vibration signals at two different spindle operation stages: before impacts were applied and after 700 impacts.

Multi-scale enveloping analysis of the vibration signals is then performed using the five complex-valued wavelet bases, respectively. Fig. 5a illustrates the spectrogram of the envelope signals extracted from the wavelet transform before impact was applied, where Morlet wavelet is used as the wavelet basis.. The only appreciable frequency peak shown in the spectrum is at 140 Hz, which corresponds to the spindle rotational speed of 8,400 rpm. No characteristic frequencies that relate to structural defects within the spindle bearing system were found, indicating the spindle bearings are in good condition.

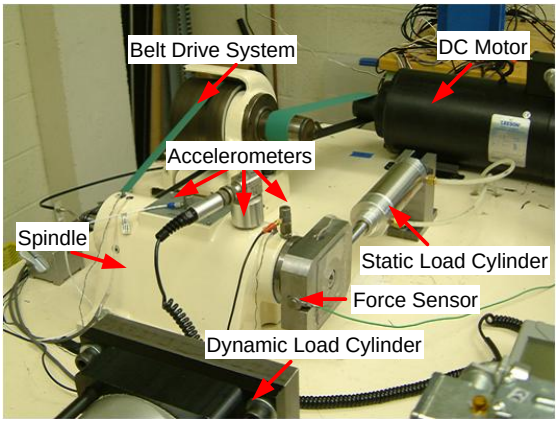

Fig. 3 Spindle-bearing test system.

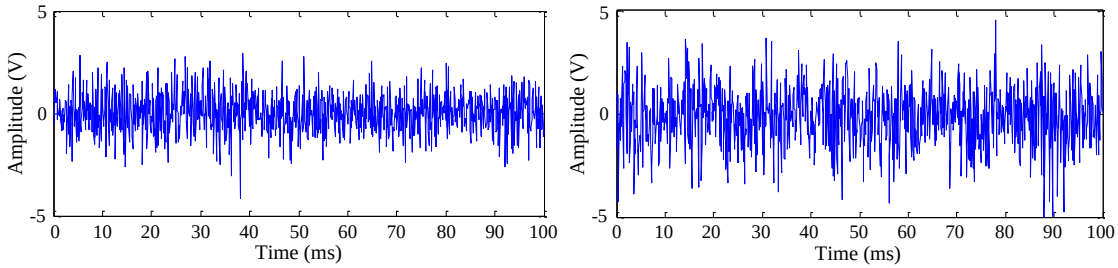

(a) before impact **(b) after 700 impacts**

Fig. 4 Vibration signals measured on the spindle test system.

After 700 impacts, the spectrogram has seen significant changes, as illustrated in Fig. 5b. In addition to an increase of the amplitude of the rotational frequency 140 Hz and its harmonics at 280 Hz, several other peaks at 885, 935, 1,075, 1,215, and 1,355 Hz, are shown respectively. Based on the geometry information of the bearing and the spindle rotational speed [26], the peak at 935 Hz is identified as the Ball Passing Frequency at the Inner Raceway (BPFI). The existence of such a frequency component indicates that one of the spindle front bearings has developed a defect on its inner raceway, as the result of dynamic impacts. Theoretically, the BPFI frequency at 8,400 rpm is calculated as 922 Hz. The 1.4% difference between the theoretical and experimental values can be traced back to the combined effect of rolling element slippage and the slight drift of spindle speed from the nominal input values to the spindle drive controller. Lastly, the frequency components at 1,075, 1,215, and 1,355

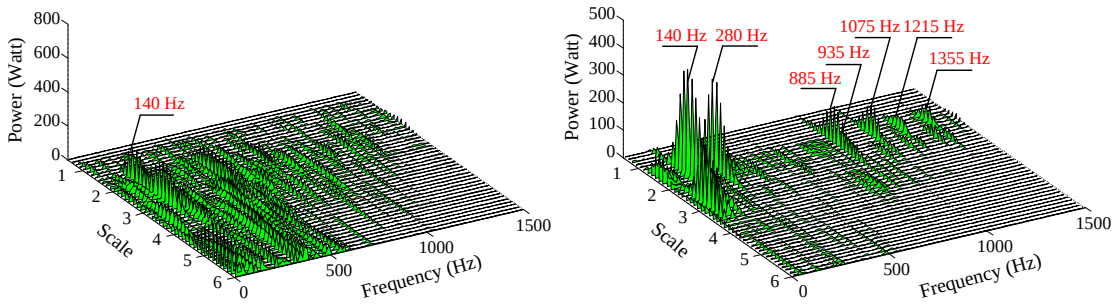

(a) before impact **(b) after 700 impacts.**

Fig. 5 Multiscale enveloping analysis results.

Hz can be specified as $f_{BPFI} + k \cdot f_r$ with k=1,2,3. These frequencies reflect upon the combined effect of spindle unbalance and inner raceway defect. The frequency component at 885Hz comes from the support bearing.

Comparison with other complex-valued wavelet bases on indentifying defect-related characteristic frequency on the inner raceway of the spindle bearing is then conducted. Fig. 6 shows the relative magnitude of the wavelet enveloping spectrum of f_{BPFI} at 935 Hz, under different number of dynamic impacts on the spindle. The Morlet wavelet has consistently output the highest magnitude at each stage of spindle operation, comparing with other wavelets. This verifies the effectiveness of the developed cross-correlation measure for performance evaluation of wavelet basis in bearing vibration analysis.

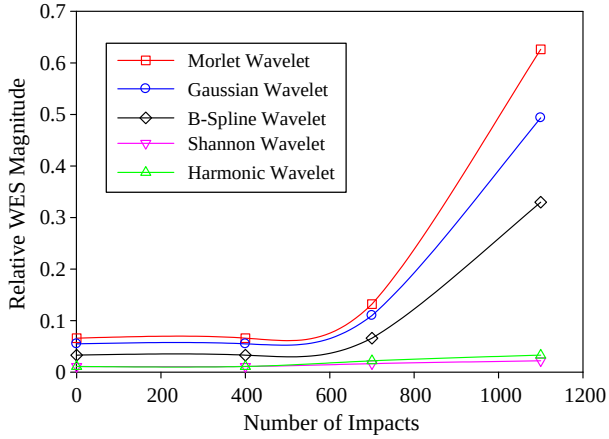

Fig. 6 Comparison among five complex-valued wavelets on defect characteristic frequency identification.

4. Conclusion

A quantitative method to guide performance evaluation of wavelet basis in bearing vibration analysis, termed cross-correlation measure, has been developed. An experimental case study has been performed, and the results have indicated that the developed measure is effective and robust. This is shown in the fact that the cross-correlation coefficient between the extracted information using the Morlet wavelet and the defect-related transient information inherent in the signal is the largest among the five candidate wavelet bases. As a result, the Morlet wavelet is effective in indentifying bearing structural defect from its vibration signals.

Acknowledgment

This work has been supported by the National Natural Science Foundation of China (No. 60874022 and No. 51175080) and US National Science Foundation under award EFRI-0735974.

References

[1] I. Daubechies. The Wavelet Transform, Time-Frequency Localization And Signal Analysis, *IEEE Transactions on Information Theory*, Vol. 36, No. 5, pp. 961-1005, 1990.

[2] D. E. Newland. Wavelet Analysis Of Vibration Part I: Theory, *ASME Journal of Vibration and Acoustics*, Vol. 116, No. 4, pp. 409-416, 1994.

[3] R. Gao and R. Yan. Non-stationary Signal Processing for Bearing Health Monitoring, *International Journal of Manufacturing Research*, Vol. 1, No. 1, pp. 18-40, 2006.

[4] W. J. Wang and P. D. McFadden. Application of Wavelets to Gearbox Vibration Signals for Fault Detection, *Journal of Sound and Vibration*, Vol. 192, pp. 927-939, 1996.

[5] Q. Sun and Y. Tang. Singularity Analysis Using Continuous Wavelet Transform For Bearing Fault Diagnosis, *Mechanical Systems and Signal Processing*, Vol. 16, pp. 1025-1041, 2002.

[6] J. Zhao, Z. He, Q. Meng and Z. Chen. Wavelet Packet- Autoregressive Spectrum Analysis and Its Application in Fault Diagnosis, *Journal of Vibration Engineering*, Vol. 8, No. 3, pp. 198-203, 1995.

[7] Z. K. Peng and F. L. Chu. Application Of The Wavelet Transform In Machine Condition Monitoring And Fault Diagnostics: A Review With Bibliography, *Mechanical Systems and Signal Processing*, Vol. 18, No. 2, pp. 199-221, 2004.

[8] J. Liu, W. Wang, and F. Golnaraghi. An Extended Wavelet Spectrum For Bearing Fault Diagnostics, *IEEE Transactions on Instrumentation and Measurement*, Vol. 57, No. 12, 2801-2812, 2008.

[9] L. Guo, J. Chen, Y. Zhu, et al. Application of Wavelet Support Vector Machine In Rolling Bearing Fault Diagnosis, *Journal of Shanghai Jiaotong University*, Vol. 43, No. 4, pp. 678-682, 2009

[10] R. Yan and R. Gao. Energy-based Feature Extraction For Defect Diagnosis In Rotary Machines, *IEEE Transactions on Instrumentation and Measurement*, Vol. 58, No. 9, pp.3130-3139, 2009.

[11] Y. Qin, S. Qin, and Y. Mao. Demodulation Approach Based On Wavelet Ridge And Its Application In Fault Diagnosis Of Rotating Machinery, *Chinese Journal of Mechanical Engineering*, Vol. 45, No. 2, pp. 231-237, 2009.

[12] J. de Jesus Rangel-Magdaleno, R. De Jesus Romero-Troncoso, R.A. Osornio-Rios, Z. Cabal-Yepez and A. Dominguez-Gonzalez. FPGA-based Vibration Analyzer For Continuous CNC Machinery Monitoring with Fused FFT-DWT Signal Processing, *IEEE Transactions on Instrumentation and Measurement*, Vol. 59, No. 12, pp. 3184-3194, 2010.

[13] X. Lou and K.A. Loparo. Bearing Fault Diagnosis Based On Wavelet Transform And Fuzzy Inference, *Mechanical Systems and Signal Processing*, Vol. 18, pp. 1077-1095, 2004.

[14] N.G. Nikolaou and I. A. Antoniadis. Rolling Element Bearing Fault Diagnosis Using Wavelet Packets, *NDT&E International*, Vol. 35, pp. 197-205, 2002.

[15] S. Fu, B. Muralikrishnan and J. Raja. Engineering Surface Analysis With Different Wavelet Bases, *ASME Journal of Manufacturing Science and Engineering*, Vol. 125, pp. 844-852, 2003.

[16] W. X. Yang and X. M. Ren. Detecting Impulses In Mechanical Signals By Wavelets, *EURASIP Journal on Applied Signal Processing*, Vol. 8, pp. 1156-1162, 2004.

[17] E. L. Schukin, R. U. Zamaraev and L. I. Schukin. The Optimization Of Wavelet Transform For The Impulsive Analysis In Vibration Signals, *Mechanical Systems and Signal Processing*, Vol. 18, No. 6, pp. 1315-1333, 2004.

[18] F. C. Li, G. Meng, K. Kazuro, Z.Q. Su and L. Ye. Optimal Mother Wavelet Selection For Lamb Wave Analysis, *Journal of Intelligent Material Systems and Structures*, Vol. 20, pp.1147-1161, 2009.

[19] J. Rafiee, P. W. Tse , A. Harifi and M.H. Sadeghi. A Novel Technique For Selecting Mother Wavelet Function Using An Intelligent Fault Diagnosis System, *Expert Systems with Applications*, Vol. 36, pp. 4862-4875, 2009.

[20] P. S. Addison. The Illustrated Wavelet Transform Handbook, IOP Publishing Ltd, 2002.

[21] X. Ma, C. Zhou, and I. J. Kemp. Automated Wavelet Selection and Thresholding for PD Detection, *IEEE Electrical Insulation Magazine*, Vol. 18, No. 2, pp. 37-45, 2002.

[22] X. Ma, C. Zhou, and I. J. Kemp. Interpretation of Wavelet Analysis and Its Application in Partial Discharge Detection, *IEEE Transactions on Dielectrics and Electrical Insulation*, Vol. 9, No. 3, pp. 446-457, 2002.

[23] J. S. Bendat and A. G. Piersol. *Random Data: Analysis and Measurement Procedures*, John Wiley & Sons, 2000.

[24] R. Yan and R. Gao. Multi-scale Enveloping Spectrogram For Vibration Analysis in Bearing Defect Diagnosis, *Tribology International*, Vol. 42, No. 2, pp. 293-302, 2009.

[25] R. Yan and R. Gao. Base Wavelet Selection For Bearing Vibration Signal Analysis, *International Journal of Wavelets, Multi-resolution, and Information Processing*, Vol. 7, No. 4, pp. 411-426, July, 2009.

[26] T. A. Harris. *Rolling Bearing Analysis*, Wiley, 1991.

Copyright © 2012 DET Corp., Japan All Rights Reserved
International Journal of Comprehensive Engineering
Part A, 1(1), 21-31, 2012
Doi: 10.14270/IJCE2012.1.1.a21
Regular paper

ISSN 2186-2680
e-ISSN 2186-2656
www.iace-journal.org

New Condition Monitoring Method of Rotary Machine Elements under the Other Operating Machineries Located Close Range

-- Extraction of Fault Components Based on Proposed Multiplex Elements AR Model

Hiromitsu Ohta [1,#], Keiji Sasada [2], Shintaro Shiota [2] and Satoru Ezoe [1]

[1] Department of Ocean Mechanical Engineering, National Fisheries Univerisity,
2-7-1, Nagatahon-machi, Shimonoseki, Yamaguchi, 759-6595, Japan
[2] Graduate Student, Graduate School of Fisheries Science, National Fisheries University.

[#] Corresponding author: ohta@fish-u.ac.jp; Tel.: +81-83-286-5111; Fax: +81-83-286-7433

Abstract: Difficulty of condition monitoring and diagnosis against machineries constructed by some mechanical elements, which are located close range increases more, because of masking in many frequency bands such as discrete frequency signals associated with shaft speed and broad band ones associated with the natural frequencies of each machinery elements and structural materials. This paper proposes a novel condition monitoring method on rotary machineries by fault vibration signals extraction algorithm based on the proposed multiplex elements Auto Regressive model (MEAR model), which can be removed influence of vibration signal components generated by other machineries located close range except for monitored and diagnosed rotary machinery. We intend to have attempted to demonstrate the effectiveness of the proposal MEAR model and its extraction algorithm using an experimental rotary machine which, is constructed by a rotor, spur gears and rolling element bearings and an induction motor, which are connected to a drive and two driven shafts. The experimental machine can be artificially assumed three common faults such as an unbalanced rotor, a gear unbalance and wear gear teeth. Good results are obtained in this article, the ability of the proposal condition monitoring method (MEAR model and its algorithm) is effectively identified. High precision condition monitoring by the method can be carried out under the environment of close range location.

Keywords: Rotary Machinery, Condition Monitoring, Multiplex Elements Auto Regressive Model, Close Range Location, Fault.

Received: May 28, 2012 / Accepted: Sept. 12,2012 / Published: Dec. 15,2012

1. Introduction

The establishment of optimum maintenance interval on machineries and equipments in operation has been one of the major sources of improving the production efficiency in manufacturing process, minimizing the maintenance cost for maintaining high production efficiency of the machineries and equipments. Condition Based Maintenance (CBM) [1] has been used as maintenance policy against significant machinery, which is strictly recommended to keep high production efficiency and reliability, to minimize the maintenance cost. CBM policy needs condition monitoring and diagnosis technology [2] of high precision and reliability to keep high production efficiency, to decrease the maintenance cost. The fault diagnosis of rotary machinery based on vibration and acoustic signals condition monitoring generated from the target machinery is the one of the effectively useful methods [3,4], however, the maintain of high precision monitoring and diagnosis of machine systems constructed many components and structural materials usually will be more difficult, these machine systems are becoming increasingly complex. An effective vibration signal associated with the fault to diagnose the machine condition is masked by other vibration signals such as other discrete frequency signals associated with shaft speed, Gaussian noise(signal), which is obeyed normal distribution in the shape of its probability density function and natural frequencies, which are generated by mechanical elements and materials located

close range. The measurement of vibration signals obtained from acceleration pickups placed in around the target machine include many frequency components such as discrete frequency signals and broad band ones associated with the natural frequencies of individual machinery elements and structural materials, even in the presence or absence of faults. Linear prediction [5, 6] is basically a method of modeling of the predictable region of a signal, based on a certain number of obtained signals in the immediate past and then using this model to predict the unknown signal in the series. The major model used for linear prediction of time series has been known as auto regressive model (AR model), which is type of parametric spectrum analysis [7, 8, 9]. The residual signal of the obtained time series is then constructed by subtraction the actual signal value from the predictable signal one. The correlation value of obtained residual component is generally used to evaluate the optimization of the constructed linear prediction model in this proposal condition monitoring method. Until now, we have attempted to implement high precision and to develop of novel condition monitoring and diagnosis technologies about mainly rotary machinery [9,10,11] and internal combustion engine [12,13,14], which are composed of many mechanical elements and materials in ship's engine room. Primary approach method to develop new monitoring and diagnosis technologies is based on the parametric and non-parametric linear predictions [15,16], which are a kind of system identification method. For example, early detection method of artificially assumed faults associated with push rod, driven rocker arm and intake exhaust valves in the four stroke twin cylinder reciprocal engine has been proposed [17]. Also, identification of above the same type faults conditions has been carried out based on the cross correlation function of close two point signals and proposed paralleled ARX (Auto Regressive with Extra Input) [18] model based on the parametric linear prediction theorem at diagnosed mechanical element within the engine. It has been possible to effectively extract only fluctuation vibration components associated with fault conditions from mechanical elements in operation. In this article, we proposes a novel condition monitoring method on rotary machineries by fault vibration signals extraction algorithm based on the named multiplex elements Auto Regressive model (MEAR model), which is a kind of parametric linear prediction method and can be effectively removed influence of vibration signal components generated by other machineries located close range from all synthesized vibration signals obtained from the acceleration pickups. When other machineries except for the target machinery are located close range, the Proposed MEAR model and its condition monitoring algorithm can be particularly shown beneficial result. When viewed as the parametric model by linear prediction method, transfer elements corresponding to several condition-monitored mechanical elements can be arranged in the block diagram of the proposed MEAR model. Individual transfer elements corresponding to condition-monitored mechanical elements are essentially modeled by the normal vibration signal generated by the no malfunction condition. When a fault vibration signal are inputted in the MEAR model constructed by the obtained normal vibration signal, A fault vibration component can be included and be emphasized in the residual vibration signal, which is obtained by subtraction the inputted fault signal from the predictable one [19]. The effectiveness of the MEAR model and its fault signal extraction algorithm will be evaluated from the obtained residual vibration signals in this study. Also, we intend to have attempted to experimentally demonstrate the effectiveness of the proposal MEAR model and its extraction algorithm using an actual experimental rotary machine which, is constructed by a rotor, spur gears and rolling element bearings and a 3 phase induction motor, which are connected to a main drive and two driven shafts. Assumed three faults types such as a rotor unbalance, a gear unbalance and wear gear teeth is artificially assumed in the experimental rotary machine. Sufficient results are obtained in this experimental demonstration, the ability of the proposal condition monitoring method (MEAR model and its algorithm) is effectively identified.

2. Theoretical Basis of Multiplex Elements Auto Regressive Model and Block Diagram for Extraction

Fig.1 shows the block diagram of proposed Multiplex Elements Auto Regressive Model (MEAR model) to extract only fault signal generated by monitored and diagnosed machineries in the case of other operated machineries located close range. In short, this MEAR model can be effectively removed influence of vibration components unrelated to fault of its machineries from other operating ones, which are located close range for the condition monitored and diagnosed ones. Transfer elements corresponding to condition monitored mechanical elements can be arranged in the above proposed block diagram in this model. Filter coefficients within respective transfer elements in the MEAR model are essentially modeled by using respective normal condition vibration (time series) data transmitted from the monitored mechanical elements. In principle, the respective predicted series $y1(t)$, $y2(t)$, $y3(t)$,$\cdots$,$yn(t)$ can be estimated by convoluting the respective filter coefficients with the respective past time series.

Furthermore, the corresponding the respective residual series $e_1(t)$, $e_2(t)$, $e_3(t)$,$\cdots$, $e_n(t)$ can be calculated by subtracting the input vibration series $u_1(t)$ or the predicted ones $y_1(t)$, $y_2(t)$, $y_3(t)$ from the final predicted ones $y_n(t)$. If the fault occurs in individual mechanical elements in operation, the input signals $u_1(t)$, $u_2(t)$, $u_3(t)$,$\cdots$,$u_n(t)$ have

direct influences of fault conditions from the mechanical elements. When the fault vibration signals generated by the individual mechanical elements are inputted in the incoming signal for the MEAR model, the obtained individual residual signals include signal components related on the faulty conditions from individual mechanical components. A part of the residual components including vibration signals on fault conditions can be emphasized and be large amplitude due to the nature of the Auto Regressive model. Consequently, although affecting other mechanical elements except for monitored mechanical ones are located close range, high precision and effective condition monitoring can be achieved by using its nature, because of by eliminating the all oscillatory signals generated by other mechanical elements. The advantage of MEAR model based monitoring can simultaneously model capturing surrounding vibration environment.

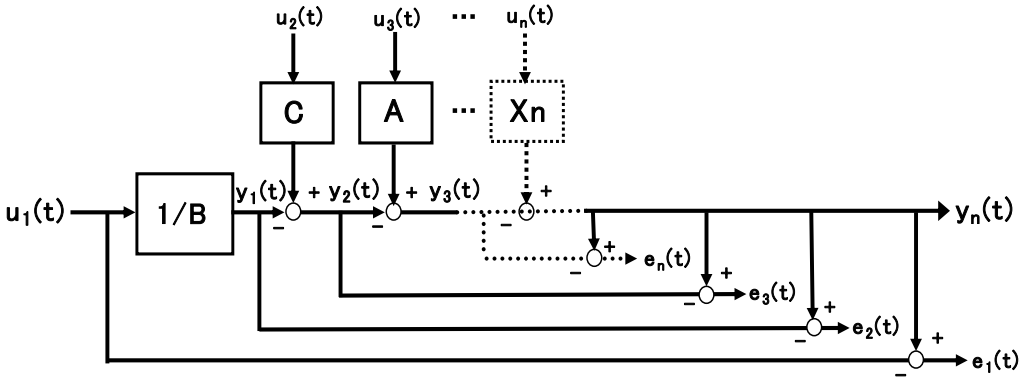

Fig. 1 Block diagram for the fault signal extraction method by proposed multiplex elements AR model

Nomenclatures:

$u_1(t)$: Input vibration signal at the location of a mechanical element No.1.
$u_2(t)$: Input vibration signal at the location of a mechanical element No.2.
$u_3(t)$: Input vibration signal at the location of a mechanical element No.3.
$u_n(t)$: Input vibration signal at the location of a mechanical element No.n.
$y_1(t)$: Predicted signal generated by a mechanical element No.1.
$y_2(t)$: Predicted signal generated by a mechanical element No.2.
$y_3(t)$: Predicted signal generated by a mechanical element No.3.
$y_n(t)$: Predicted signal generated by a mechanical element No.n.
$e_1(t)$: Residual signal obtained from subtracting predicted signal $u_1(t)$ from $y_n(t)$.
$e_2(t)$: Residual signal obtained from subtracting predicted signal $y_1(t)$ from $y_n(t)$.
$e_3(t)$: Residual signal obtained from subtracting predicted signal $y_2(t)$ from $y_n(t)$.
$e_n(t)$: Residual signal obtained from subtracting predicted signal $y_3(t)$ from $y_n(t)$.
A: Filter coefficients of corresponding to a normal condition mechanical element No.3.
B: Filter coefficients of corresponding to a normal condition mechanical element No.1.
C: Filter coefficients of corresponding to a normal condition mechanical element No.2.
Xn:Filter coefficients of corresponding to normal condition of a mechanical element No.n.

In this research, in order to model the time series of condition monitored mechanical elements, acceleration pickups as a sensor measuring the vibration are directly located on the condition monitored mechanical ones. The prediction output $y_1(t)$ shown in Eq.(1) can be estimated from time series data obtained at the location corresponding to filter coefficient B.

$$y_1(t) = \frac{1}{B(q)} u_1(t) \tag{1}$$

Furthermore, the prediction output $y_2(t)$ can be constructed from the time series data obtained at the location corresponding to filter coefficients B and C respectively. The $y_2(t)$ can be written by Eq.(2).

$$y_2(t) = \frac{1}{B(q)} u_1(t) + C(q) u_2(t) \tag{2}$$

Similarly, the prediction output $y_3(t)$ shown in Eq.(3) can be estimated by corresponding to filter A ,B ,C

$$y_3(t) = \frac{1}{B(q)} u_1(t) + C(q)u_2(t) + A(q)u_3(t) \tag{3}$$

The general form of prediction output $y_n(t)$ corresponding to the nth measuring location can be obtained from Eq.(4).

$$y_n(t) = \frac{1}{B(q)} u_1(t) + C(q)u_2(t) + A(q)u_3(t) + \cdots + X_n u_n(t) \tag{4}$$

A discrete representation of a system possessed auto correlation can be given by Eq.(5).

$$\begin{aligned} & y(t) + a_1 y(t-1) + \cdots + a_{n_a} y(t-n_a) \\ & = \left(1 + a_1 q^{-1} + \cdots a_{n_a} q^{-n_a}\right) y(t) \end{aligned} \tag{5}$$

Where, the symbol q is the shift operator and having the following relationship shown in Eq.(6)

$$qu(t) = u(t+1) \tag{6}$$

Filter coefficient A shown in Eq.(7) can be expressed by using Eq.(5)

$$A(q) = 1 + a_1 q^{-1} + \cdots + a_{n_a} q^{-n_a} \tag{7}$$

Also, filter coefficient B and C can be respectively expressed in the following Equation Eq.(8) and Eq.(9). Applied filter are described in polynomial equation.

$$B(q) = b_1 q^{-1} + \cdots + b_{n_b} q^{-n_b} \tag{8}$$

$$C(q) = c_1 q^{-1} + \cdots + c_{n_b} q^{-n_b} \tag{9}$$

In this paper, optimum order to be firstly construct the filter coefficients A,B,C・・・, Eq.(7), (8), (9) are determined by the autocorrelation values of the respective residual components $e_n(t)$ which can be obtained by taking the difference between the respective prediction outputs $y_1(t)$, $y_2(t)$,$y_3(t)$ to the respective input ones $u_1(t)$, $u_2(t)$, $u_3(t)$. For example, autocorrelation function $R_c(\tau)$ which is evaluation criteria to determine the order of filter coefficient C can be defined as Eq.(10). Here, T and τ shown in Eq.(10) indicate a finite measurement time and delay time respectively.

$$R_C(\tau) = \lim_{T \to \infty} \frac{1}{T} \int_0^T \{y_1(t) - u_1(t)\}\{y_1(t+\tau\} - u_1(t+\tau) dt \tag{10}$$

In conclusion, the lower one of the autocorrelation values $R_C(\tau)$ obtained by using normal condition time series data is firstly selected as the optimum coefficients composed the MEAR model. If the fault condition time series data will input in the MEAR model previously composed by the normal condition ones, signal components related the fault condition will be contained and be emphasized in the obtained residual components $e_1(t)$, $e_2(t)$, $e_3(t)$ by depending on the characteristics of the MEAR model. The residual fault components generated by the all n monitored mechanical elements corresponding to the respective transfer elements in the block diagram shown in Fig.1 can be expressed by the below Eq.(11).

$$e_1(t) = y_n(t) - u_1(t) \tag{11}$$

In the case of the n-1 residual fault components $e_2(t)$, which will be shown in below Eq.(12).

$$e_2(t) = y_n(t) - y_1(t) \tag{12}$$

Similarity, in the case of the n-2 residual fault components $e_3(t)$, which can be estimated by Eq.(13).

$$e_3(t) = y_n(t) - y_2(t) \tag{13}$$

Finally, the fault signal components corresponding to the transfer element (Filter coefficient) A,C,B can be obtained from the prediction signal $y_3(t)$-$y_2(t)$, $y_2(t)$-$y_1(t)$ and $y_2(t)$-$y_1(t)$, $y_1(t)$-$u_1(t)$ respectively.

3. Condition Monitored Machinery and its Assumed Fault Conditions

The general view of the applied rotary machinery facility for verification of the proposal monitoring method is shown in Fig.2. The vertical, horizontal and height direction dimensions of the facility are 620×1570×1460(including the control board)[mm] respectively. The facility consists of one main drive shaft and two driven ones that are placed on the both sides of the main shaft. The main shaft sustained by three deep groove rolling element bearings NSK6206 is driven by a three-phase induction motor (output power 0.75[kw]) via a coupling and other top of the main shaft is connected to electro-magnetic brakes to give an arbitrary load to the 3 phase induction motor and mounted mechanical elements. The main shaft attaches two spur gears (number of teeth 40) and one rotor which can be assumed fault conditions. The driven shaft sustained by two deep groove rolling element bearings attaches two spur gears (number of teeth 43) which can be classified into a normal condition and fault one. Fig.3 shows a picture of monitored mechanical elements and the locations of applied three

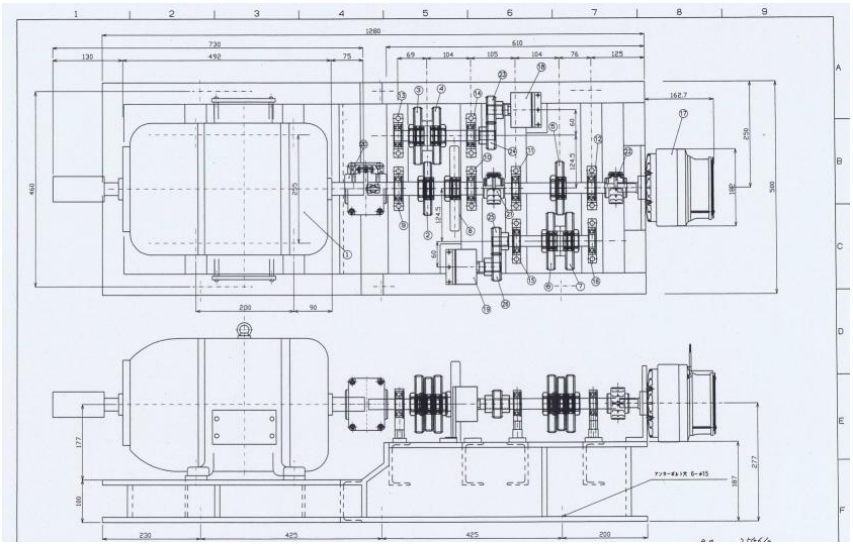

Fig. 2 The general view of applied rotary machinery for condition monitoring

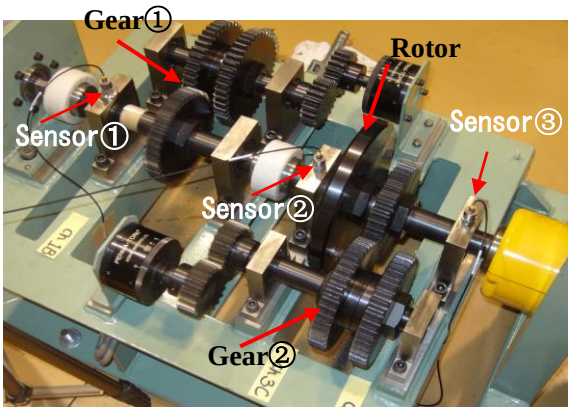

Fig. 3 Applied rotary machinery for condition monitoring

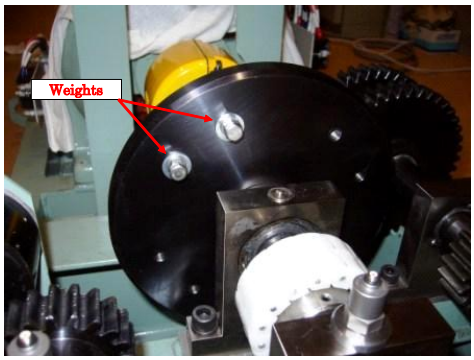

Fig. 5 An applied unbalanced rotor

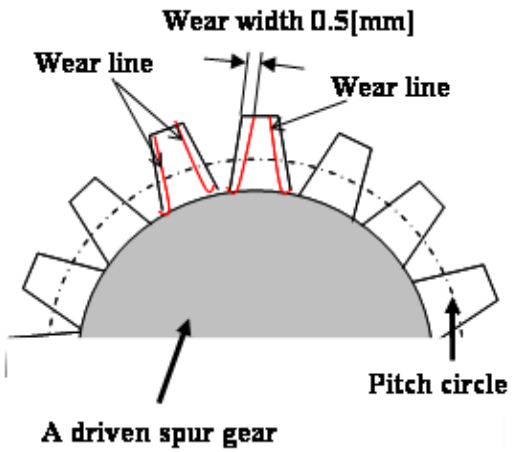

Fig. 4 Schematic diagram of the adjacent two wear teeth **Fig. 6 M6 bolts as load weight for rotor unbalance**

acceleration pickups indicated as "Sensor①,②,③". As the fault condition, surface wears of adjacent two teeth on driven side indicated as "Gear①" has been assumed in the monitoring. Schematic diagram of the surface wear of adjacent two teeth on driven gear side is shown in Fig.4. The both sides wear width of a tooth are 1.0[mm]. Moreover, the rotor unbalance in the main shaft and a gear unbalance in the driven shaft side indicated as "Rotor" and "Gear②" have been assumed respectively. Fig.5 shows the picture of unbalanced rotor which, is made by mounting the two M6 bolts and the six nuts (weight 42.1[g]) shown in Fig.6 using as load weight. The rotational speed of the main shaft during the verification is 500 [rpm] (8.33[Hz]) constantly, sampling and cutoff frequencies are set to 5[kHz], and 400[Hz] respectively, sampling time per one time is 1.0[s], measuring point per one time is 5000[points]. The programming of proposed MEAR model and its extraction algorithm has been performed by Lab VIEW software made of National Instruments Corp, and fundamentally analyzed under the online state.

4. Verification of Effectiveness of MEAR model and its Monitoring Method and Discussion

At first, the filter coefficients and related optimum orders at the location "Sensor①,②,③" indicated in Fig.3 must be determined by a time series data associated with vibration acceleration, which is obtained from normal condition. The filters at the location "Sensor ①","②"and"③" are respectively called filter "B", "C" and "A" in this article for convenience. Although applied "Sensor①,②,③" are located on the deep groove rolling element bearings, the influence of pass frequency associated with its rolling elements cannot be completely appeared the respective sensors because of using the no fault bearings. A vibration acceleration time series data obtained from "Sensor①" under the normal condition so as to construct the MEAR model is shown in Fig.7, Similarly, Fig.8 and Fig.9 represent the acceleration time series ones obtained from "Sensor②,③" under normal condition respectively. The modeling of transfer elements correspond to the block diagram MEAR model shown in Fig.1 have been used by the previous normal vibration acceleration time series. The transfer element correspond to the

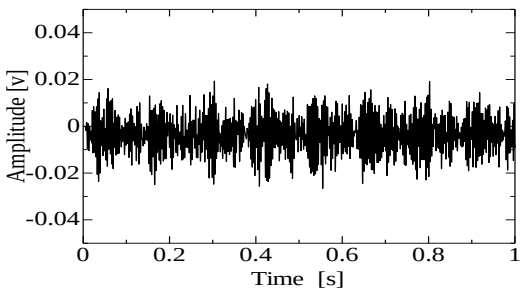

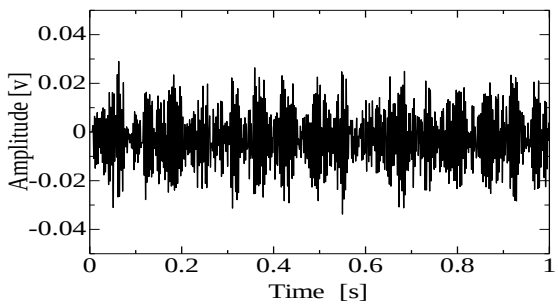

Fig. 7 The normal condition series used by modeling filter B **Fig. 8 The normal condition series used by modeling filer C**

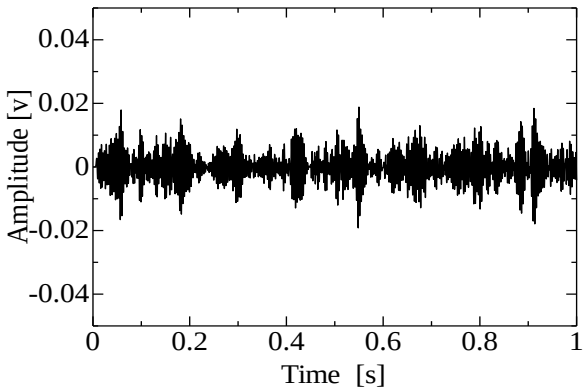

Fig. 9 The normal condition series used by modeling filter A

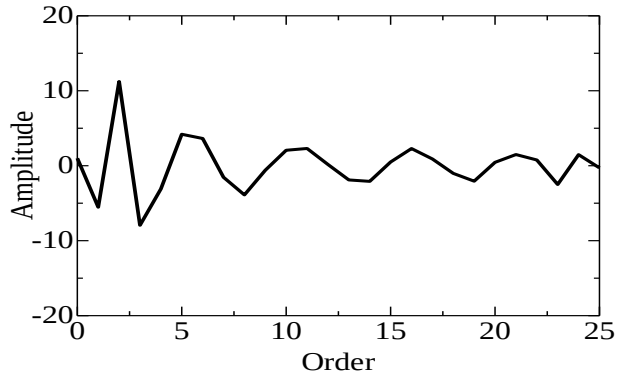

Fig. 10 The applied filter coefficient B for the MEAR model

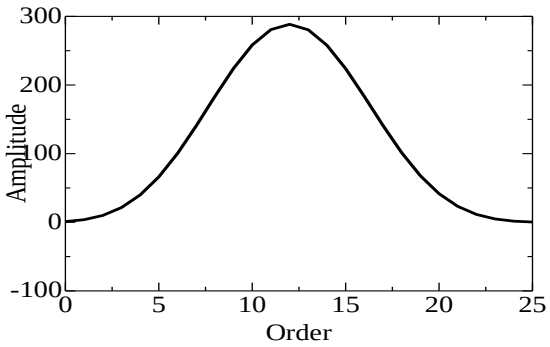

Fig. 11 The applied filter coefficient C for the MEAR model

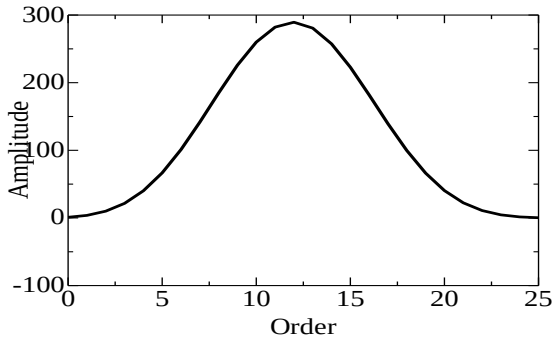

Fig. 12 The applied filter coefficient A for the MEAR model

filter "B" supports the vibration acceleration received in the location in "Sensor①" ,furthermore, filter "C" and filter "A" can support the vibration acceleration received by the locations in "Sensor②,③" respectively. Fig.7, Fig.8 and Fig.9 show normal vibration acceleration time series to constitute the MEAR model which can be measured at the individual locations "Sensor①", "Sensor②" and "Sensor③". Filter coefficients that applied in the MEAR model shown in Fig.10, Fig.11 and Fig.12 are essentially obtained by using the previous time series data shown in Fig.7, Fig.8 and Fig.9 respectively, in this article, optimum orders of these filters have been determined from the viewpoint of repeatability of estimated prediction output and the degree of calculation load to do the online condition monitoring system. Its repeatability will be satisfied by evaluating the correlation values, which can be obtained by subtracting required prediction outputs from the previous normal vibration acceleration time series. The more obtained correlation value is high, the more its repeatability of the estimated prediction output is really satisfied, however the load to our online condition monitoring system is extremely increased because of increasing the selected filter order, what is called, trade-off relationship based on the uncertainly principle affects the construction of MEAR model constructed by the optimum order. As a result, 25th as the optimum orders of our filter coefficients "A", "B" and "C" are experimentally chosen and unified by referring to the convergence property of the obtained autocorrelation values shown in Fig.13. Fig.14 shows the acceleration time series measured by "Sensor②" under only unbalanced rotor before applying the proposal MEAR model which emphasized its fault components. It is obviously hard to detect the existence of unbalanced rotor by visual recognition of the obtained acceleration time series shown in Fig.14, by reason of masking by multiple waveform generated by other mechanical elements and structural materials located close range except for the target machinery for the condition monitoring. On the other side, residual component e3(t)-e2(t) shown in the block diagram Fig.1 obtained by applying our proposal model can be shown in Fig.15. Large amplitudes correspond to the period of rotation speed, which is specific to the unbalance phenomenon of rotary machinery can be apparently seen in this figure. Furthermore, enveloped spectrums to apply Fast Fourier Transform to the previous acceleration time series and residual component can be shown in Fig.16. Black and red lines in the figure are correspond to the in the case of applying MEAR model and not applying one, respectively. Rotation

frequency associated with unbalanced rotor, which is fundamental, second and third harmonics components, which are generated by interference with between fundamental frequency can be apparently confirmed at applying the MEAR model, in contrast, in the case of not applying the MEAR model, frequency components of the unbalanced rotor are not clear. Considering the above result, effectiveness of the proposal model has been sufficiently demonstrated. Fig.17, Fig.18 and Fig.19 show an acceleration time series, a residual component and its enveloped spectrum in the case of surface wears of adjacent two teeth on driven side indicated as "Gear①" measured by "Sensor①"shown in Fig.3 and 4. Fig.17 is correspond to the not applying MEAR model, Fig.18 is the residual component e2(t)-e1(t) shown in the Fig.1, when the applying the proposal model to conventional acceleration times series. It is obviously hard to detect the existence of surface wear on the driven gear by visual recognition of the obtained acceleration time series shown

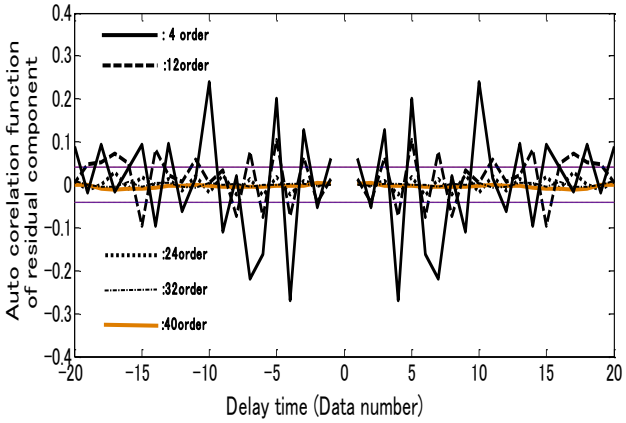

Fig. 13 The autocorrelation function of the obtained residual component

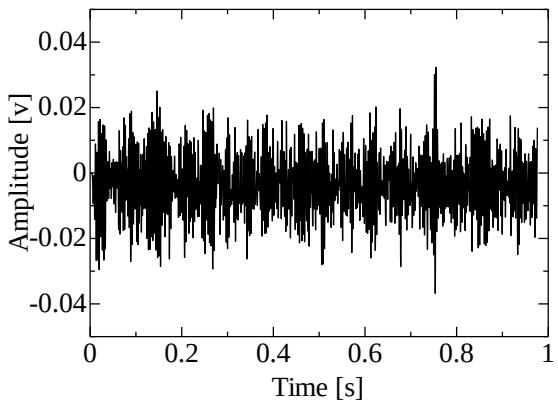

Fig. 14 The unbalanced rotor series before applying the MEAR model

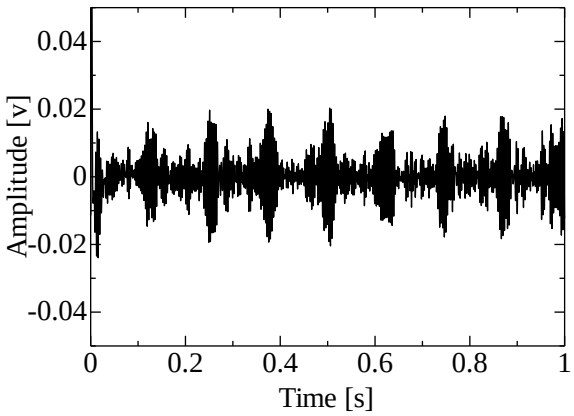

Fig. 15 The unbalanced rotor residual component the MEAR model

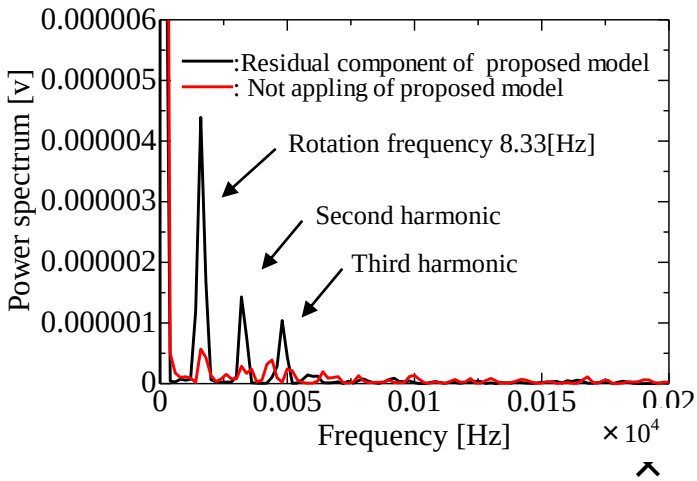

Fig. 16 The enveloped spectrum of Fig.14 and Fig.15

in Fig.17, on the other side, residual component $e_2(t)$-$e_1(t)$ shown in the block diagram Fig.1 obtained by applying the MEAR model can be shown in Fig.18.When the spur gear of adjacent two wear teeth on driven gear is seated, the impulsive wave correspond to the period of rotation speed can be apparently appeared in this figure.Still more, rotation frequency associated with surface ware of adjacent two teeth, which are fundamental and second harmonics components, which can be apparently confirmed at applying the MEAR model in enveloped spectrum shown in Fig.19, on the other hand, in the case of not applying the MEAR model, above frequency components of the associated with surface ware on driven spur gear can not be apparently confirmed. Fig.19 shows the acceleration time series measured by "Sensor③" under only an unbalanced spur gear indicated in "Gear②" shown in Fig.3.before applying the MEAR model. It is obviously hard to detect the existence of the unbalanced spur gear by visual recognition of the obtained acceleration time series shown in Fig.19. On the other side, residual component $e_n(t)$-$e_3(t)$ obtained by applying the proposal model can be shown in Fig.21. Large amplitudes correspond to the period of rotation speed of the driven spur gear, which is specific to the unbalance phenomenon can be apparently seen in this figure. Furthermore, enveloped spectrums to the previous acceleration time series

and residual component $e_n(t)$-$e_3(t)$ can be shown in Fig.22. The rotation frequencies associated with unbalanced rotor can be apparently confirmed at applying the MEAR model, in contrast, in the case of not applying the MEAR model, frequency components of the unbalanced rotor are not clear. Considering these results, effectiveness of the proposal MEAR model can be sufficiently demonstrated and confirmed.

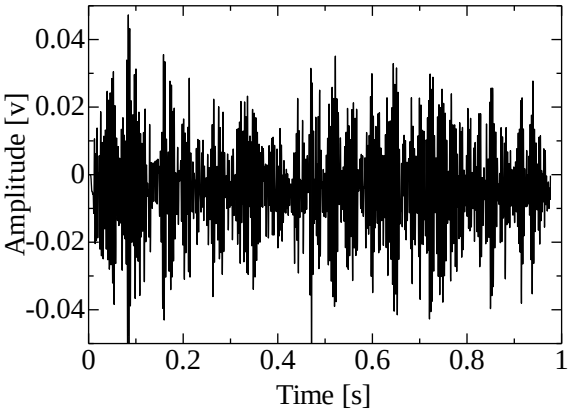

Fig. 17 The surface wear of spur gear before applying the MEAR model

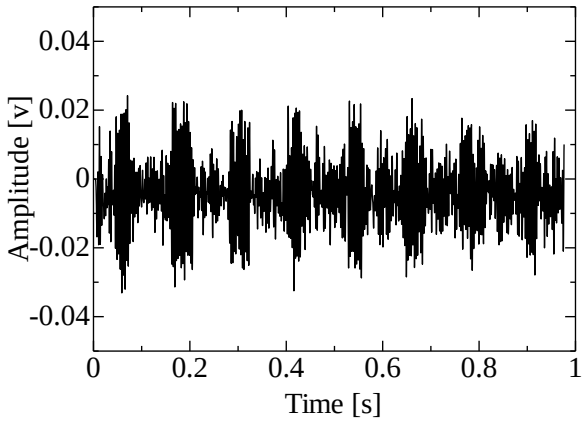

Fig. 18 The surface wear of spur gear residual component applying the MEAR model

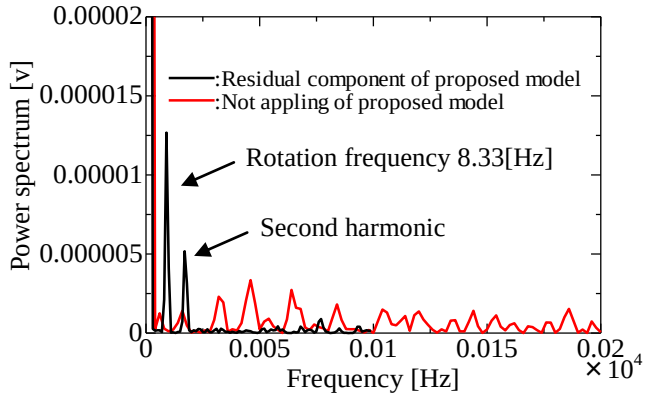

Fig. 19 The enveloped spectrum of Fig.17 and Fig.18

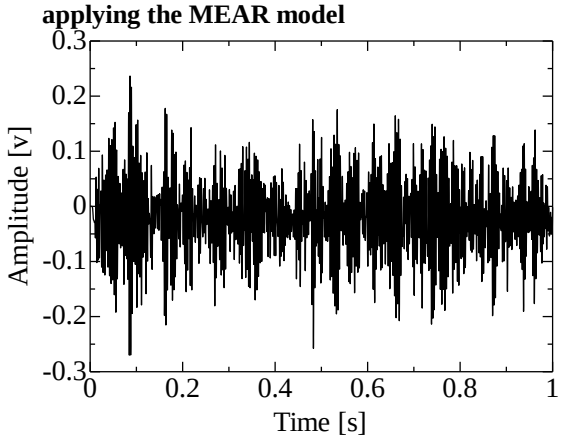

Fig. 20 The unbalanced spur gear before the MEAR model

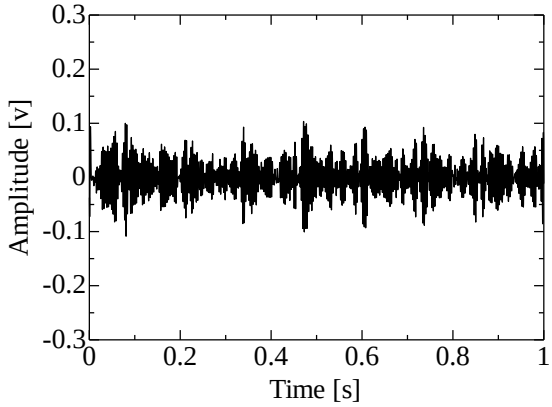

Fig. 21 The unbalanced spur gear residual component applying the MEAR model

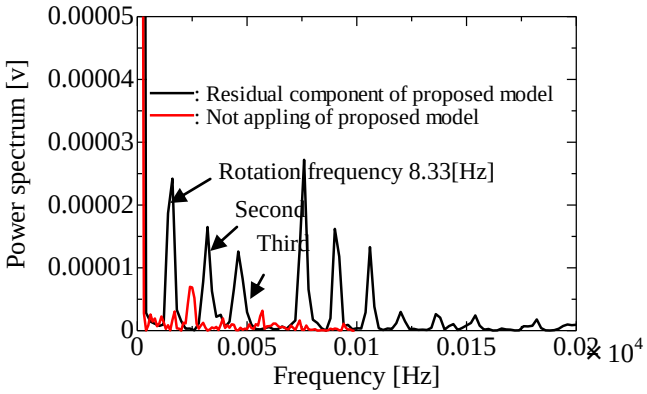

Fig. 22 The enveloped spectrum of Fig.20 and Fig.21

5. Conclusions

This paper proposes a new condition monitoring method on rotary machineries by fault vibration signals extraction and emphasis algorithm based on the proposed multiplex elements Auto Regressive model (MEAR model), which can be removed influence of vibration signal components generated by other machineries located close range except for condition monitored and diagnosed rotary machinery. We intend to have attempted to demonstrate the effectiveness of the proposal MEAR model and its extraction and emphasis algorithm using an experimental actual rotary machine which, is constructed by a rotor, spur gears and rolling element bearings and a 3phase induction motor, which are connected to a drive and two driven shafts. The experimental machine can

be artificially assumed three common faults such as an unbalanced rotor, a gear unbalance and surface wears of adjacent two teeth on a spur gear. Good results are obtained in these verifications, the high ability of the proposal condition monitoring method is effectively identified. High precision condition monitoring by the method can be carried out under the environment of close range location.

Acknowledgment

This work was supported by Japan Society for Promotion of Science (JSPS), Grant-in-Aid for Science Research (C) (No.20560752). Therefore, the authors wish to express our deep gratitude to all JSPS partners.

References

[1] *Handbook of Condition Diagnosis Technology*, *1st ed.*, Iron and Steel Institute of Japan, Maruzen Press, 1986, pp. 1-4.

[2] R. B. Randall. *Vibration-based Condition Monitoring: Industrial, Aerospace and Automotive Applications*, Wiley Press, 2011.

[3] L. Wang and R. Gao. *Condition Monitoring and Control for Intelligent Manufacturing*, Springer Press, pp. 109-136, 2005.

[4] Eric Walter and Luc Pronzato. *Identification of Parametric Models: From Experimental Data (Communications and Control Engineering)*, Springer London Press, 1997.

[5] R. S. Sanchez-pena, J. Q. Casin and V. P. Cayuela. *Identification and Control: The Gap Between Theory and Practice*, Springer, 2007.

[6] L. Wang and R. Gao. *Condition Monitoring and Control for Intelligent Manufacturing*, Springer Press, pp. 219-244, 2005.

[7] H. Ohta, S. Ezoe and K. Seto. Acoustic Diagnosis for Rotary Machinery Based on Liner Auto Regressive Model, *Proceedings of 8th International Congress on Sound and Vibration*, pp. 1699-1706, 2001, Hong Kong, China.

[8] R. Pintelon, G. Vandersteen, J. Schoukens and Y. Rolain. Improved (non-)parametric identification of dynamic system excited by periodic signals－The multivaariate case, *Mechanical Systems&Signal Processing*, Vol. 25, No. 8, pp. 2892-2922,2 011.

[9] H. Ohta and K. Seto. Acoustic Diagnosis on Rolling Bearing Based on Presumption of a Division Term by Locally Stationary AR model, *Transactions of the Japan Society of Mechanical Engineers*, Vol. 70, No. 691(C), pp. 56-62, 2004.

[10] H. Ohta, K. Seto and T. I. Khan. Acoustic Diagnosis Technique for a Failure Rolling Bearing by Adaptive Signal Processing Algorithm (Characteristics of Appling Adaptive Line Enhancer), *Eleventh International Congress on Sound and Vibration (ICSV11)*, pp. 949-955, 2004.

[11] N. Sawalhi and R. B. Randall. Vibration response of spalled rolling element bearings: Observations, simulations and signal processing techniques to track the spall size, *Mechanical Systems&Signal Processing*, Vol. 25, No. 3, pp. 846-870, 2011.

[12] H. Ohta, M. Tuda, Shin-ya Shimokawa and K.Maeda. A Diagosis Method of Torque Rich by Use of Vibration Acceleration and Hear Release Rate, *The 9th Western Pacific Acoustic Conference (WESPAC IX)*, pp. 352-358, 2006.

[13] H. Ohta, K. Seto and T. I. Khan. Dynamic Characteristic Analysis in the Abnormal Condition on Pistorn Crank Mechanism for Small Fishing Boat Engines, *Proceedings of JSME 12th Asia Pacific Vibration Conference (APVC2007)*, pp.1-7, 2007.

[14] H. Ohta, T. Aikawa and M. Tuda. Diagnosis of Abnormal Conditions on a Single Cylinder Reciprocal Engine by Generated Vibration and Acoustical Signals, *Engineering Asset Manegement*, Vol. 3, No. 1, pp. 1215-1221, 2008.

[15] R. B. Randall and Jerome Antoni. Rolling element bearing diagnostics—A tutorial, *Mechanical Systems&Signal Processing*, Vol. 25, No. 2, pp. 486-520, 2011.

[16] H. T. Pham and Bo-Suk Yang. Estimation and forecasting of machine health condition using ARMA/GARCH model, *Mechanical Systems&Signal Processing*, Vol. 24, No. 2, pp. 546-558, 2010.

[17] H. Ohta, T. Ailawa and M. Tuda. Diagnosis of Abnormal Condition on Twin Cylinder Reciprocal Engine by Vibrational Signal, *Proceedings of the 22nd International Congress Condition Monitoring and Diagnostic Engineering Management (COMADEM 2009)*, pp. 158-164, 2009.

[18] H. Ohta and T. Aikawa. Extraction Method of Failure Component on Vibration and Acoustic Signals Generated by a Reciprocal Engine Based on Cross Correlation of Close Two Point Signals and Characteristic of Paralleled Auto Regressive Model with Extra Input, *Proceedings of the 23nd International Congress Condition Monitoring and Diagnostic Engineering Management (COMADEM2010)*, pp. 333-340, 2010.

[19] T. Toyota. *How to Proceed Signal Processing for Condition Diagnosis*, Japan Institute of Plant Maintenance, 1996.

Copyright © 2012 DET Corp., Japan All Rights Reserved
International Journal of Comprehensive Engineering
Part A, 1(1), 32-37, 2012
Doi: 10.14270/IJCE2012.1.1.a32
Regular paper

ISSN 2186-2680
e-ISSN 2186-2656
www.iace-journal.org

Numerical and Experimental Research on Pitch Mechanism of Gun with Clearances

Bing Li [1,#], Hongrui Cao [1], Zhengjia He [1]

[1] State Key Lab. for Manufacturing Systems Engineering, Xi'an Jiaotong University, Xi'an, 710049, China

[#] Corresponding author: bli@mail.xjtu.edu.cn; Tel.: +86-29-82663689-602; Fax: +86-29-82663689-605

Abstract: The clearances in pitch mechanism of gun have an important influence on firing concentration. The present study designs a set-up of experimental research on pitch mechanism of gun with clearances and carries out corresponding numerical simulations and experiments. The clearance in slider-guide joint, a typical clearance in pitch mechanism of gun, is considered in the set-up. Sinusoidal excitation is used to get dynamical response signals of gun; results of the experiments show that the response signals in time domain reflect clearance size. In the same intensity under sinusoidal excitation, the peak value of gun barrel's time-domain signal is larger with the clearance enlargement. The current work can be referred as a basis for dynamical clearance adjustment and the gun design.

Keywords: Clearance, Gun, Dynamic, Firing Concentration.

Received: May 11,2012 / Accepted: Sept. 12,2012 / Published: Dec. 15,2012

1. Introduction

Since high-tech was applied in weapon system, guns have been the most frequently used type of weapons with the largest number in the world. The modern warfare puts forward higher requirements for gun performance. The clearances in pitch mechanism of gun have an important influence on firing concentration in the war [1]. There is an optimum interval of clearance. The fire concentration of gun is accurate inside the interval but inaccurate outside the interval. In practice, the fire concentration is weakened because of the clearance change as a result of powder explosion. So soldiers need adjust clearance dynamically to ensure firing concentration. In fact, it is hard to measure clearance dynamically and quickly. However, the response signal of gun can be easily obtained. Therefore, research on this clearance is of great significance for extracting clearance features from the dynamic response signal, determining the size of the clearance, adjusting the clearance and improving the firing concentration accordingly.

For the sake of secrecy, few documents have been published in this field. Some scholars have studied the clearance dynamic. In 2004, Tasora [2] et al. built a special experimental device for measuring the effect of clearance in revolute joints of a four-bar mechanism in terms of accelerations and surface wearing. In 2005, Barthels and Wauer [3] calculated modal parameters of rotating machinery with clearance based on the condition monitoring information. In 2006, Zhu and Parker [4] conducted a perturbation analysis of a clearance-type nonlinear system. In 2008, Khemili and Romdhane [5] studied the dynamic behavior of a planar flexible slider-crank mechanism with clearance and built an experimental set-up to perform some experiments. Shiau [6] et al. made a nonlinear dynamic analysis of a parallel mechanism in consideration of joint effects. In 2009, Ishida [7] et al. researched nonlinear resonances and self-excited oscillations of a rotor caused by radial clearance and collision. In 2010, Chen [8] took ANSYS simulation to compute the flexibility of clearance of gun barrel and found that clearance value was a function of the flexibility and stiffness of a small gap.

The present study designs a set-up of experimental research on pitch mechanism of gun with clearances and carrys out corresponding numerical simulations and experiments. The clearance in slider-guild joint, a typical

clearance in pitch mechanism of gun, is considered in the set-up. Sinusoidal excitation is used to get dynamical response signals of gun barrel. The experimental results indicate that the response signals in time domain reflect clearance size. In the same intensity under sinusoidal excitation, the peak value of gun barrel's time-domain signal is smaller with the clearance enlargement. The research results provided an important basis for dynamical clearance adjustment between slider plate of gun barrel and guide and the gun firing concentration.

2. Design of a Set-up of Pitch Mechanism with Clearance in Gun

Gun is a complex mechanical system including thousands of parts and assembles, among which pitch mechanism is its key one influencing firing concentration. In view of the expensiveness of firing experiment, a simple experimental set-up is demanded to study the dynamic characters of clearance. Fig. 1 is the experimental set-up we designed to test the dynamic behaviors of clearance.

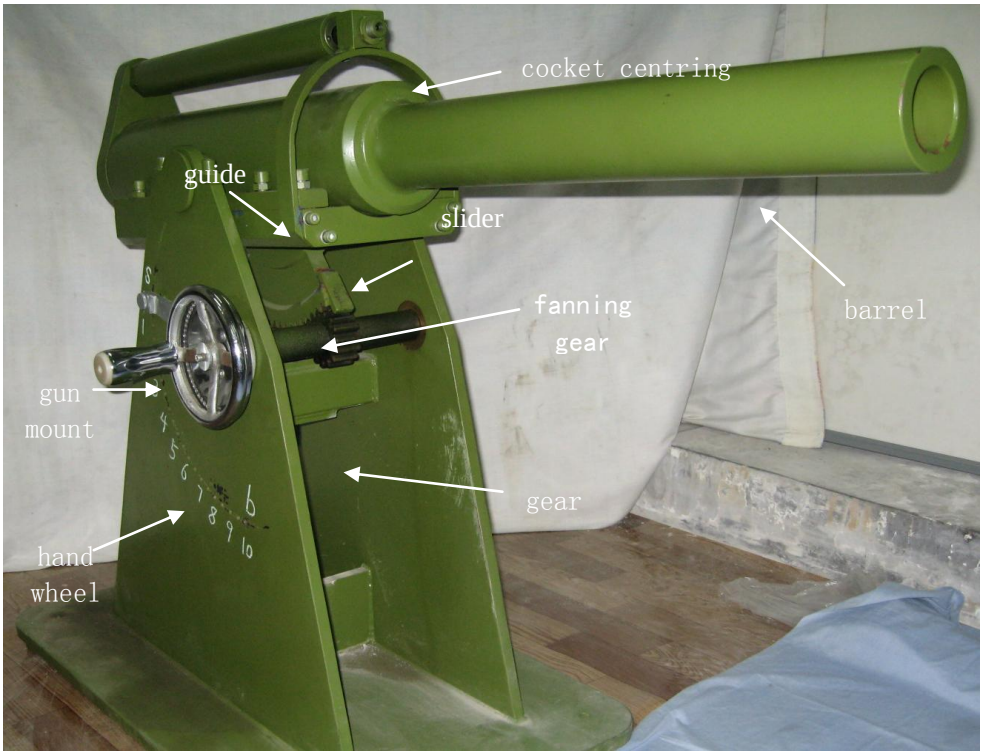

Fig. 1 A set-up of pitch mechanism with clearance in gun

The set-up includes eight elements: gun mount, hand wheel, gear, fanning gear, guide, slider, cocket centring and barrel. The pitch of barrel can be adjusted by the hand wheel. Before firing, the slider of barrel contacts with the guide rail. In the firing process, the slider departs with the guide due to the impact force. And then, the slider returns to the contact state. The contact-depart-contact procedure introduces the vibration of barrel. According to the structure of slider and guide, we designed the slider-guild mechanism with clearance (Fig. 2). The clearance is adjusted by the 8 M8 bolts with pitch of 0.5mm. We can tight the bolts to decrease the clearance of slider-guide (Fig. 3).

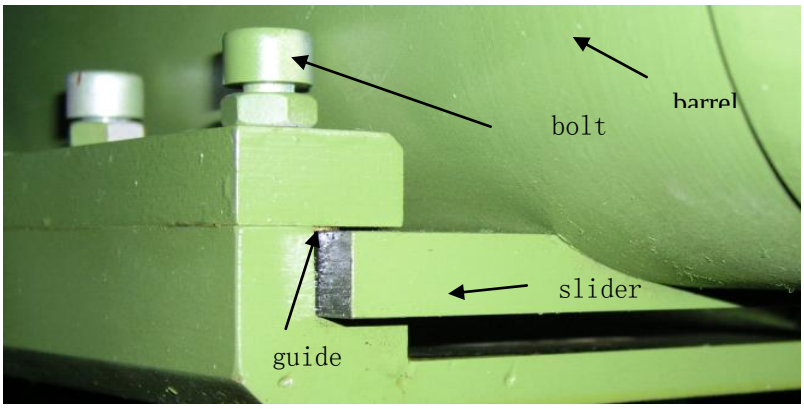

Fig. 2 The slider and guide rail mechanism with clearance

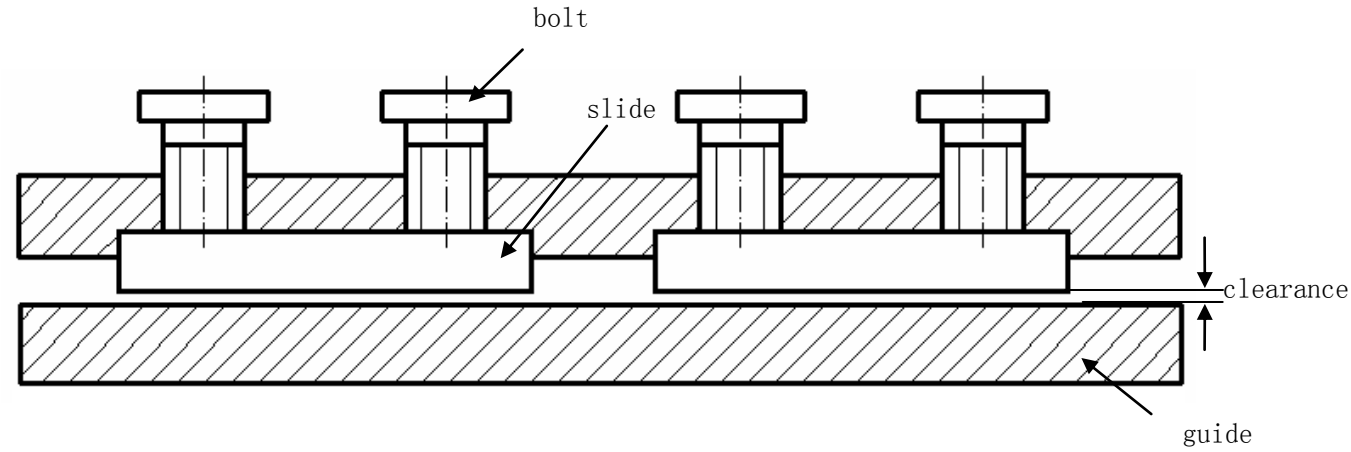

Fig. 3 The CAD draw of slider and guide rail mechanism

3. Numerical Simulation of Experimental Set-up

In order to study the dynamic behaviors, we modeled the experiment set-up of gun by the finite element method (FEM) software, ANSYS. Fig. 4 is the geometry model of the set-up in ANSYS environment. All elements including pitch mechanism are imported into ANSYS from CAD software PROE. In ANSYS, the contact relations are defined manually, the clearance of slider-guide can be adjusted by moving slider model.

The model are meshing firstly by using the tetrahedron element (solid185 of ANSYS). In total, 513090 elements were utilized to mesh the model. The part near the clearance of slider-guide is refined with small-size elements. The FEM model of set-up is given in Fig. 5.

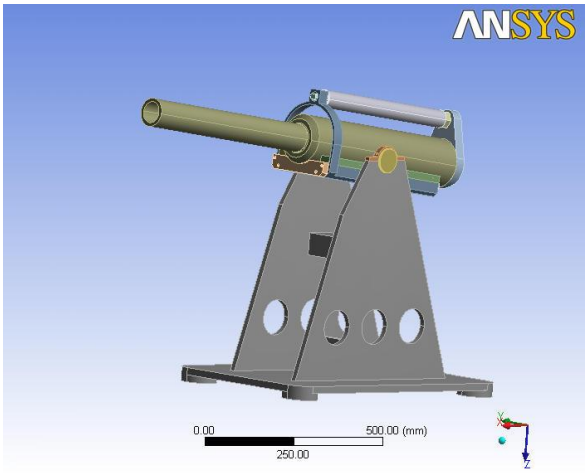

Fig. 4 The CAD model of experimental set-up of gun

Fig. 5 The FEM model of set-up in ANSYS environment

The model analysis and harmonic analysis of the set-up were carried out. The boundary conditions including material properties, and displacement constraints are used to construct the FEM model, which are listed as follows.

Material properties: structural steel with Young's modulus 2.1e11 Pa, Poisson rate 0.3 and density 7890 kg/m3.

Displacement constraints: The gun mount are fixed on the ground, degree of freedom (DOFs) of all the six displacement are zero.

The results of modal analysis are given in Fig. 6. From the results, we can find that the clearance of slider-guide mechanism influences the dynamic characters, especially the pitch modal of set-up. However, the FEM model cannot simulate the contact-depart-contact phases of clearance, the relations between clearance and dynamic characters of gun cannot be obtained by numerical simulation.

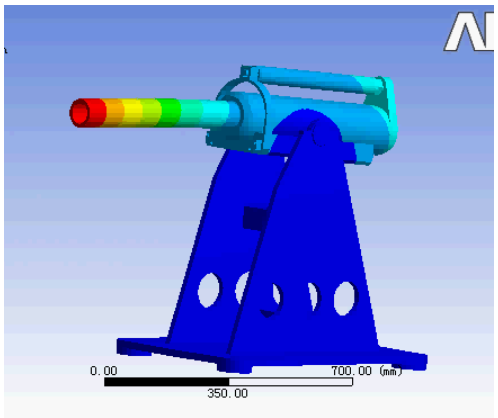

(a) Pitch modal of set-up with clearance 0.2mm

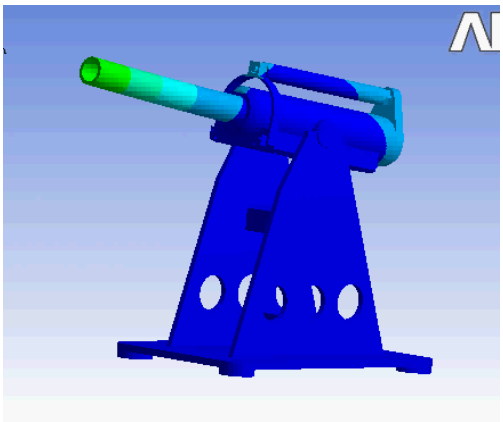

(b) Pitch modal of set-up with clearance 0.4mm

Fig. 6 The modal results of set-up

4. The Experimental Research on the Barrel Clearance

The experimental set-up is given in Fig. 7 (①: gun barrel, ②: acceleration transducer, ③: vibration exciter, ④: signal generator, ⑤: LMS signal picking box, ⑥: PC). The signal generator ④ provides the sinusoidal signal, which drives the vibration exciter ③. The gun barrel ① is vibrating when the exciter is operating with

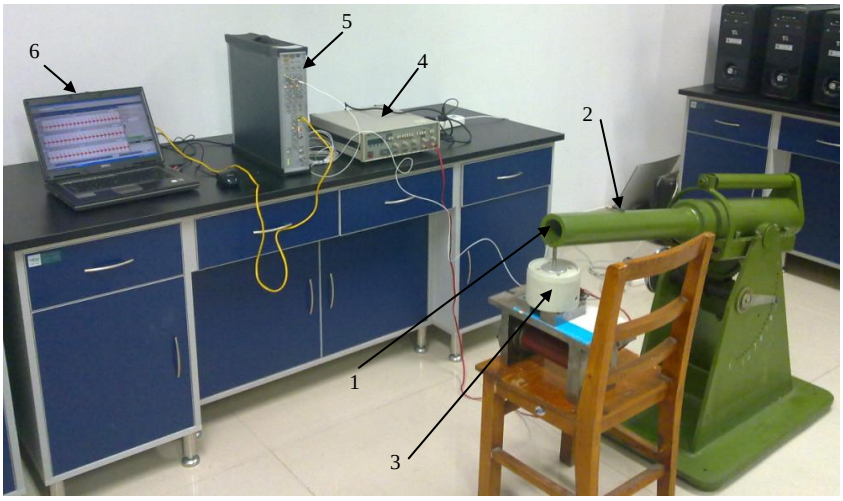

Fig. 7 The set-up of experiment

1: gun barrel; 2: acceleration transducer; 3: vibration exciter
4: signal generator; 5: LMS signal picking box; 6: PC

different input signals. The vibration response of the barrel is picked by the vibration acceleration transducer ②, and the vibration displacements of the cantilever beams can be obtained after the signal analysis. The signals are sent to the LMS signals picking box ⑤ and the PC ⑥. The vibration response can be showed with the time

signals wave figure in PC. The contact clearance can be adjusted by the different value of the bolt’ s tightening force and moment worked on the barrel and slider.

In the experiment, we change the bolt’s tightening force to decrease the clearance in the joint of slider-guild. The final time is marked with the clearance δ_1 = 0. The clearance value is corresponding to the round number of pitch and bolt. The signal generation’s output is sinusoidal signal with a frequency of 20 Hz. We max its output signal’s amplitude and keep it in order to optimize the response. The right measure data are recorded when the experimental system is steady. Fig. 8 shows the six groups of measure we do and the relations between the clearance and peak value .

Fig. 8 reveals that the signal character reflects clearance size. Peak values of the time signal increase when the clearances grow. The clearance of slider-guild increases, then the constraints working on the slider and guide rail decreases. So the vibration of the gun barrel increases, the time signal’s peak value picked also increase:

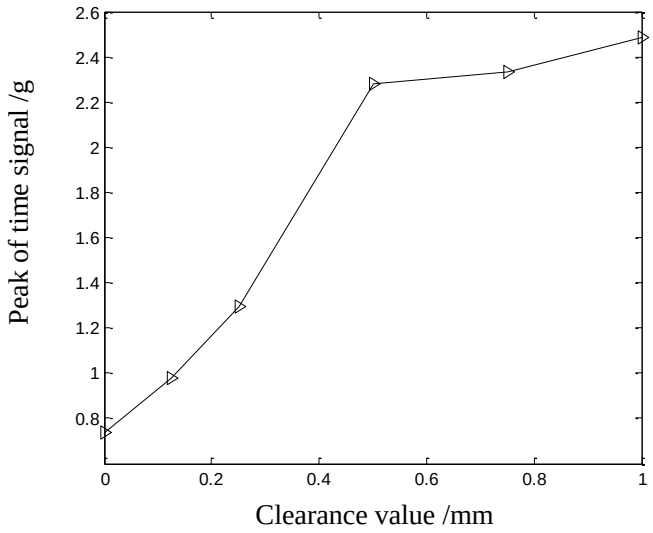

Fig. 8 The curve of clearance signal

5. Conclusions

In the present study we investigated the dynamic behavior of pitch mechanism of gun with clearance. The experimental set-up was designed and built with the clearance of slider-guild adjusted by the bolt. Sinusoidal excitation was used to get dynamical response signals of gun barrel; the results of the experiments are that the response signals in time domain reflect clearance size. In the same intensity under sinusoidal excitation, the peak value of gun barrel’s time-domain signal is larger with the clearance enlargement. The current work can be referred as a basis for the dynamical clearance adjustment in pitch mechanism and the gun design.

Acknowledgment

This work is supported by the National Natural Science Foundation of China (No. 11176024).

References

[1] S. L Wu and B Wen. *The Dynamic Experiment of Gun*,The Press of Defense Industry, China, 1999.

[2] A. Tasora, E. Prati and M. Silvestri. Experimental investigation of clearance effects in a revolute joint, *Proceedings of AIMTEA International Tribologie Conference*, pp. 871-882, 2004, Rome, Italy.

[3] P. Barthels and J. Wauer. Modeling and Dynamic Analysis of Telescopic Systems of Structural Members with Clearance, *Nonlinear Dynamics*, Vol. 42, pp. 371-382, 2005.

[4] F. R. Zhu and R. G. Parker. Perturbation analysis of a clearance-type nonlinear system, *Journal of Sound and Vibration*, Vol. 292, pp. 969-979, 2006.

[5] T. N. Shiau, Y.J. Tsaim and M. S. Tsai. Nonlinear dynamic analysis of a parallel mechanism with consideration of joint effects, *Mechanism and Machine Theory*, Vol. 43, pp. 491-505, 2008.

[6] I. Khemili and L. Romdhane. Dynamic analysis of a flexible slider-crank mechanism with clearance, *European Journal of Mechanics A/Solids*, Vol. 27, pp. 882-898, 2008.

[7] Y. Ishida, M. Inagaki and R. Ejima. Nolinear resonances and self-excited oscillations of a rotor caused by radial clearance and collision. *Nonlinear Dynamic*, Vol. 57, pp. 593-605, 2009.

[8] R.Y. Chen. Dynamic Modeling and Experimental Research on the Slide Plate of Gun Barrel and Guide with Clearances. Master thesis, Xi'an jiaotong University, Xi'an, China , 2010.

Copyright © 2012 DET Corp., Japan All Rights Reserved
International Journal of Comprehensive Engineering
Part A, 1(1), 38-43, 2012
Doi: 10.14270/IJCE2012.1.1.a38
Regular paper

ISSN 2186-2680
e-ISSN 2186-2656
www.iace-journal.org

Experimental Research on Vibration Control of High-rise Petrochemical Equipment with Lumped-mass Tuned Mass Damper

Wei Hao, Lidong He [#], Wanfu Han and Jian Chang

Diagnosis and Self-Recovery Engineering Research Center, Beijing University of Chemical Technology, Beijing, 100029, China

Corresponding author: 1963he@163.com; Tel.: +86-010-64443098; Fax: +86-010-64446043

Abstract: The wind-induced vibration of high-rise petrochemical equipment would do great harm to equipment operation and cause fatigue damage easily. Thus it is very necessary to install some control device to reduce the vibration actively. Therefore, the tuned mass damper (TMD), rarely used in high-rise petrochemical equipment, is studied by experiment to minimize wind-induced vibration, ensure safety operation and prolong service life. In the experiment, the high-rise petrochemical equipment is properly simplified in order to verify the feasibility of the TMD. Parameter matching of the TMD is mainly researched, which includes mass ratio and damping ratio. Experimental results show that the TMD is feasible for the wind-induced vibration control of high-rise petrochemical equipment. When parameters are not properly matched, the effect of vibration suppression is not the best. However, the top maximum displacement of the simulator reduces by 38.51% under optimal matching parameters in the experimental condition. The experimental research has provided certain valuable references for practical application of the TMD in petrochemical field.

Keywords: High-rise Petrochemical Equipment, Wind-induced Vibration Control, Tuned Mass Damper.

Received: May 16,2012 / Accepted: Sept. 12,2012 / Published: Dec. 15,2012

1. Introduction

In petrochemical enterprises, there are many kinds of high-rise petrochemical equipments, such as fractionating tower, distillation column, industrial smokestack, etc [1]. For these high-rise equipments, as shown in Fig.1a, the ratio of height to diameter is much larger, which leads to the greater flexibility and lower natural frequency [2]. Therefore, the intensive wind will have a greater effect on the vibration and deformation of high-rise petrochemical equipment. Thus it is very necessary to install some control device to reduce the vibration actively.

As a method of vibration suppression, the tuned mass damper (TMD) has many advantages, such as low cost, small mass and size, vibration control of each direction, easy installation and maintenance [3]. The TMD has also plenty of different kinds of structure styles, e.g., cistern type, ring-mass type, lumped-mass type [4]. In China, the TMD is widely applied to TV tower, skyscraper and bridge [5-8], but rarely used in high-rise petrochemical equipment. Therefore, it is well worth researching that how the TMD is effectively applied in petrochemical field. So it is studied by experiment in this paper.

In accordance with the structural features of actual high-rise petrochemical equipment, the authors plan to install the lumped-mass TMD on the top of the equipment, as shown in Fig.1b. When the TMD is working, generated inertial force will act on the equipment. It will lead to resonance when the frequency of TMD approaches the inherent frequency of the equipment. At that time, the TMD can absorb part of the energy to reduce the wind-induced vibration of high-rise equipment. However, when parameters of the TMD are not properly matched, the effect of vibration suppression is not the best and even counterproductive sometimes. In view of this, the wind-induced vibration is compared before and after the using of the TMD in order to study control effect of different parameters and seek for optimal matching parameters in this paper.

(a) (b)

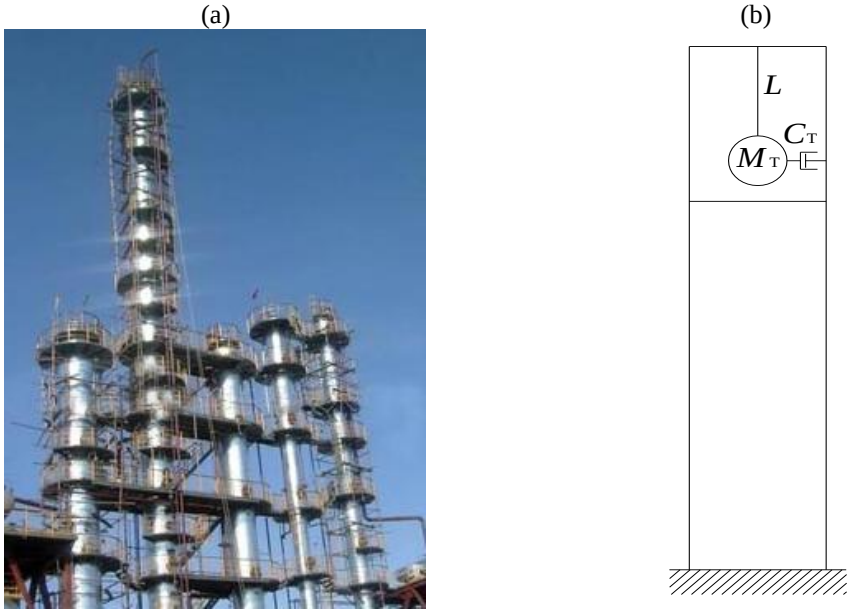

Fig. 1 High-rise petrochemical equipment. (a) Actual image. (b) Vibration control with TMD schematic.

2. Experimental system and TMD structure

Experimental system mainly consists of the simulator, fan, TMD, computer, eddy-current sensor and OR38 dynamic signal analyzer. They are shown in Fig.2.

The simulator includes windward baffles, additional mass and supporting tube. Among them, the windward baffle bears the fluctuating wind from fan and drives the supporting tube to swing, which simulates the wind-induced vibration of high-rise equipment. Besides, additional mass strengthens the swing of the simulator.

The sensors start to work in two perpendicular directions when the simulator swings. Collected signals are transmitted to OR38 analyzer and then displayed, recorded and processed by the computer.

In this experiment, the TMD system mainly consists of counterweight, iron wire and damping liquid (Fig.2f). The length, diameter and thickness of supporting tube are respectively 1020mm, 32mm and 2mm. The weight of the simulator is 43kg and its inherent frequency is 1.57 Hz by measuring. The frequency of the TMD is determined by $f=(g/l)^{1/2}/2\pi$. When the frequency f is 1.57 Hz, the length l is 101mm, which determines the length of iron wire. Ensure that the frequency of TMD is 1.57 Hz through adjustment.

(a) (b)

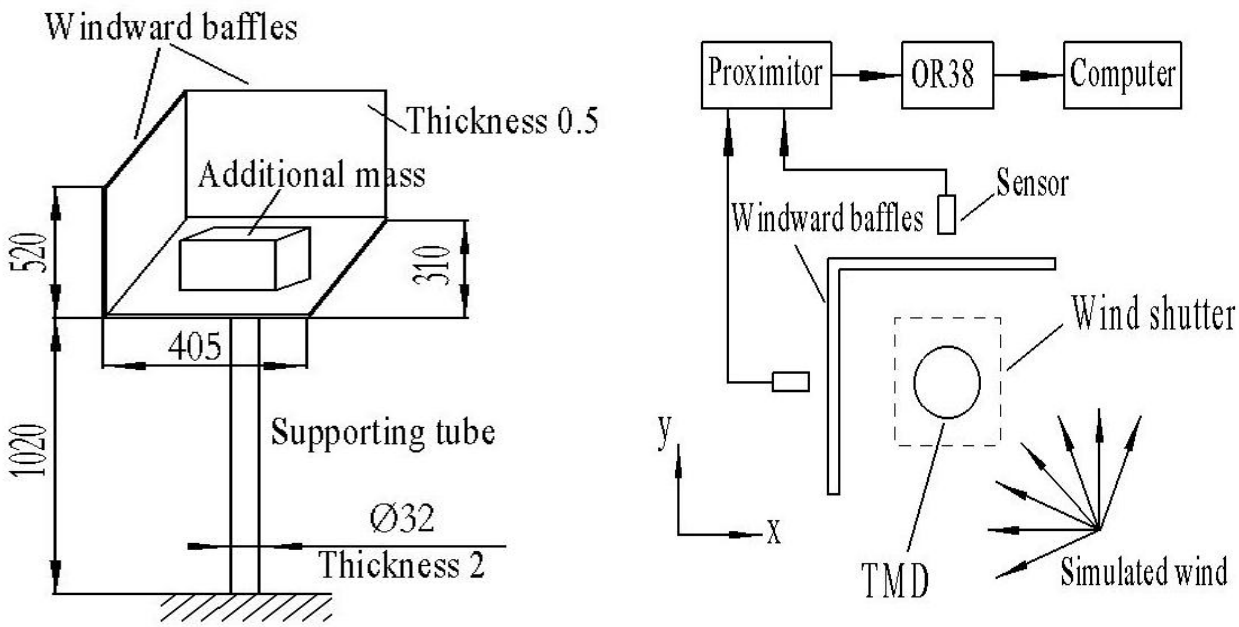

(c)

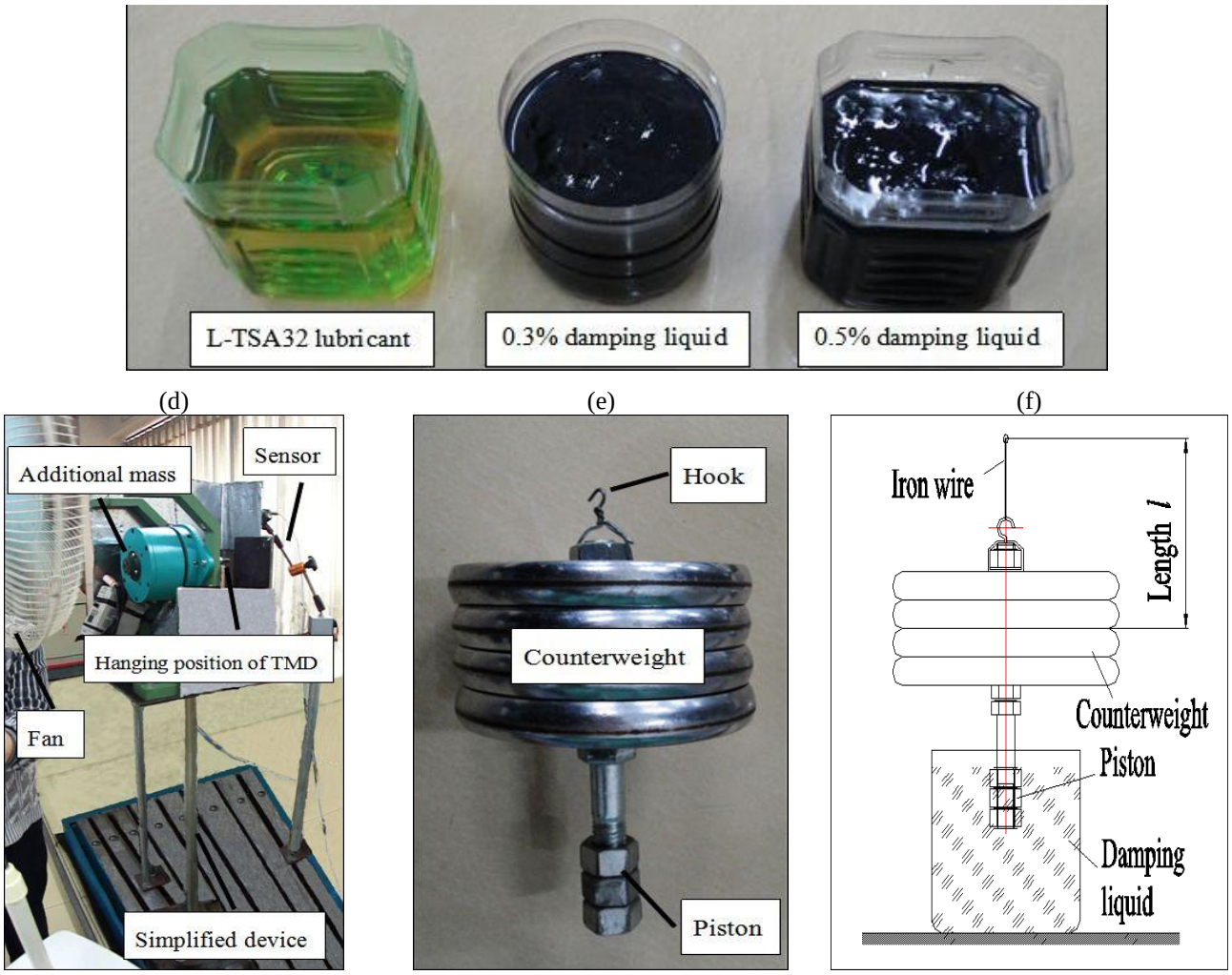

Fig. 2 Experimental system and schematics. (a) The simulator schematic. (b) Experimental system schematic. (c) Three kinds of damping liquids. (d) Experimental system photo. (e) Counterweight. (f) TMD schematic.

(2) The damping liquid is made up of pulverized carbon fibre sheet and L-TSA32 turbine lubricant with different mass ratios (0, 0.3% and 0.5%), which is shown in Fig.2c. Under the condition of certain mass ratio, the piston is immersed in different damping liquid to research the control effect.

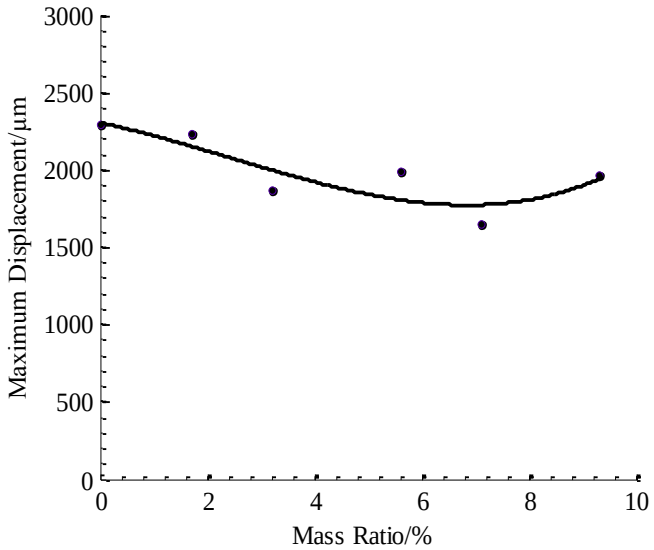

Fig. 3 The relationship between maximum displacement and mass ratios without damping.

In order to minimize errors, the above experiments will be repeated 5 times to get the average. And the vibrations in two directions will be synthesized to obtain the actual displacement.

3.1 The effect of different mass ratios without damping

It can be seen from Fig.3 that the maximum displacement has a certain degree of reduction under different mass ratios without damping. Under the condition of 7.1% mass ratio, the maximum displacement is minimum, which is 1650 μm, reducing by 28.04% relative to 2293 μm without TMD.

3.2 The effect of different mass ratios with damping

It can be seen from Fig.4 that the maximum displacement has a certain degree of reduction under different mass ratios when the piston is immersed in L-TSA32 turbine lubricant. Under the condition of 9.3% mass ratio, the maximum displacement is minimum, which is 1777 μm, reducing by 22.50%. Compared with the control effect in section 3.1, the result is not good. The reason may be that parameters are not properly matched.

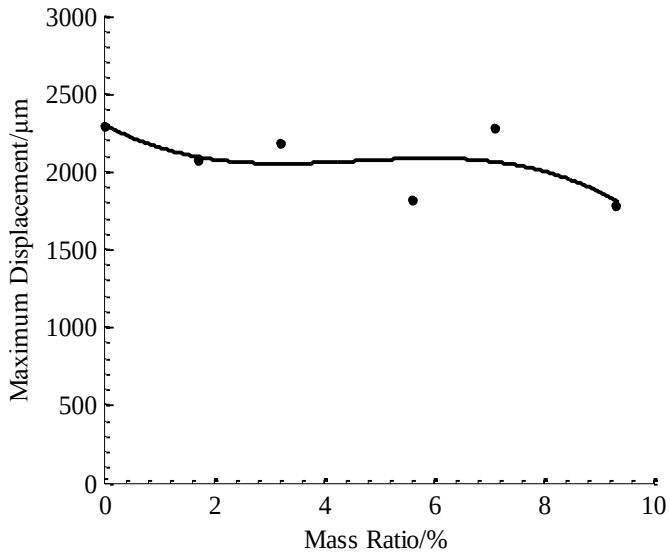

Fig. 4 The relationship between maximum displacement and mass ratios with damping.

3.3 The effect of different dampings under 3.2% mass ratio

It can be seen from Fig.5 that the maximum displacement has a certain degree of reduction under different working conditions with 3.2% mass ratio. Under the condition of 3.2% mass ratio and 0.3% damping liquid, the maximum displacement is minimum, which is 1710 μm, reducing by 25.43%. The control effect is better than section 3.2. However, parameters are still not properly matched when compared with the control effect in section 3.1.

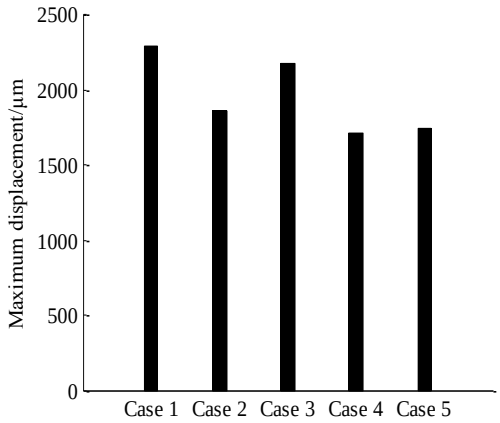

Case 1: no TMD; Case 2: 3.2% mass ratio; Case 3: 3.2% mass ratio and L-TSA32 lubricant;
Case 4: 3.2% mass ratio and 0.3% damping liquid; Case 5: 3.2% mass ratio and 0.5% damping liquid

Fig. 5 The maximum displacement under 3.2% mass ratio.

It can be seen from Fig.6 that the maximum displacement has a certain degree of reduction under different working conditions with 9.3% mass ratio. Under the condition of 9.3% mass ratio and 0.3% damping liquid, the maximum displacement is minimum, which is 1410 μm, reducing by 38.51%. Therefore, it can be known that optimal matching parameters have been found. Fig.7 compares the time-domain waveform under optimal matching parameters with the one without TMD.

3.4 The effect of different dampings under 9.3% mass ratio

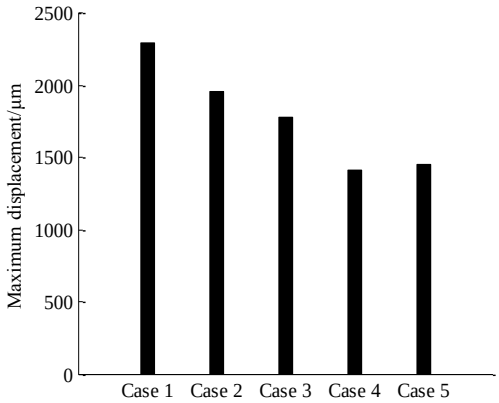

Case 1: no TMD; Case 2: 9.3% mass ratio; Case 3: 9.3% mass ratio and L-TSA32 lubricant;
Case 4: 9.3% mass ratio and 0.3% damping liquid; Case 5: 9.3% mass ratio and 0.5% damping liquid

Fig. 6 The maximum displacement under 9.3% mass ratio.

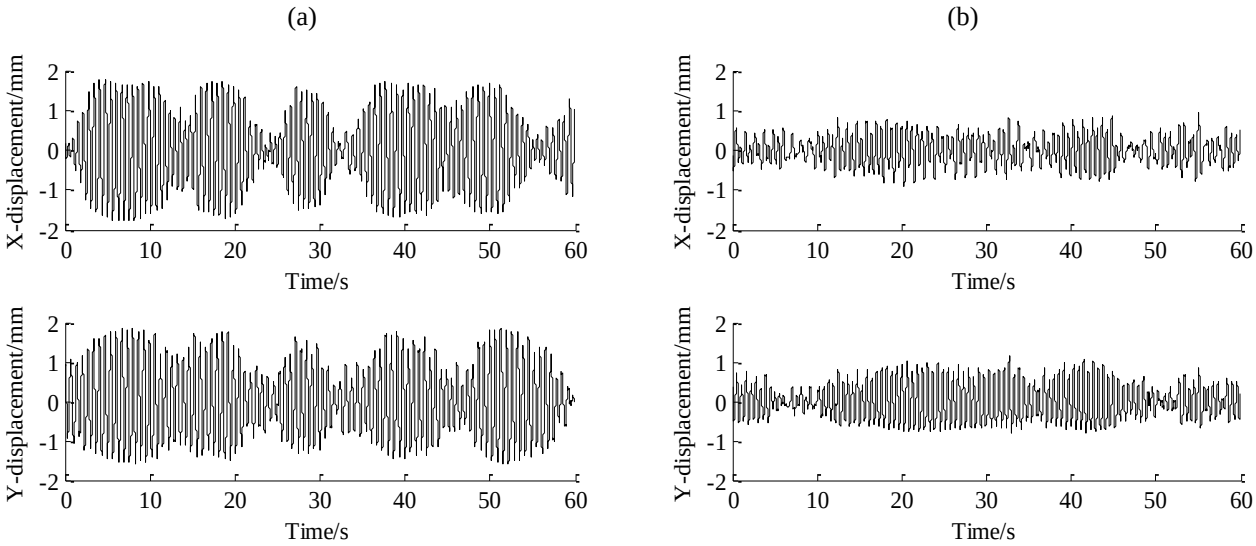

Fig. 7 Time-domain waveforms under different working conditions.
(a) No TMD. (b) 9.3% mass ratio and 0.3% damping liquid.

3.5 Results discussion

Table 1 summarizes the above experiment results. From that, some conclusions can be drawn:

(1) Mass ratio and damping ratio must be properly matched in order to get the best control effect.

(2)Under the condition of 9.3% mass ratio and 0.3% damping liquid, the maximum displacement is minimum, reducing by 38.51%, which demonstrates that there are optimal mass ratio and damping ratio for the TMD.

Table 1 Summarized Results

Mass Ratio（%）	Damping liquid（%）	Reduction（%）
7.1	——	28.04
9.3	0	22.50
3.2	0.3	25.43
9.3	0.3	38.51

3. Conclusions

In this work, the effectiveness of the TMD used for the vibration control of high-rise petrochemical equipment under intensive wind has been investigated. During the process of seeking for the optimal matching parameters, different mass ratios and damping ratios have been taken into account in order to understand the characteristics of the TMD under different working conditions.

When mass ratio and damping ratio are properly matched, the control effect is the best. Otherwise, the effect of vibration suppression is not the best and even counterproductive sometimes. Therefore, theory calculation or model test must be carried out to obtain the optimal matching parameters before the TMD is applied in petrochemical enterprises.

On the basis of the experimental data, the TMD is very feasible for the wind-induced vibration control. The experimental research has provided valuable preferences for practical application and laid good foundation for further optimization of the TMD.

Acknowledgment

The authors gratefully acknowledge the financial support provided by Joint Project Special Fund of Education Committee of Beijing, the Ph. D. Programs Foundation of Ministry of Education of China (Item No.: 20110010110009) and National Basic Research Program of China (973 program) (Item No.: 2012CB026000).

References

[1] H. H Gao and J. L Jiang. Tower Vibration and Kaman Vortex Solution, *Gansu Science and Technology*, Vol. 21, No. 6, pp. 35-36, 2005.

[2] S. Feng and J. Jin. Simulation of Fluctuating Wind Load on High Rise Tower and Analysis of Wind Induced Vibration Response, *Journal of Nantong University (Natural Science Edition)*, Vol. 6, No. 1, pp. 67-71, 2007.

[3] L. Qin, W. M Yan, X. J Hu, et al. Study on Seismic Control Effectiveness of TMD System of Symbolic Tower of Henan Art Center, *Journal of Beijing University of Technology*, Vol. 35, No. 6, pp. 761-768, 2009.

[4] Z. M Wang. *Vibration Control of High-rise Structures*, Tongji University Press, 1997.

[5] R. X Huang, A. Q Li, Z. Q Zhang, et al. TMD Vibration Control of Beijing Olympic Center Broadcast Tower under Fluctuating Wind Load, *Journal of Southeast University (Natural Science Edition)*, Vol. 39, No. 3, pp. 519-524, 2009.

[6] M. J He and R. L Ma. Measurements and Analysis of the Vibration of Heilongjiang Broadcast and TV Steel Tower Controlled by PendulousTank, *Journal of Building Structures*, Vol. 22, No. 1, pp. 39-41,2001.

[7] J. Ren, J. Teng and L. P Ye. Research on Vibration Control of Hybrid Mass Damper for Diwang Tower under Wind Loading, *Earthquake Engineering and Engineering Vibration*, Vol. 23, No. 6, pp. 187-193, 2003.

[8] M. Wang and P. Gu. Damping Suppression of Vibration for Half-through Steel Truss Bridges Using TMD, *Journal of Shijiazhuang Railway Institute*, Vol. 19, No. 1, pp. 14-17, 2006.

[9] X. J Hu and J. P Ge. Study on Wind-induced Vibration TMD Control of a High-rise Structure, *Shanxi Architecture*, Vol. 33, No. 32, pp. 81-82, 2007.

Copyright © 2012 DET Corp., Japan All Rights Reserved
International Journal of Comprehensive Engineering
Part A, 1(1), 44-50, 2012
Doi: 10.14270/IJCE2012.1.1.a44
Regular paper

ISSN 2186-2680
e-ISSN 2186-2656
www.iace-journal.org

A Selection Method of Vibration Signal Feature Based on Mutual Information and Distance Measurement

Hongfang Yuan [1], Changdui Zhu [1], Xi Cao [1], Huaqing Wang [2,#], Wenbin Liu [2] and Jianfeng Yang [2]

[1] School of Information Science and Technology, Beijing University of Chemical Technology, Beijing, 100029, China
[2] School of Mechanical and Electrical Engineering, Beijing University of Chemical Technology, Beijing, 100029, China

[#] Corresponding author: wanghq_buct@hotmail.com; Tel.: +86-10-64443037

Abstract: Feature selection is an important problem for fault diagnosis systems. This paper proposes a selection method of characteristic parameters based on mutual information theory and distance measurement between parameters. Its core goal is to search the parameter subset which has higher relevance between the selection and state class, the lower redundancy and the longer distance measurement between the parameters. The experiment compared the new algorithm with traditional methods by using Particle Swarm Optimization. The results prove that the new method leads to improvement on feature selection and classification accuracy.

Keywords: Vibration Signals, Mutual Information, Distance Measurement, Fault Diagnosis.

Received: Apr. 25,2012 / Accepted: Sept. 12,2012 / Published: Dec. 15,2012

1. Introduction

When the fatigue spalling, indentation and local corrosion occur on the working surface of a rotating machine, the cyclical pulse signal is released in this running process [1]. These signals are received by the acceleration sensor on bearing chock and analyzed to diagnose the faults. However, this diagnosis method is mostly applied under extreme and dangerous environments. So the application of wireless transmission can get rid of the environment restrictions and reduce the cost compared with the traditional Industrial Ethernet. Because the data quantity of vibration signals is quite huge, the wireless transmission speed is not high enough to transmit the original signals. Thus, the vibration signals are preprocessed, and then the characteristic parameters is calculated and transmitted to the upper computer for state analysis. There are many kinds of characteristic parameters of vibration signals, so selecting the characteristic parameters which are mostly effective for classification and recognition can improve the accuracy and real time of state recognition.

This paper proposes a selection method of characteristic parameters subset based on mutual information and distance measurement. Compared with the traditional method, it can increase the classification performance of characteristic parameters subset, overcome the disadvantages of traditional method and achieve the effective recognition to the running state.

2. The Selection Method Based on Distance Measurement

2.1 Distance Measurement

Distance measurement is a method used to select the characteristic parameters through distance. The longer the distance between the same characteristic parameters with different states is, the better the classification performance of characteristic parameters. The most common distance calculating methods include Euclidean distance, Minkowski distance, squared distance, and nonlinear measurement [2-4].

Currently, Minkowski distance is commonly used in calculating the difference of characteristics parameters of vibration signals. It is easy to be calculated and understood, but it only considers the difference between the same parameters in different fault state. Besides, it might be easily disturbed by the noises, so the characteristic parameters subset cannot reach the requirements of state recognition.

2.2 Procedures of Distance Measurement

To the characteristic parameters X, if using benchmark state as normal state, the value is $X_0 = (x_{01}, x_{02}, ..., x_{0n})$. Under the fault state, the characteristic parameter is $X_m = (x_{m1}, x_{m2}, ..., x_{mn})$, so it can be defined X_m and X_0's relative Minkowski (Minkowski) distance as follows:

$$d_{m0i} = |x_{mi} - x_{0i}| \tag{1}$$

The greater of the d_{m0} value is, the easier to distinct the fault classes by characteristic parameter. This paper chooses the ratio of difference X_m and X_0 to the length of X_0 as a reference.

$$S_{m0i} = \frac{|x_{mi} - x_{0i}|}{|x_{0i}|} \tag{2}$$

In order to prevent the over sensitivity of some characteristic parameters, the following rule has been proposed: if $S_{m0i} > 10$, then $S_{m0i} = 10$, keep $S_{m0i} = [0,10]$.

To rank the S_{m0i} in descending order and pick several top characteristic parameters as a subset, then this subset can be used in fault diagnosis.

3. The Selection Method Based on Mutual Information and Distance Measurement

3.1 Evaluation Standard

The mRMR (maximum Relevance Minimum Redundancy) is a characteristic parameters selection standard [5]. The core method is using the correlation between the characteristic parameter and the classification target, as well as the redundancy between the parameters.

Suppose there were two characteristic parameters, X and Y. Their probability are $p(x)$, $p(y)$, and the joint probability is $p(x, y)$, so the mutual information between X and Y is

$$I(x, y) = \sum_i \sum_j p(x_i, y_j) \log \frac{p(x_i, y_j)}{p(x_i) p(y_j)} \tag{3}$$

In fault diagnosis, the maximum relevance is that the correlation between characteristic parameter x_i and fault class C of the mutual information should be the maximum. The subset generally consists of the first m characteristic parameters which have maximum correlation with fault class [6].

Suppose D indicates the correlation between characteristic parameter subset S and fault class C, so the maximum relevance principle is

$$\max(D), D = \frac{1}{|S|} \sum_{X_i \in S} I(x_i, C) \tag{4}$$

$|S|$ indicates the number of parameters in subset S.

However, the subsets which only rely on maximum relevance principle may cause some redundancy problems [7]. If these two characteristics are close to the fault class C and the mutual information between the characteristic parameters is high, it means high redundancy. If one of them is removed, it will reduce computation cost and not affect the classification ability of subset.

Therefore, better classification characteristic parameters subset can be collected if both minimum redundancy and maximum relevance are considered. Make R indicate the subset S redundancy, and the minimum redundancy can be defined as follows:

$$\min(R), R = \frac{1}{|S|^2} \sum_{x_i, x_j \in S} I(x_i, x_j) \tag{5}$$

In addition to mRMR principle, this method also includes the distance measurement. Make M indicate the distance between the parameter and the reference state.

$$M = \frac{|x_i - x_{0i}|}{|x_{0i}|} \tag{6}$$

x_0 is average value of the parameter in reference state.

The selection method of characteristic parameters based on mutual information and distance measurement (MIDM) can be defined as the Eq. (7) by combining mRMR and distance measurement.

$$\max(\phi), \phi = D - R + \partial * M \tag{7}$$

3.2 Procedures of MIDM

At first, characteristic parameters of vibration signals are abstracted through characteristic parameter acquisition functions. Then each characteristic parameters threshold is set according to the training data. Assuming the each state probability is same. After comparing the characteristic parameters of each fault and threshold and getting the number which is greater than the threshold, $p(x_i)$ can be calculated [8-9].

Hypothesis: A is the number of quantity which is greater than the threshold in class C, B is the number of quantity which greater than the threshold but not included in class C , D the number of quantity which is less than the threshold in class C, N is the number of quantity of total samples. The mutual information of characteristic parameter x_i and class C as follows:

$$I(x_i, C) = \log \frac{p(x_i, C)}{p(x_i) * p(C)} \approx \log \frac{A * N}{(A + D) * (A + B)} \tag{8}$$

If characteristic parameter x_i and fault class C are independent to each other, then $I(x_i, C) = 0$.

According to the above formula, the $\max(I(x_i, C))$ can be inferred. In the same fault class, the mutual information can be defined as follows:

$$I(x_i, x_j) = H(x_i) + H(x_j) - H(x_i, x_j) \tag{9}$$

$H(x_i)$, $H(x_j)$ is Shannon entropy, $H(x_i, x_j)$ is the joint entropy.

$$H(x) = -\sum p(x) \log p(x) \tag{10}$$

$$H(x_i, x_j) = -\sum p(x_i, x_j) \log p(x_i, x_j) \tag{11}$$

It uses the greedy algorithm based on the mRMR and distance measurement, and then gets the characteristic parameters subset which meets the condition which is

$$\max_{x_i \in \{X - S_{t-1}\}} [I(x_i, C) - \frac{1}{t-1} \sum_{j=1}^{t-1} I(x_i, x_j) + \partial \frac{|x_i - x_{i0}|}{|x_{i0}|}] \tag{12}$$

∂ is an impact factor of distance measurement. Through several experiments, $\partial = 0.8$ can help get the better result.

The subset is satisfying the maximum mutual information of characteristic parameters and fault class, and the minimum mutual information of the characteristic parameters, as well as the maximum distance with reference state.

4. Experiments and Analysis

4.1 Experimental Data

This experiment used NTN 204 rolling bearing with rotating speed at 600r/min. The vibration signals included normal state, inner race fault and outer race fault. Sampling frequency was 100 kHz, and the length of each data was 10000. There are 200 samples from every state had been chosen and the first 100 of them were treated as training samples, the second 100 of them were used as testing samples.

The characteristic parameters universal set selected in this experiment includes Average amplitude, RMS, Mean square value, Skewness, ASL, Peak-to-peak value, Maximum, Minimum, Kurtosis, Energy, Variance, Absolute peak, Waveform index, Peak index, Impulse factor, Average frequency, Frequency centroid and Peak frequency[10-11].

4.2 The Result and Analysis of Distance Measurement

Fig.1 (a) shows the parameter sensitivity to inner race fault state by traditional distance measurement. The sensitivity of Skewness, Impulse factor, Kurtosis, Minimum and Absolute peak is higher than the others. Fig.1 (b) outlines the each characteristic parameter's sensitivity to outer race fault state. It is shown that Kurtosis is as high as 10, and Average frequency, Minimum, Skewness and Impulse factor are also relatively higher than the others. According to the conditions required in fault recognition and wireless transmission, the quantity of one subset is fixed on 6. So the selected characteristic parameters subset included Skewness, Kurtosis, Average frequency, Impulse factor, Absolute peak, Minimum.

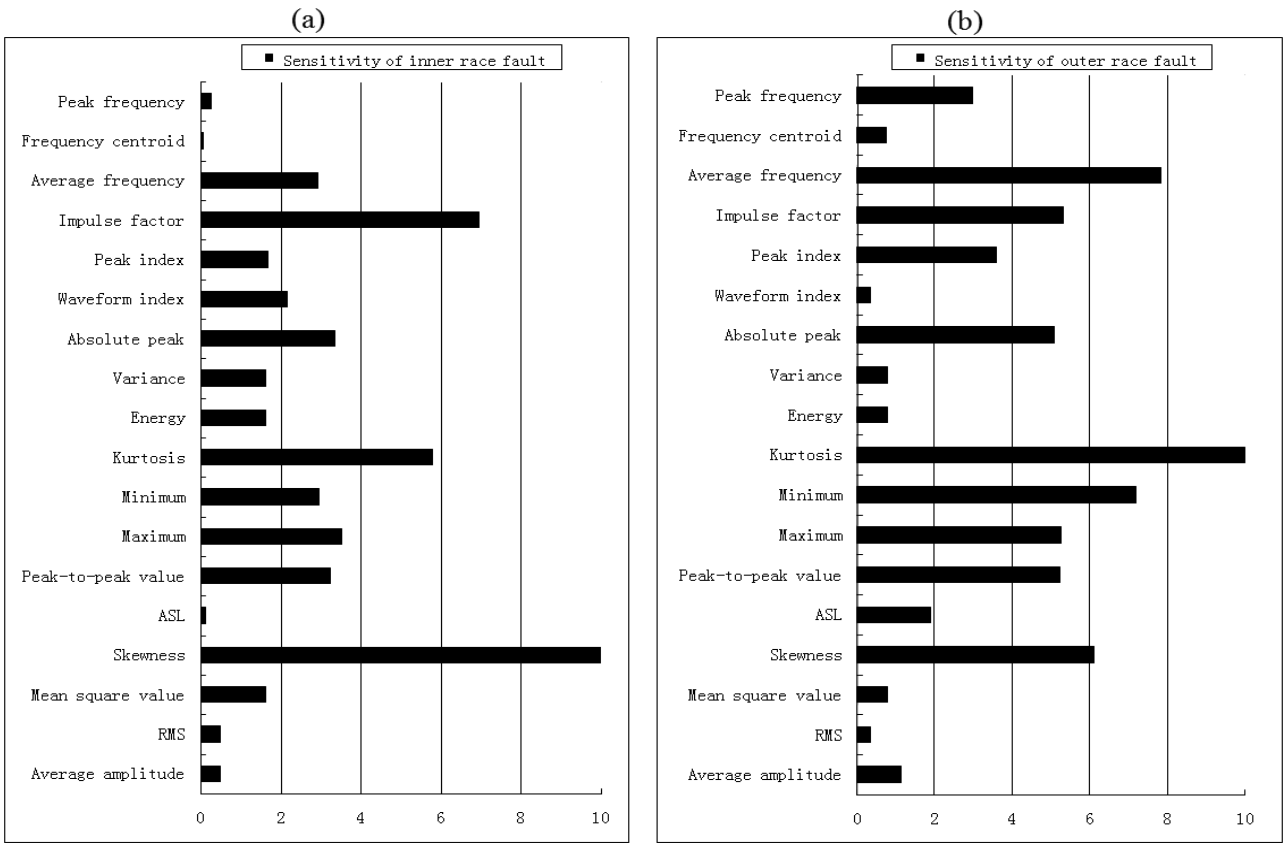

Fig. 1 Result of distance method .(a) Sensitivity of inner race fault. (b) Sensitivity of outer race fault.

4.3 The Result and Analysis of MIDM

Fig.2 is the value arrangement generalized according to the function of MIDM. Among these parameters, Peak frequency, Waveform index, Impulse factor are mostly relevant to the Normal state. Frequency centroid,

Average amplitude and Skewness are mostly relevant to the inner race fault state. Besides, Characteristic parameters, such as Waveform index, Impulse factor and Average frequency, have the best relevancy to the outer race fault state. According to the same conditions required in the fault recognition and wireless transmission, the selected characteristic parameters subset included Peak frequency, Waveform index, Frequency centroid, Impulse factor, Average amplitude, Skewness.

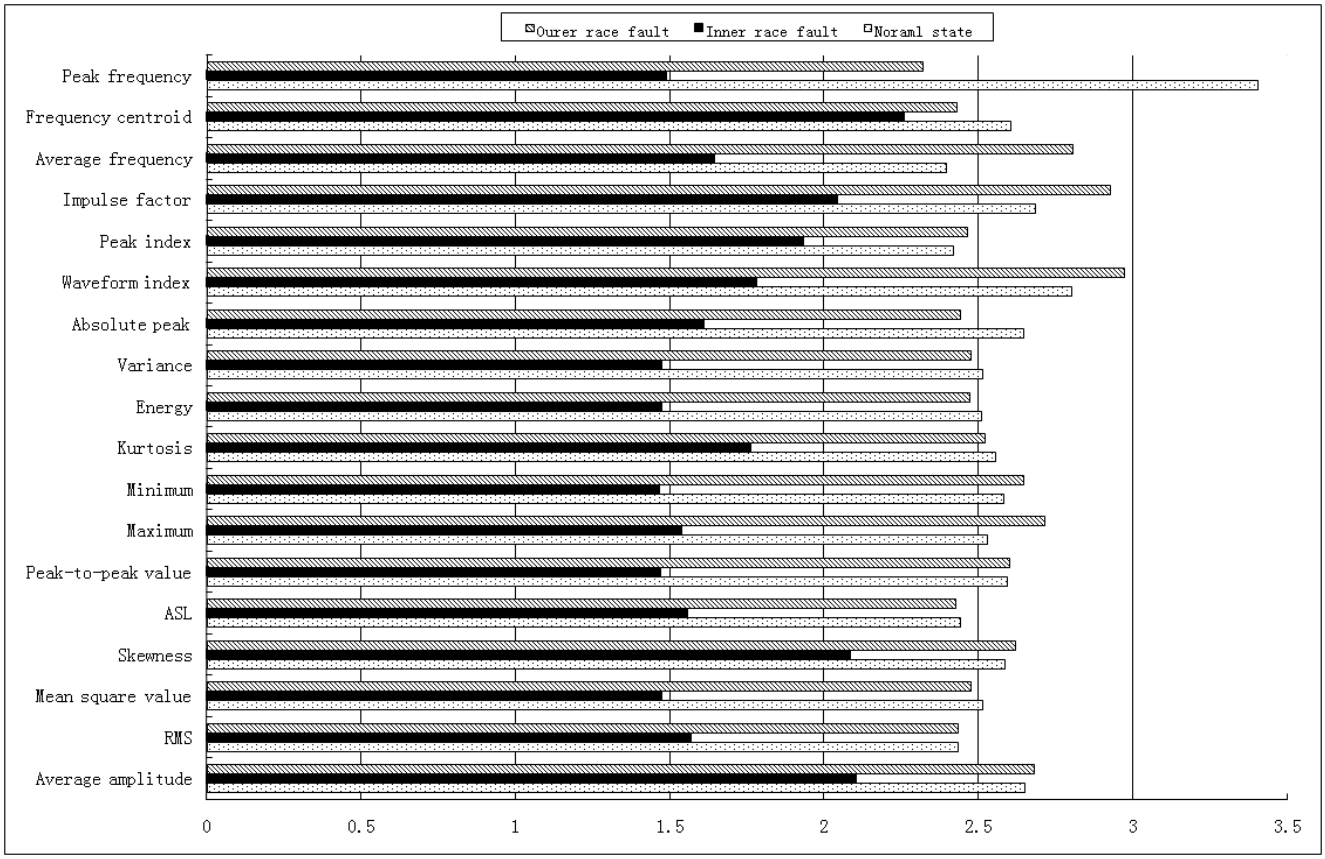

Fig. 2 The result based on MIDM

4.4 Diagnosis result analysis

Table 1 Contrast classification result of two methods

Fault class	Normal state	Inner race fault	Outer race fault
Subset based on distance	99%	85%	91%
Subset based on MIDM	99%	88%	96%

The cluster analysis of experiment data is conducted by Ant Colony Clustering [12-15]. Fig.4 and Fig.5 shows the clustering effect of the two methods and the classification result is represented in Table 1. As to the normal states, the performance of characteristic parameters subset based on both approach is quite similar, which reached to 99%. There is an obvious increase in the performance of MIDM on the recognition of outer race fault state compared with the distance measurement. Nevertheless, the recognition rate of characteristic parameters subset based on distance measurement is only 85% to the inner race fault state recognition. This rate can reach 88% based on MIDM, which is 3% higher than that based on distance measurement. So both methods' performance is unsatisfactory in recognizing the inner race fault because vibration signals of inner race fault is disturbed by the outer race.

5. Conclusion

Because the monitoring of vibration signals is generally operated in dangerous or remote areas, the use of wireless transmission technology can reduce the cost and improve the efficiency of detecting. The following

strengths of MIDM have been proposed in this paper compared with the traditional distance measurement. First, the relevance between the characteristic parameters and fault class has been involved in the analysis. This provides a better recognition to the different fault class. Secondly, the redundancy between the characteristic parameters has been considered, so the selected parameters can help to get rid of the redundancy parameter and collect characteristic parameters subset with high efficiency. What's more, the distance measurement is combined based on relevance and redundancy, so the cluster analysis could be conducted more easily through characteristic parameters subset. Therefore, MIDM could improve the efficiency and resolution, lower the bandwidth requirements. It also could reduce the necessary computing cost and increase the working efficiency of real-time wireless monitoring equipments.

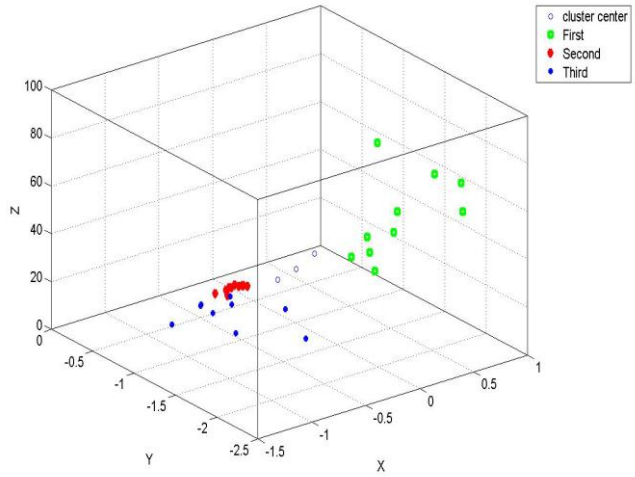

Fig. 4 The effect diagram of subset based on distance measure

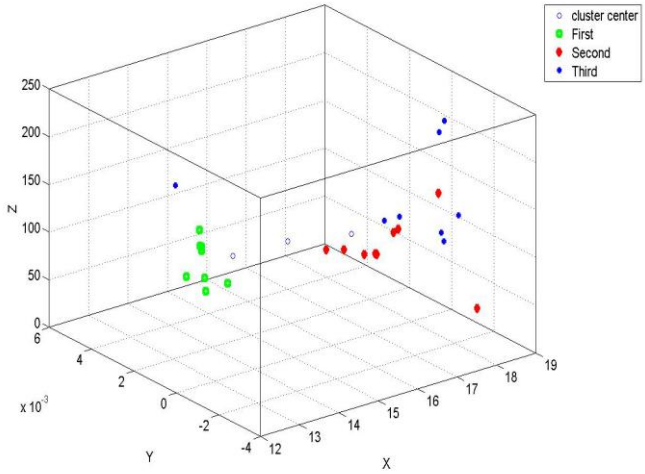

Fig. 5 The effect diagram of subset based on MIDM

Acknowledgment

This project is supported by National Program on Key Basic Research Project (Grant No. 2012CB026000), National Natural Science Foundation of China (Grant No.51075023, 51135001) and National Key Technologies R&D Program (Grant No. 2011BAK06B02), and Fundamental Research Funds for the Central Universities (Grant No. ZZ1124) and SRF for ROCS, SEM

References

[1] H. B Mei. *Rolling Bearing Vibration Detection and Diagnosis*, China Machine Press, 1995.

[2] Toussaint, G. T. On a Simple Minkowski Metric Classifier, *IEEE Transactions on Systems Science and Cybernetics*, vol. 6, No. 6, pp. 360-362, 1970.

[3] Pourhossein.K, Gharhpetian.G.B and Ranhimpour.E. Buckling Severity Diagnosis in Power Transformer Windings using Euclidean Distance Classifier, *Electrical Engineering Conference on*, pp. 1, IEEE xplore, May 17-19, 2011, Iranian.

[4] Yeary. M. B, Nemati. S, T. Y Yu, Y. D Wang and Y. Zhai. A Support Vector Machine Based Approach to RF Sensor Spectral Signature Classifications, *IEEE Transacions on Instrumentation and Measurement*, vol. 58, No. 1, pp. 221-228, 2008.

[5] H. C Peng, F. H Long and D. Chen. Feature Selection Based on Mutual Information Criteria of Max-dependency, Max-relevance, and Min-redundancy, *IEEE Transactions on Pattern Analysis and Machine Intelligence*, vol . 27, No. 8, pp. 1226-1238, 2005.

[6] K. Torkkola. Nonlinear Feature Transforms Using Maximum Mutual information, *International Joint Conference on Neural Networks*, pp. 2756-2761, IEEE xplore, July 15 - 19, 2001, Washington, DC, United states.

[7] B. Li, P. L Zhang, G. Q Ren, D. S Liu and S. Mi. Feature Selection for Rolling Bearing Fault Diagnosis Based on Muatual Information, *Journal of Test and Measurement Technology*, vol . 23, No. 2, pp. 183-188, 2009.

[8] L. Tang, J. G Duan, H. B Xu and L. Liang. Mutual Information Maximization Based Feature Selection Algorithm in Text Classification, *Computer Engineering and Applications*, vol. 44, No. 13, pp. 130-133, 2008.

[9] Nugraha. I, Ayuningtyas. C. H and Saptawati.G. A. P. Performance Analysis of Relief and Mrmr Algorithm Combination for Selecting Features in Iupus Genome-Wide Association Study, *Electrical Engineering and Informatics International Conference on*, pp. 1-5, IEEE xplore, July 17-19, 2011, Bandung, Indonesia.

[10] Y. Sha, X. H Yu and G. Y Zhang. A Feature Selection Algorithm Based on Boosting for Road Detection, *Fuzzy Systems and Knowledge Discovery International Conference on*, pp. 257-261, IEEE xplore, Oct 18-20, 2008, Beijing, China.

[11] J. B Chang, T. F Li and Q. Luo. Fault Dignosis of Rolling Bearing Based on Time Domain Parameters, *Control and Decision Conference*, pp. 2215-2218, IEEE xplore, May 26-28, 2010, Chongqing, China.

[12] Kalousis.A, Prados.J, and Hilario. M. Stability of Feature Selection Algorithms, *Data Mining International Conference on*, pp. 8, IEEE xplore, Nov 27-30, 2005, Switzerland.

[13] J. H Yan and D. B Zhao. Condition-Based Early Stage Diagnosis Robust Ant Colony Clustering Algorithm and Feature Mapping, *Industrial Engineering and Engineering Management International Conference on*, pp. 927-931, IEEE xplore, Oct 29-31, 2010, Harbin, China.

[14] J. H Liu and G. X Wang. A Hybrid Feature Selecion Method for Data Sets of Thousands of Variables, *Advanced Computer Control International Conference on*, pp. 288-291, IEEE xplore, March 27-29, 2010, Shenyang, China.

[15] S. Y Yang. *Pattern Recognition and Intelligent Computation*, Publishing House of Electronics Industry.

Copyright © 2012 DET Corp., Japan All Rights Reserved
International Journal of Comprehensive Engineering
Part B, 1(1), 51-59, 2012
Doi: 10.14270/IJCE2012.1.1.b51
Regular paper

ISSN 2186-2680
e-ISSN 2186-2656
www.iace-journal.org

The Research of Intelligent Diagnosis Expert System on Pumps Group

Bo Ma [1, #], Kun Feng [1] and Yujie Xi [2]

[1] Diagnosis and Self-Recovery Engineering Research Center, Beijing University of Chemical Technology, Beijing, 100029, China
[2] China Paper Machinery Corporations, Beijing, 100025, China

[#] Corresponding author: mabo@mail.buct.edu.cn; Tel.: +86-10-64439699; Fax: +86-10-64446043

Abstract: The pumps group dispersed in the oil refining enterprises is commonly monitored by off-line patrol management system, by which inspection and data analysis are limited. Automatic diagnosis for pump faults cannot be performed, and maintenance of pumps cannot be relied on in this system. Therefore, a task-based intelligent diagnosis expert system is proposed to solve this problem. The diagnostic reasoning of the system is implemented by formulating a general rule based on the failure mechanism of the pump, and establishing customized special diagnosis rules for different pumps on the basis of general rules. Different tasks can be selected to diagnose faults according to different types of centrifugal pump. According to this design strategy, an intelligent diagnosis expert system for the pumps group is developed and used in the refining enterprises. Practical examples of diagnosis for the pumps group are given to verify the effectiveness of the approach proposed in this paper.

Key Words: Pumps Group, Fault Diagnosis, Expert System, Off-line Patrol.

Received: May 20,2012 / Accepted: Sept. 12,2012 / Published: Dec. 15,2012

1. Introduction

There are a large number of pumps being used as power source for fluid delivery in the process industries such as oil refining, chemical, metallurgy and power, while the running condition of them would directly affect the production and safety of the enterprises [1]. In recent years, major accidents occurred in the refining factories because of the pump faults which lead to the leakage of flammable liquid and cause explosions. It is important for preventing the machine accidents and ensuring the safety and efficient operations to enhance the maintenance and management of the pumps.

Currently, main condition monitoring and fault diagnosis for the pumps group dispersed in the process enterprises uses the portable inspecting instruments to collect signals of the pumps regularly, such as vibration and temperature. The collected data will be uploaded to off-line patrol management system on a computer. By determining whether the vibration or temperature exceeds the alarm limits or not, whether the pump is down or not can be known. The technology of portable inspecting and off-line patrol management system has been developed well. Although the functions such as various signal acquisition and advanced analysis have been included by the inspecting instruments generally, expert diagnostic capabilities are still commonly absent. In a nutshell, these systems are better for detection but weaker for diagnosis. The differences between different pumps or fans in the enterprises make it difficult to determine the machine's fault accurately only by vibration and temperature. It is especially hard to decide whether the failure is serious enough for shutting down and repair. It requires that the person who is in charge of the machine must have enough knowledge of fault diagnosis. Trend analysis, spectrum analysis, envelop analysis, etc must be mastered by the person. As a result, the usability of the portable inspecting instruments is limited severely .Furthermore, in the oil refining and chemical enterprises, there are hundreds pumps, some even have thousands. Therefore, the basic fault diagnosis research and expert system is necessary to help the enterprises solve the machine management problem.

Currently, the study on the fault diagnosis of pumps group mainly focuses on three areas: (1) the specific mechanism of the pump fault and the methods for extracting the fault feature; (2) the fault classification methods,

such as based on neural networks, support vector machines, rough set, and so on; (3) model-based fault diagnosis of pumps and so on. Literature [2] analyzed the mechanism of rolling bearing failure, while the literature [3, 4] researched the feature extraction of the signals about rolling bearings through enveloping demodulation and wavelet respectively, and the literature [5] studied the classification about the bearing fault feature with the neural network method. Extract fault feature for gearbox with Empirical Mode Decomposition and Hibert spectrum method in literature [6], while using Discrete Wavelet transformation technique method to extract fault feature and via fuzzy inference to identify the fault in literature [7]. Literature [8] developed study on the corresponding relationship between the failure cause of the shaft of the rotating machine and the dominant frequency in the spectrum analysis of the vibration signal and proposed a reason concept of the vibration fault, which correct the traditional fault cause and classification method for characteristic frequency. Literature [9] used the current spectrum analysis of motor to determine and predict pump's fault. Literature [10, 11] studied on the acoustic emission technique in diagnosing these pump faults, such as cavitation and bearing wear. Literature [12] used support vector machine to classify these faults, including blade damaged, shaft cracks, bearing fault. Literature [13] studied the classification and diagnosis of the fault feature with the fuzzy decision tree and rough set methods. Literature [14, 15] studied estimation on the fault signals of the centrifugal with the nonlinear modeling technology, which achieved the fault detection of the centrifugal. To sum up the above literatures, it is visible that the research on pump intelligent diagnosis expert system and diagnosis logic is still lacking.

In order to improve the security management of the pumps group in the enterprises, the intelligent diagnosis expert system based on the information such as vibration, temperature, visual inspection, and the diagnostic reason will be presented in this paper. Through analyzing the management feature and fault mechanism and feature extraction method of the pumps group in the refining enterprises, the expert system is developed and integrated into the off-line patrol management system for the pumps group. The system not only can diagnose the pump's fault but also can assess the seriousness of the fault, so that it can propose the recommendations about pump operation and maintenance for the machine personnel.

2. The diagnostic object and design of the intelligent expert system

2.1 The diagnostic object of the expert system

The diagnosis object of the intelligent expert system is the pumps group in the process industry, according to the management model and diagnosis feature of the pumps group in the process industry. The system adopts the automatic diagnosis, semi-automatic diagnosis and human-computer interaction diagnosis, and can be integrated with the off-line patrol system flexibly.

2.2 Expert system design

The working principle of the machine in the pumps group is almost the same, while there are differences among different pumps in structure. In order to improve the diagnostic accuracy, practicality and ease of maintenance, on the basis of a set of foundation rules library, the diagnostic rule logic of the expert system customizes rules respectively according to the structural differences of the pumps. In order to meet the demand, expert system adopted MAS-CommonKADS methodology [16] and put forward Task-based Expert System framework on the basis of traditional product-based reasoning framework, which optimized the expression of rules and facts. The system frame graph is shown in Fig.1, where the expert system kernel and operating principle processing diagram is in the dotted box. As shown in Fig.1, the intelligent diagnosis expert system has two ways it can be used: one is independent use that users can select different tasks to do fault diagnosis and set fact value through the man-machine interaction; the other is the use that integrated into the off-line patrol management system. The system can automatically obtain the fact value from the off-line patrol management system.

The feature of the TBES architecture calls different diagnosis rule logic according to different structure types of machine and improving the diagnostic accuracy. The types of the machine structure can be classified according to different factors, such as supporting pattern, whether there is a gearbox or not, bearing type, pump series and so on.

The rule representation adopts a general rule structure (GRS) rather than production rules. Under the thought that variable precision logic for GRS, the using rules can be dynamically adjusted according to the task and facts' value in the reasoning process, which support both forward and backward reasoning technique[17]. Here a fact is expressed as a triple structure of "object-attribute-value"[18], for example, for the fact 'dominant frequency', the property is 'frequency', and the value includes '1X、2 X、3 X frequency'.

2.3 Integrated design of expert system and off-line patrol management system

As shown in Fig.1, expert system and off-line patrol management system are integrated with each other through the knowledge interaction interface of the expert system. Calling the knowledge interaction interface of the expert system, setting the characteristic parameters, and calling rule reasoning are all executed in the off-line patrol management system to achieve the fault diagnosis. The knowledge interaction forms of the integrated system include automatic and semi-automatic.

Automatic knowledge interaction of the expert system is an interaction mode that does expert diagnosis after integrating the expert system into the off-line patrol management system. Without interaction with the operators in the reasoning process, so we can automatically obtain the facts and calling the characteristic indexes of the inspection data after being processed.

Semi-automatic knowledge interaction mode is also integrated into the off-line patrol management system like the automatic mode, and the value data that can be obtained automatically is assigned by the condition monitoring system; but the difference is that the operator can assign the value through the dialog box popped up automatically when meeting the knowledge which can't be obtained by the off-line system. The reasoning of the semi-automatic acquisition mode can improve the accuracy of the expert diagnosis because that some facts could not be obtained in the off-line patrol management system, such as vibration noise, oil spills and other on-site visual inspection data.

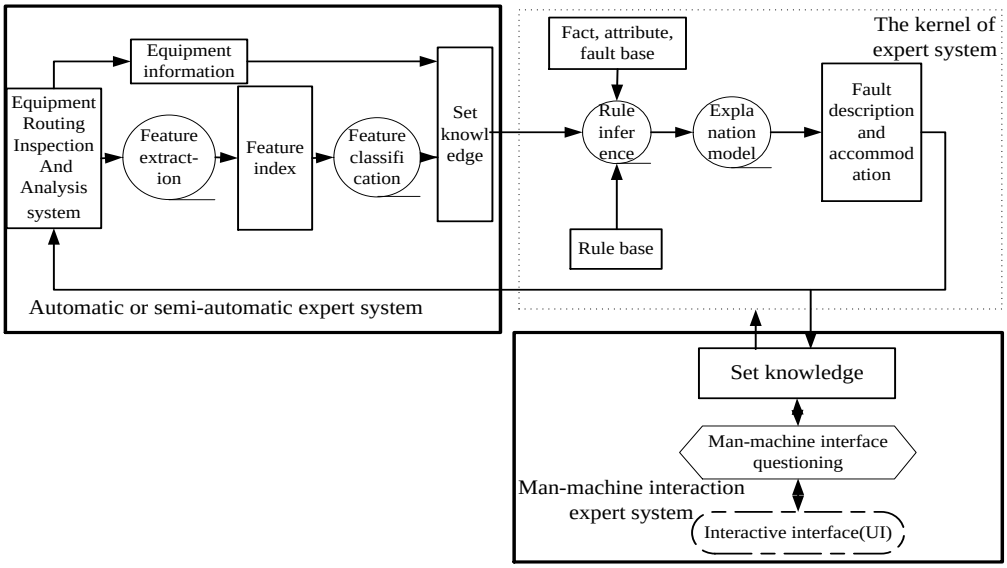

Fig. 1 Schematic overview of task-based expert system (TBES)

3. Design and implementation of the intelligent diagnosis logic

According to the structure composition of the pump, fault mechanism, the relation between fault cause and fault symptom, and taking advantage of the characteristic information, such as vibration, temperature, lubricating oil, noise and so on, which is detected in the inspection process, multiple diagnosis logical rules can be constructed.

3.1 Diagnosis logic design principles

In order to improve the performance of the expert system, such as accuracy, practicability, maintainability, the diagnosis logic design principle of the pump fault is proposed as the following four aspects:

(1)Formulate the main frame based on the pump structure and the differences between the components, and segment different faults

The structure principle of the rotating pumps in the enterprises is same, but the structure between the pump has differences because of the requirements of technology and production. For example, not only the sleeve bearing, but also the rolling bearing is used in the pumps. Both the diagnostic commonality and differences are considered in the diagnosis logic based on pump structure and components. For example, some pumps use the gearbox while other pumps do not. Some units use rolling bearings but others use the sleeve bearings. In addition, several faults can only occur at specific circumstances. Therefore, the groups structure and components not only can be regarded as the primary condition for diagnosis logic, but also can be used as the basis for distinction between the various faults.

(2)Formulating diagnosis logic based on fault mechanism

According to the differences of the failure mechanism and the failure symptom between different components of the pump, the diagnosis logic can be divided into three parts: rotor faults based on velocity-power spectrum, gear faults based on acceleration-power spectrum and envelop spectrum, and rolling bearing faults based on acceleration-envelop spectrum. The diagnostic logic of the three parts covered a series of pumps group faults. Therefore, using the principles of classifying the fault feature designed the diagnostic logic in determining structure of the pumps group.

(3) Improving the diagnostic efficiency and accuracy with the principle of coarse and fine combination

While the fault characteristic of the pump is diversity, the distinction feature between fault categories is more obvious. In order to improve the efficiency of the diagnostic reasoning logic and the accuracy of the diagnostic result, fault diagnosis is performed firstly by a rough distinction, then by an exact diagnosis in the reasoning process. Fault diagnosis is divided into preliminary diagnosis and precise diagnosis [19]. The preliminary diagnosis can exclude parts of faults according to several characteristic values, so that the fault position can be localized. Precise diagnosis is further performed to ensure fault position, fault type, fault severity and so on by according to the fault symptoms after completing the preliminary diagnosis.

(4) Assessing the deterioration degree of the fault with the diagnostic principle of multi information fusion

The enterprises users not only concern the fault location and fault type, but also the severity of the fault, which is whether the pump can continue to run or should be shut down for maintenance. Most of the fault diagnosis is based on the single point vibration analysis. However, multiple parts of the pump would be abnormal when the pump breaks down, especially in the later period of the failure. Therefore, in order to assess the deterioration degree to improve the availability of diagnostic result, this paper adopts the diagnostic logic of multiple points and different parameters and the method of multiple points authenticated with each other. For example, for the imbalance fault diagnosis of the pump rotor, we can verify whether the rotor is imbalanced or not according to whether the dominant frequency of the vibration signal spectrum between the two supporting position of the rotor is 1X frequency or not. With the deterioration degree of the bearing fault, comprehensive evaluation with the combination information that combined the viscosity of the lubrication oil and the impurity of other particle can be done.

3.2 The implementation of diagnostic reasoning logic

When designing the intelligent diagnosis expert system, the faults that can be diagnosed are as following:

(1) Rotor faults: mass unbalance of rotor, shaft crack, shaft bending, blade wear, and fluid vibration, etc.

(2) Supporting system fault: foundation loosen, bearing base loosen, sleeve bearing injury, oil film whirl, and oil film oscillation.

(3) Shaft fault: misalignment, coupling wear, etc.

(4) Impact fault: gear fault, rolling bearing fault, etc.

Diagnostic reasoning logic formulates the main frame based on the structure of the pump, as shown in Fig. 2. The main frame is designed on the first principle of the diagnostic logical design principles. The main frame includes three diagnostic reasoning logical branches: rotor and support fault diagnosis, bearing fault diagnosis, and gearbox fault diagnosis. The three branches are designed by the main process according to the principle of fault mechanism. The fault exclusion and fault deterioration degree evaluation are conducted based on the coarse-fine combination and multiple information fusion.

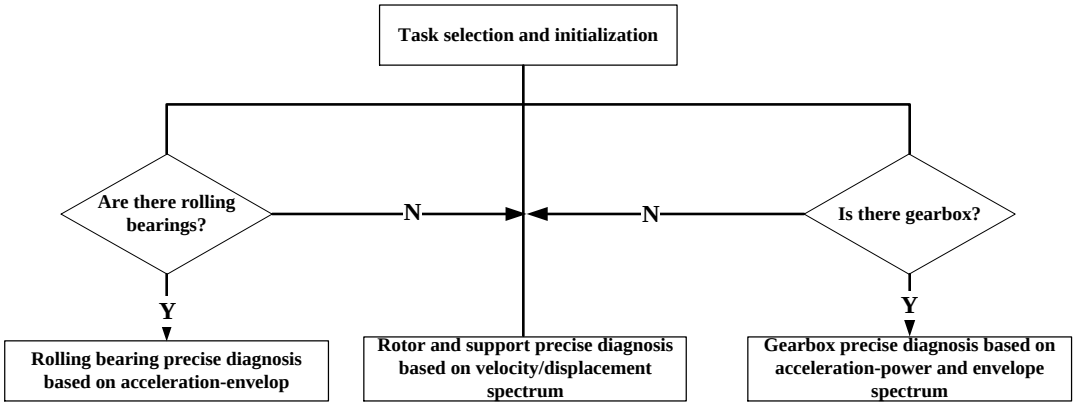

Fig. 2 Main frame of the diagnostic reasoning logic

Velocity-displacement spectrum based fault diagnostic branch does the diagnostic reasoning logical settings according to the rotating machinery fault mechanism. Main characteristic parameters are based on spectrum. The

faults that can be diagnosed by this branch include faults of rotor itself, shaft faults, supporting system faults, etc. This branch of diagnostic reasoning logical design makes determination not only based on frequency information like pass frequency of the impeller, but also trends change and in-site visual inspection. The simplified diagnostic logic is shown in Fig.3. The dominant frequency is the frequency components which have largest amplitude in the spectrum, and the often accompanied frequency is the frequency components with higher amplitude apart from the dominant frequency in the spectrum. For the vibration fault of the rotating machinery, the dominant frequency is the most effective recognizing feature used for diagnosing [8]. In-site visual inspection refers to using these means, such as "seeing, hearing, touching, smelling," to obtain the running status information, which include noise information, seal leakage, the level of the lubricating oil, whether the oil is metamorphic, whether the connection of the anchor bolt is intact.

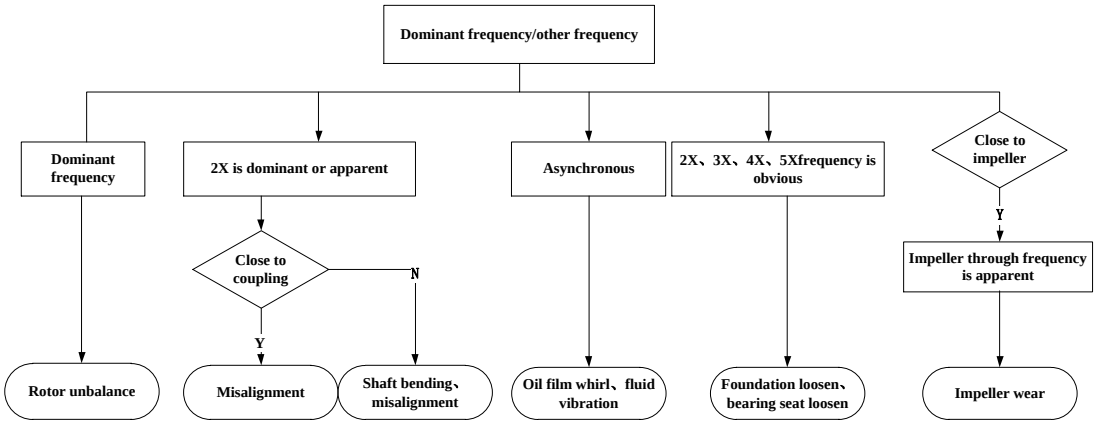

Fig. 3 The flow chart of velocity/displacement based diagnostic branch

The rolling bearing fault diagnostic branch based on acceleration-envelop spectrum formulates diagnostic reasoning logic according to the fault mechanism of rolling bearing, and the simplified diagnostic logic is shown in Fig.4. The branch of diagnostic reasoning logic is based on: impulsive energy in gIE (scale of it represents the severity of shocking fault for the rolling bearing),the fault frequency of the rolling bearing, gIE trend, and so on.

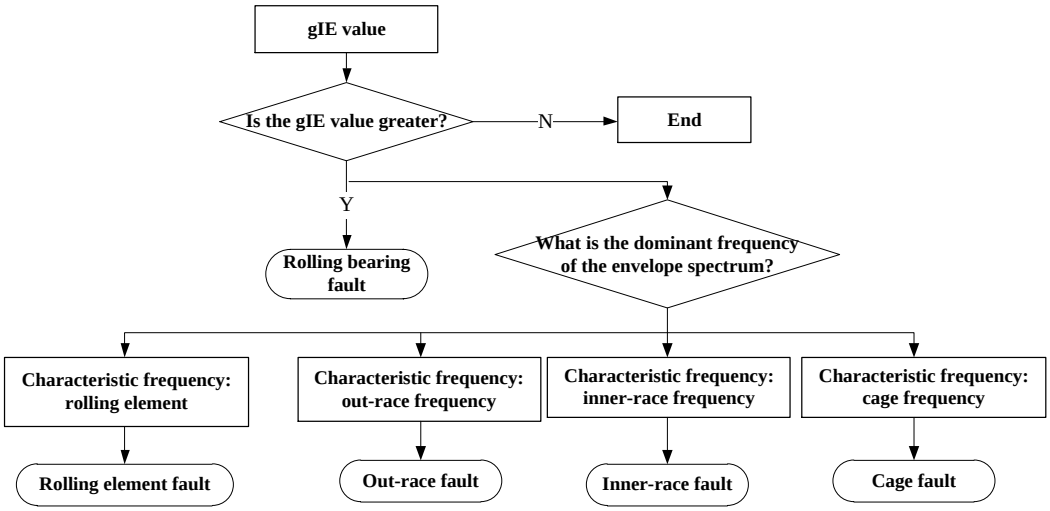

Fig. 4 The flow chart of the diagnostic branch based on the acceleration-envelop spectrum

The branch of gearbox fault, which based on the acceleration-power and envelop spectrum, formulates diagnostic reasoning logic in accordance with the mechanism of the fault for the gearbox, and the simplified diagnostic logic is shown in Fig. 5. The design of the diagnostic reasoning logic branch mainly consider: gIE of the acceleration signal, the dominant frequency of the acceleration power spectrum, the dominant frequency of the envelop spectrum, gIE trend, etc.

The fault deterioration assessment is done according to three aspects information: fault mechanism and evolution, multiple information fusion, and trend change. As illustrated in Fig. 6, the deterioration degree of the rolling bearing can be known by comparing the gIE trend of the bearing with the gIE trend of the next

measurement point. And the repairing advices can be put forward according to the inspection condition of the oil lubricating.

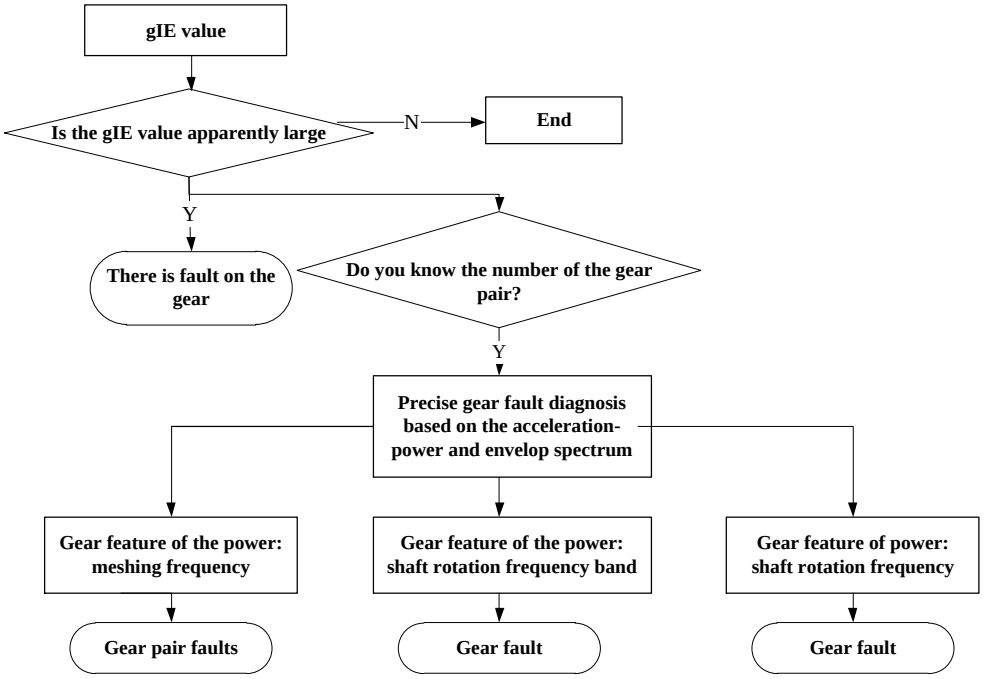

Fig. 5 The flow chart of the gearbox fault diagnostic branch based on the acceleration-power and envelop spectrum

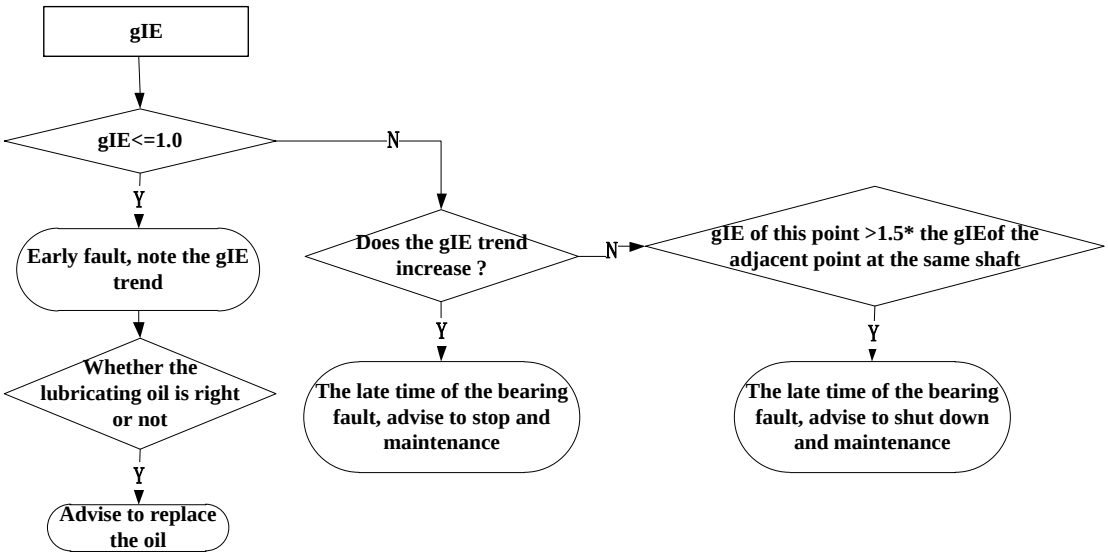

Fig. 6 The evaluation of the deterioration degree for the rolling bearing fault

4. Application cases study

According to the above design, integrating the intelligent diagnostic expert system into the off-line patrol management system of the pumps group has been applied in the pump management of the China oil refining enterprises. The applications are introduced below by two typical cases.

4.1 Bearing out race fault

Take the diagnosis for circulating water pump of external heat exchanger in heavy oil catalytic cracking unit of one petrochemical industry as example. The circulating water pump is composed by turbine, gearbox and cantilever centrifugal pump, in which the rotating speed of the turbine is 4500 rpm, the rotating speed of the centrifugal is 1480 rpm and the delivering medium of the centrifugal is steam water. Centrifugal pump adopts the

rolling bearing (SKF NU324E), whose characteristic frequencies of the out-race fault is 131HZ. The vibration signal is collected by the accelerometers with sampling rate 15360HZ and the sampling number 5120. The arrangement of the measuring points in the unit is shown in Fig.7.

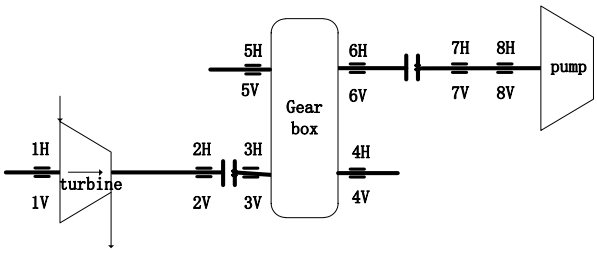

Fig. 7 The measuring point layout of the circulating water pump

As shown in Fig.8, the gIE of the 7V point was abnormal in the period of time from 13:14:09 November 17th, 2010 to 12:31:02 November 21th, 2010 from the historical trend graph. Spectrum displayed that 130HZ and its harmonic frequency played the dominant roles that were the same with the frequency of outer race fault. Selecting this segment data to diagnose, and the diagnostic result was late time of the outer race fault for rolling bearing, which was consistent with the diagnostic result when repaired after stop.

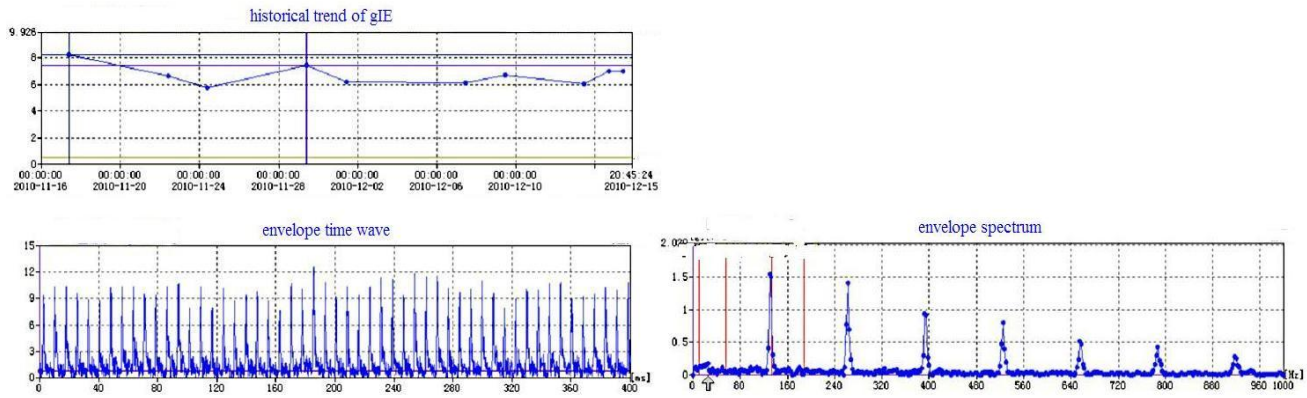

Fig. 8 The out race fault of the rolling bearing

4.2 Rotor misalignment fault

Take the forced circulation hot water pump of triple-combined in a petrochemical company as an example. The circulation water pump is composed of motor, cantilever centrifugal pump that working speed is 2980 r/min. Its vibration signal is collected by the acceleration sensor, which recollected and integrated can be the displacement signal. The sampling rate of the displacement signal after being integrated is 5120 HZ, and the sampling number is 1024. Layout of the unit points is shown in Fig. 9.

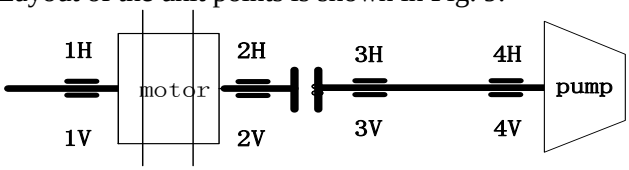

Fig. 9 The measuring point layout of the circulating heat-water pump

The diagnosis adopted the semi-automatic diagnostic model. As shown in Fig.10, from the historical trend chart, selecting the 2H vibration point in the period time that from 15:14:01 of April 14th, 2010 to 12:30:03 of April 18th, 2010 to diagnose and choosing the semi-automatic as the diagnostic model. The human-machine dialog box is shown in the diagnostic process to put out the question that where the measurement point is, then selected closing to the coupling as the point position, and finally obvious misalignment of the rotor as the diagnostic result. In Fig.11, the analysis for the velocity spectrum of the two points in the two sides of the coupling showed that the 2X frequency of the 2H velocity spectrum was obvious and the amplitude of it had exceeded the 1X frequency, so that we could determine that the fault was a more serious misalignment fault which was in accordance with the practical situation.

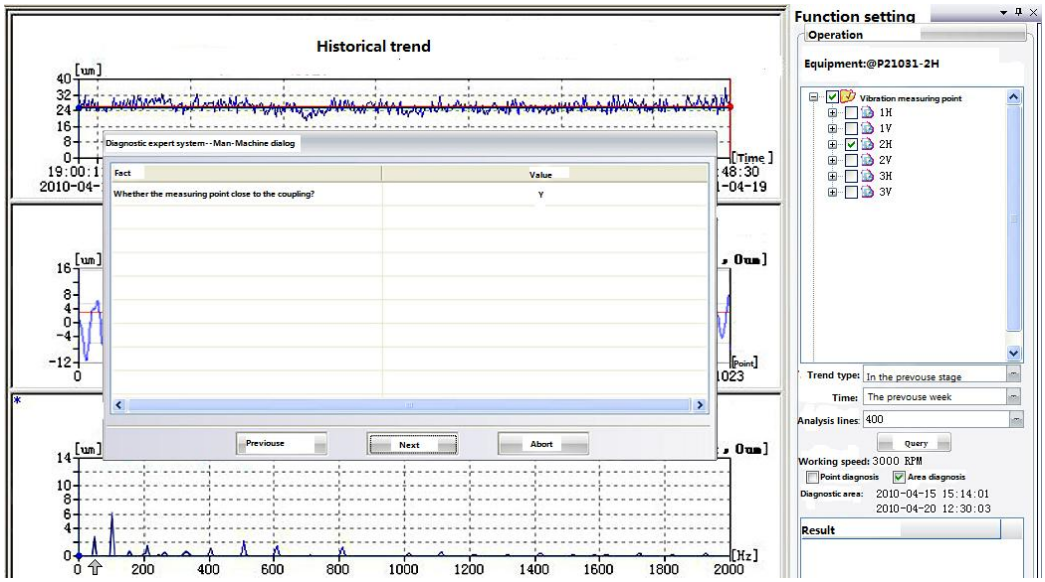

Fig. 10 Rotor misalignment fault—human-machine dialog interface

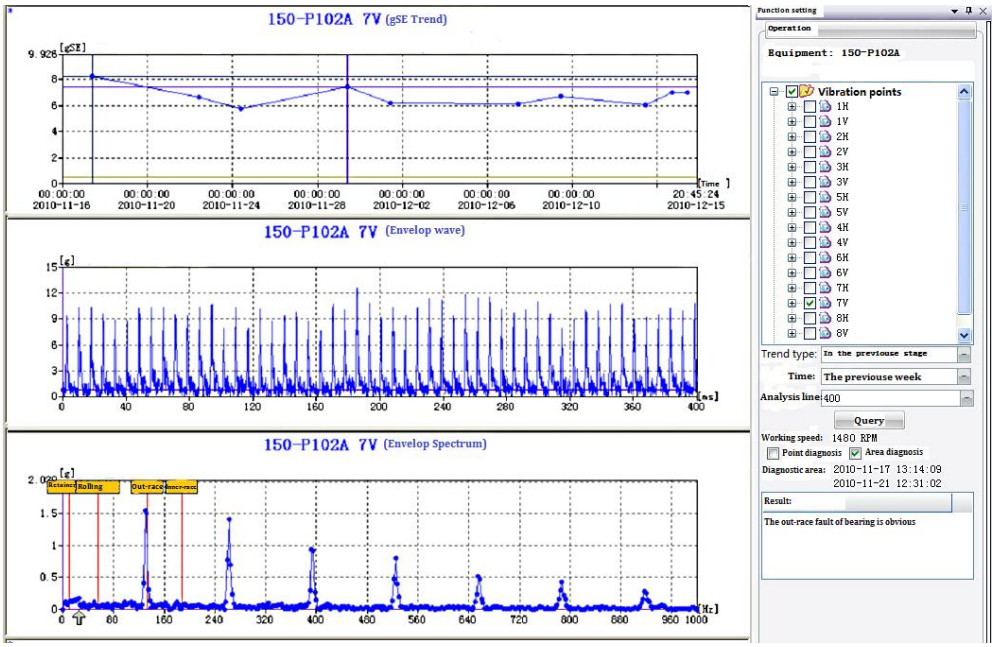

Fig. 11 Rotor misalignment fault

5. Conclusion

With the development of the refining and chemical enterprise's size and the condition based maintenance system, refining enterprises not only increasingly recognize the necessity of developing machine condition monitoring and the technology of the fault diagnosis, but also put forward new demands for the condition monitoring: condition monitoring system not only be restricted to preventing the accidents, but also needs to guide the maintenance. Though it is especially important for the large and dispersed pumps, the traditional off-line patrol management system focuses on the inspection and signal analysis that is difficult to adapt to the new requirements of the refining enterprises. Therefore, the paper researched and designed the intelligent expert system that can be integrated to the off-line condition monitoring system for the pumps group. Two application cases show that the effect of the off-line patrol management system is improved and more direct and reliable basis for the enterprise to carry out condition based repairing are provided.

Acknowledgment

The work is supported by Major Program of National Natural Science Foundation of China (NO. 51135001).

References

[1] J. J Gao. A Real-Time Monitoring Network and Fault Diagnosis Expert System for Compressors and Pumps, *China Engineering Science*, Vol. 3, pp. 41-47, 2001.

[2] P. D. McFadden and J. D. Smith. Model for the Vibration Produced by a Single Point Defect in A Rolling Element Bearing, *Journal of Sound and Vibration*, Vol. 96, No. 1, pp. 69-82, 1984.

[3] B. Ma, Q. Wei, C. L Xu and Z. N Jiang. Envelope Analysis Based on Hibert Transformation and Its Application in Ball Bearing Fault Diagnosis, *Journal of Beijing University of Chemical Technology*, Vol. 31, pp. 95-97, 2004.

[4] Q. Y Fu, Y. C Zhang, L. J Ying and G. S Li. Extraction of Failure Character Signal of Rolling Element Bearings by Wavelet, *Chinese Journal of Mechanical Engineering*, Vol. 37, pp. 30-33, 2001.

[5] H. Q Wang and P. Chen. Intelligent Diagnosis Method for Rolling Element Bearing Faults Using Possibility Theory and Neural Network, *Computers & Industrial Engineering*, Vol. 60, pp. 511-518, 2011.

[6] B. Liu, S. Riemenschnieder and Y. Xu. Gearbox Fault Diagnosis Using Empirical Mode Decomposition And Hilbert Spectrum, *Mechaninal Systems and Signal Processing*, Vol. 20, No. 3, pp. 718-734, 2006.

[7] J. D Wu and C. C Hsu. Fault Gear Identification Using Vibration Signal with Discrete Wavelet Transform Technique and Fuzzy－Logic Inference, *Expert System with Applications*, Vol. 36, No. 2, pp. 3785-3794, 2009.

[8] J. J Gao. Approach to Mechanical Vibration Faults and Distinctive Symptoms in Rotating Machinery. *Journal of Vibration, Measurement & Diagnosis*, Vol. 15, No. 3, pp. 1-8, 1995.

[9] S Perovic, P. J Unsworth and E. H Higham. Fuzzy Logic System to Detect Pump Faults from Motor Current Spectra, *IEEE Industry Applications Conference*, Vol. 1, pp. 274-280, IEEE xplore, September 30-Octorber 4, 2001, Chicago, IL, USA

[10] L. Alfayez, D. Mba and G. Dyson. The Application of Acoustic Emission for Detecting Incipient Cavitation and the Best Efficiency Point of A 60 KW Centrifugal Pump: Case Study, *NDT & E International*, Vol. 38, No. 5, pp. 354-358, 2005.

[11] D. Mba and R. B. K. N Rao. Development of Acoustic Emission Technology for Condition Monitoring and Diagnosis of Rotating Machines; Bearings, Pumps, Gearboxes, Engines and Rotating Structures, *The Shock and Vibration Digest*, Vol. 38, No.1, pp. 3-16, 2006.

[12] S. F Yuan and F. L Chu. Support Vector Machines-Based Fault Diagnosis for Turbo-Pump Rotor, *Mechaninal Systems and Signal Processing*, Vol. 20, No. 4, pp. 939-952, 2006.

[13] N.R Sakthivel, V Sugumaran and B.B Nair. Comparison of Decision Tree-Fuzzy and Rough Set-Fuzzy Methods for Fault Categorization of Mono-Block Centrifugal Pump, *Mechaninal Systems and Signal Processing*, Vol. 24, No. 6, pp. 1887-1906, 2010.

[14] A. Wolfram, D. Fussel, T. Brune and R. Isermann. Component-Based Multi-Model Approach for Fault Detection and Diagnosis of a Centrifugal Pump, *Proceedings of the American Control Conference*, Vol. 6, pp. 4443-4448, IEEE xplore, June 25-27, 2001, Arlington, VA, USA.

[15] C. S Kallesoe, V. Cocquempot and R. Izamanabadi. Model Based Fault Detection in a Centrifugal Pump Application, *IEEE Transactions on Control Systems Technology*, Vol. 14, No. 2, pp. 204-215, 2006.

[16] P. Farzd and T. Fattaneh. Applying the MAS-CommonKADS methodology to the Flights Reservation Problem: Integrating Coorination and Expertise, *Proceedings of the 5th joint conference on knowledge-based software engineering*, 2002, Maribor, Slovenia.

[17] N. M Hewahi. A General Rule Structure, *Information and Software Technology*, Vol. 44, pp. 451-457, 2002.

[18] H. Antonio. A New Algebraic Model for Implementing Expert Systems Represented under the 'Concept-Attribute-Value' Paradigm, *Mathematics and Computers in Simulation*, Vol. 82, No. 1, pp. 29-43,2008.

[19] J. J Gao. A Mechanical Fault Diagnosis Expert System Based on Matrix Distinguishing Sieve Method, *Journal of Vibration, Measurement & Diagnosis*, Vol. 18, No. 2, pp. 120-124, 1998.

Copyright © 2012 DET Corp., Japan All Rights Reserved
International Journal of Comprehensive Engineering
Part B, 1(1), 60-66, 2012
Doi: 10.14270/IJCE2012.1.1.b60
Regular paper

ISSN 2186-2680
e-ISSN 2186-2656
www.iace-journal.org

Numerical Calculation of Transient Characteristics in Centrifugal Pump Speed Regulation process based on CEL language

Shouqi Yuan [1], Lingdi Tang [1, #], Erhui Liu [1] and Yue Tang [1]

[1]Research Center of Machinery Engineering and Technology, Jiangsu University, Zhenjiang, Jiangsu 212013, China

[#] Corresponding author: angealt@sina.com; Tel.: +8651188782641; Fax: +8651188782641

Abstract: Analysis of the transient hydraulic characteristics of a centrifugal pump during its speed regulating process was carried out based on the approaches of both quasi-steady-state and transient numerical simulation with the CEL languages function applied by using the commercial software ANSYS CFX 12.0. Meanwhile, the effect of different impeller acceleration and regulating flow on the transient pump head was also studied in the paper. To avoid the influence of the artificial factor in the simulations, a software Flowmaster was used for boundary condition definitions. The numerical results show that pump head deviation between the transient state and quasi-steady-state becomes large with the impeller acceleration increasing and the regulating flow rate decreasing. The influence of impeller and flow acceleration in speed regulating period can be accurately predicted by transient simulation method based on CEL languages function. Additionally, by investigating flow section in the centrifugal pump, the transient flow in its speed regulating process was obtained, which can be used to judge the speed regulating schemes from the inner flow pattern, and find the dynamic root for induced unsteady total pressure and its generated positions, as well as provide certain reference for the centrifugal pump hydraulic design.

Keywords: Transient Characteristics, Regulating, Steady Calculation, Transient Calculation, Flow Section.

Received: May 20,2012 / Accepted: Sept. 12,2012 / Published: Dec. 15,2012

1. Introduction

Operating condition regulation of centrifugal pump contains flow regulation and speed regulation. As the Intelligent Power Technology has developed in recent years, speed regulation has become more and more widely used. The pattern of speed regulation has a direct influence on transient process for pump, improper regulation can lead to pressure fluctuation in centrifugal pump system, even oscillation phenomenon and so on. Factors mentioned above have effects on daily live, so the research for transient characteristics in speed regulation process of centrifugal pump is important and significant to promote the Energy Conservation and Emission Reduction. However, the research on transient process on centrifugal pump are mostly focused on power on and off process, or regarding pump as a boundary condition when calculating for water hammer within pump pipelines, as well as using complete characteristic curves to describe performance. For instance, Daigo and Ohashi [1] studied the pump initial stage in 1972, which occurs with rapidly increased rotational speed, and obtained deviation value between steady and transient state. However, they failed to explain why this phenomenon appears. Lefebvre [2] carried out a test on a centrifugal pump for transient characteristic on startup process in 1995, and the result revealed that the faster acceleration startup process had, the more obviously transient effect behaved. Meanwhile, Tsukamoto [3, 4] did relevant research for centrifugal pump on transient characteristics.

Wang Leqin, Wu Dazhuan, et al. [5, 6] numerically calculated transient hydraulic characteristic at startup stage for two different sizes mixed-flow pumps in 2004. They built a transient hydraulic characteristic analyticequation on the basis of mixed-flow internal character and a pipeline characteristicequation under

transient condition. Then they combined these two equations, solved the simultaneous equations, and came up with the conclusion that numerical results at early initiating stage had a big deviation compared with experimental results, while at the post stage these two fit well. And the possible reason was miscalculating the resistance loss coefficient in pipeline.

For now, the way of quasi-steady-state calculation [7] and dynamic meshes calculation [8] are usually used to calculate centrifugal instantaneous conditions. The former is easer but not accurate enough under high impeller acceleration [1], at the same time the latter ensures the real-time variation of rotational speed but the amount of work is enormous due to continual meshes update. Furthermore, the latter is mainly used at the startup and shoutdown stages instead of speed regulating process. This paper researches the internal transient flow of centrifugal pump in speed regulating process by using CEL language transient simulation method.

2. Numerical Model

The centrifugal pump 3D model completed by using the commercial software Pro/E is shown in Fig.1**.** It is composed of inlet pipe, outlet pipe, and an impeller with six twisted blades as well as volute. The parameters of the test pump are presented in Table1.

Table 1 design parameters of the model centrifugal pump

Type	Q_d (m^3/h)	H_d (m)	N(r/min)	n_s
IS65-50-160	25	32	2900	66

Unstructured tetrahedron grids of the whole computation domains were generated by ICEM CFD 12.0. Especially, the grids around volute tongue were locally refined. A final grid with about 1,542,460 cells was used in the model pump, as is shown in Fig.2.

Fig. 1 3D view of the centrifugal pump

Fig. 2 Calculation grids

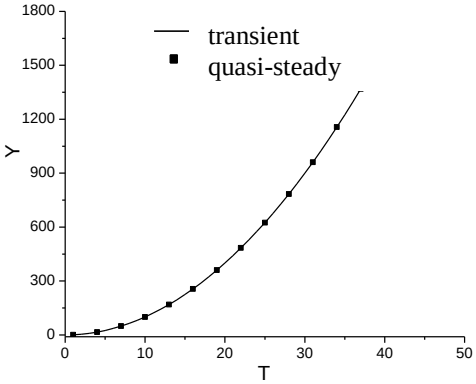

Fig. 3 Boundary curves of steady and transient

3. Numerical results under different speed regulating schemes

To analyze the effect of different impeller acceleration and regulating flow in regulation process, both the quasi-steady-state calculation method and CEL language transient simulation method were applied in this paper. Fig.3 shows that the difference between quasi-steady-state calculation and transient state calculation. The former method was based on discrete points, and the latter defines boundary condition as continuous variation, whose variation curves are artificially defined.

The calculation schemes of speed regulating process are listed in Table 2.The initial and the steady flow rate values were both measured by experiments. Regulation time was chosen by integrating with motor acceleration limit and simulation computing time. Too short regulating time is likely to damage motor, while too long is likely to build up computational time. Therefore, taking the above factors into account, regulation times were selected at 0.4s and 2s, rotational speed and outlet velocity were selected as continuous variation in transient calculation.

In order to quantitatively analyze the different values between transient head and quasi-steady-state head, the deviation is normalized using the following equation:

$$\Delta H = H_s - H_w,$$

where H_s means the transient head value of CEL language transient simulation calculation method, H_w represents the head value of quasi-steady-state calculation method. The deviation was varying with time, whose variation curves are shown in Fig.4, which was obtained from the quasi-steady-state calculation of regulation operating condition ranging from 1 to 6.

From the comparison between operating condition 1 (Fig.4(a)) and 2 (Fig.4(b)) in regulation scheme 1, the impeller acceleration differs with different regulation time. Fig.4(a) shows that the deviation between transient head and quasi-steady-state head is fluctuating from 0.6m to 0.7m., while that value is from 0.3m to 0.55m as shown in Fig.4(b). Generally, the deviation mainly varies between 0.35m and 0.5m. By comparing Fig.4(c) and Fig.4(d), Fig.4(e) and Fig.4(f) respectively, it can be achieved that the higher impeller acceleration causes the deviation larger.

Table 2 Regulation schemes

Regulation scheme		Regulation time/s	Initial rotational speed/rpm	Steady rotational speed/rpm	Initial flow rate/m^3^h^{-1}	Steady flow rate/m^3^h^{-1}
Scheme 1	Regulating operating condition 1	0.4	3000	1800	46	25
	Regulating operating condition 2	2	3000	1800	46	25
Scheme 2	Regulating operating condition 3	0.4	3000	1800	25	15
	Regulating operating condition 4	2	3000	1800	25	15
Scheme 3	Regulating operating condition 5	0.4	3000	1800	15	5
	Regulating operating condition 6	2	3000	1800	15	5

The same impeller acceleration with different regulating ranges were defined for operating conditions of 1, 3, and 5. From regulation scheme 1 to 5, the deviation ΔH increases from 0.7m to 3.5m, and its value in regulation 2, 4 and 6 has experienced the similar change. The deviation between transient state and quasi-steady-state gradually becomes much larger (see in Fig.4) as the regulation flow decreases. The transient head of the centrifugal pump varies not only with the impeller acceleration, but also the flow regulating range in its speed regulating process.

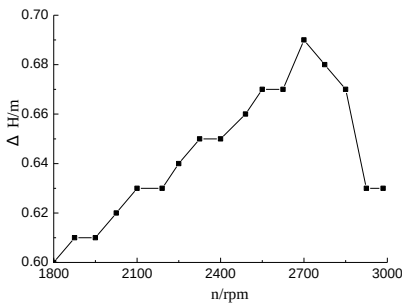

(a) Regulating operating condition 1

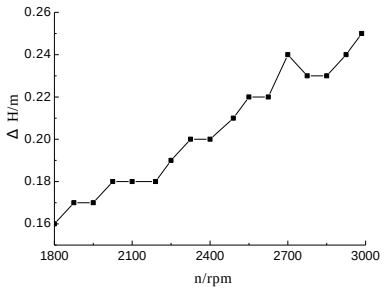

(b) Regulating operating condition 2

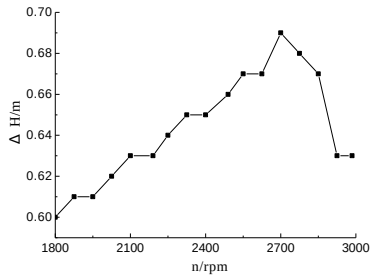

(c) Regulating operating condition 3

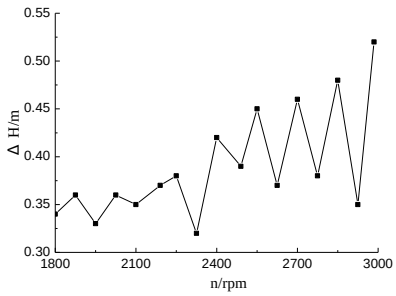

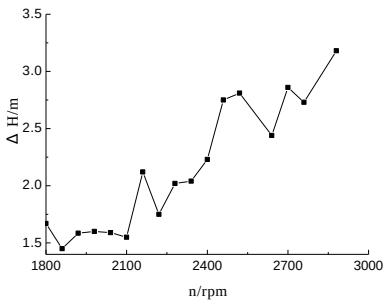

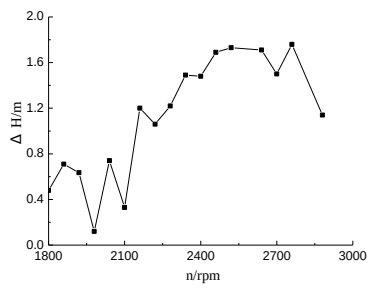

(d) Regulating operating condition 4 (e) Regulating operating condition 5 (f) Regulating operating condition 6

Fig. 4 Difference head of transient and steady curve

It can be initially concluded that the transient characteristic of the centrifugal pump performed in its speed regulating process is caused by both the impeller acceleration and the flow acceleration, as obtained from the numerical calculation. The quasi-steady-state method cannot reflect the influence of impeller acceleration and flow acceleration. The transient state method basing on CEL language can accurately consider this influence, but cannot exactly get the centrifugal pump hydraulic characteristic curves in its starting process, for the reason that boundary conditions such as rotational speed and flow rate were artificially defined according to ratiolaw, and inlet pressure was set as a constant going against the fact.

4. Flow Regime Analysis

4.1 Boundary condition

It has a long period, a high cost, and is difficult to obtain the accurate flow evolution curve at initial design phase to get pump hydraulic characteristic parameters in speed regulating process with experimental tests. Therefore, the software Flowmaster was applied to simulate the speed regulating process of the centrifugal pump system. The various curves of pump rotational speed and outlet flow were obtained. The parameters of the model pump hydraulic characteristic are shown in Fig.5. It can be seen that rotational speed and flow rate rapidly change from 0 to 2 seconds, gradually rise from 2 to 5 seconds, and basically remained steady after rising to a certain value. This study mainly focused the pump characteristic in its speed regulating process, and the simulation time from 0 to 5 seconds was selected.

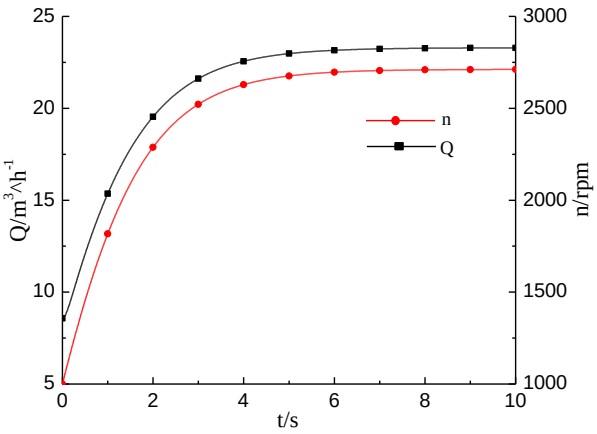

Fig. 5 Rotation and flow regulation curves of the pump

The equations were achieved by fitting the data from the numerical calculation during the time from 0 to 5 seconds. The equations were regarded as the boundary conditions. Then this curve of the data was quadratic fitted as the following equations:

$$n(t) = 16.810t^3 - 220.04t^2 + 1017.4t + 999.56 \quad (1)$$

$$R^2 = 1.000$$

$$Q(t) = 0.1487t^3 - 1.9529t^2 + 9.0441t + 8.0759 \quad (2)$$

$$R^2 = 0.9998,$$

where Equ.1 is rotational speed variation, Equ.2 is flow variation. the inlet boundary condition was set as total pressure, and mass flow rate was applied for outlet, as can be calculated by dividing 3.6 in Equ.2. The time step was set as 0.001s, and the total time step was1000.

4.2 Results and Discussions

In unsteady numerical results of the regulation process of the centrifugal pump, five points (0.1s, 1s, 2s, 3s, 4s) were picked out to analyze the internal flow in cross section of impeller and volute. In order to obtain the energy variation within centrifugal pump and judge whether the energy mutations have occurred or not in speed regulating process, vortex dynamics was analyzed [9]. To further understand the transient flow pattern, energy distribution and the effort of this distribution on transient characteristic within the centrifugal pump, the transformation between impeller mechanical energy and fluid energy was analyzed by studying the total pressure

in the flow section, based on the numerical simulation results of the transient flow in the speed regulating process of the centrifugal pump.

The total pressure distribution at different moments at the radius of 40mm (closes to impeller inlet) is shown in Fig.6. The nonuniform distribution of inlet energy can be found at every moment. High local energy lies where is close to the blade suction side. The total pressure equally increases step by step with the rotational speed and time increasing. The energy distribution gradually goes well as time goes. It was not until 4s that the energy distributed uniformly except the place around the cutwater.

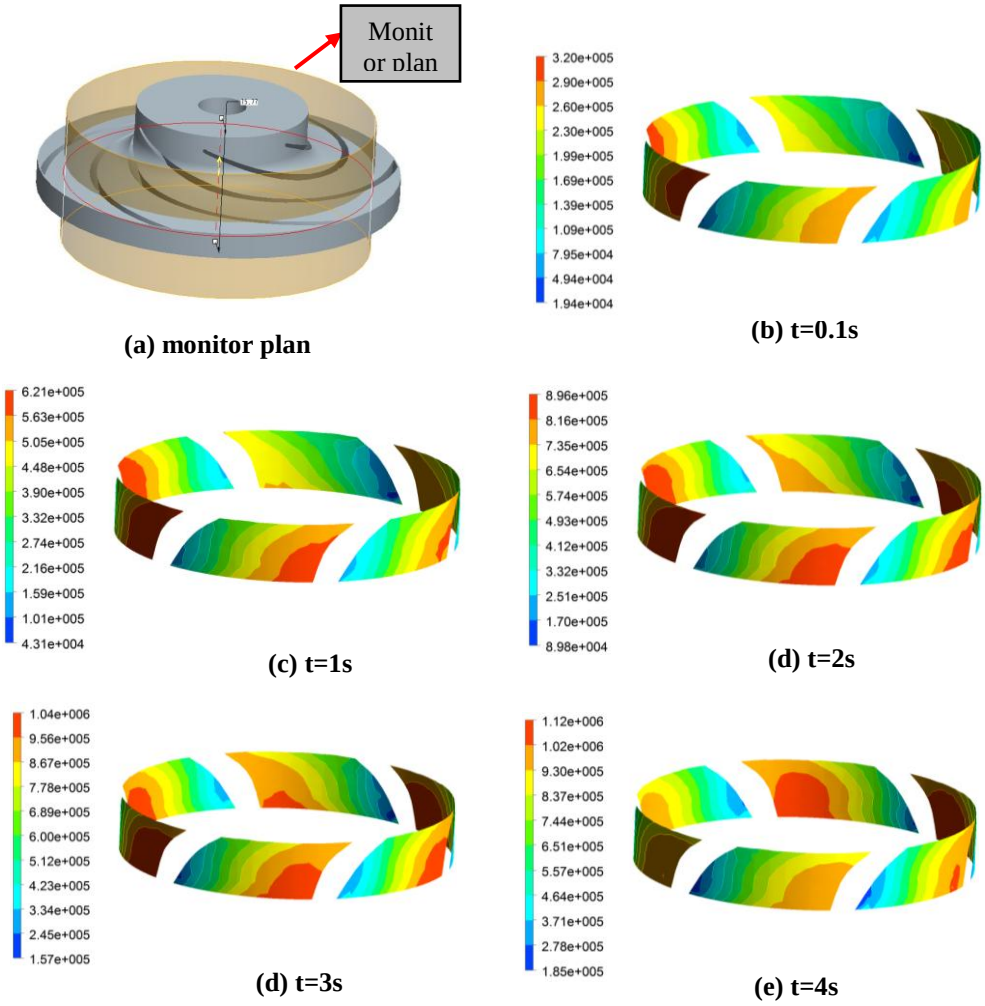

(a) monitor plan **(b) t=0.1s**

(c) t=1s **(d) t=2s**

(d) t=3s **(e) t=4s**

Fig.6 Total pressure distribution at the suction of r=40mm

Fig.7 shows total pressure distribution at different radius in the same time. Flow energy gradually increases along the direction of flow, representing the process that fluid increases work. There is no significant increase and decrease in the total pressure of different sections, and the energy variation in speed regulating process was smooth and steady.

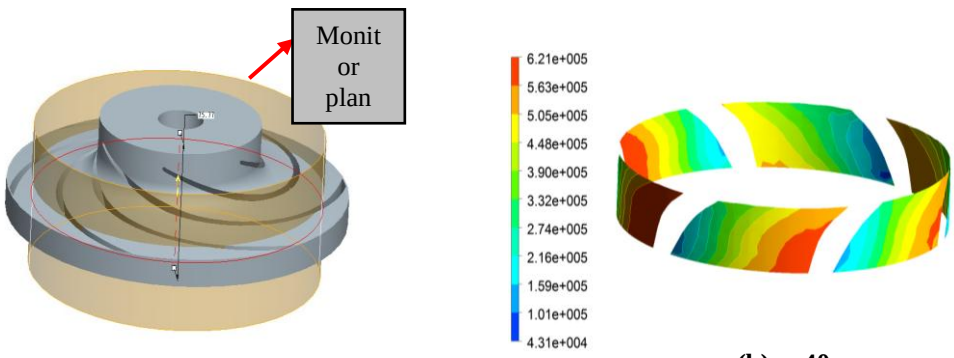

(a) monitor plan **(b) r=40mm**

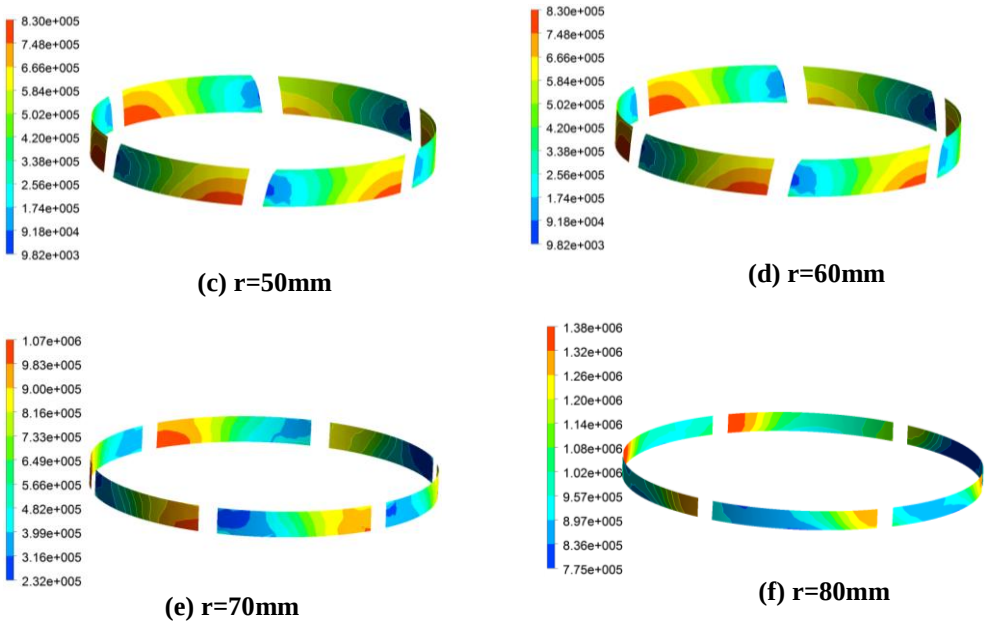

Fig. 7 Total pressure distribution at the time of t=1s

Based on the study of the flow section through analyzing total pressure integrals at any vertical section in flow direction, the dynamic root and its location which has a negative influence on the total pressure can be obtained. In addition, it can provide certain reference for centrifugal pump hydraulic design and to judge the rationality of speed regulating scheme.

5. Test Verification

Regulation scheme 2 was tested to verify the accuracy of transient numerical simulation. Due to the filtering process was required in data collection, partial values of transient calculation and whole test values were extracted to have a comparison as is shown in Fig.8. The results obtained by the test have a good agreement with the numerical calculation, so the numerical simulation in this paper is certainly reliable.

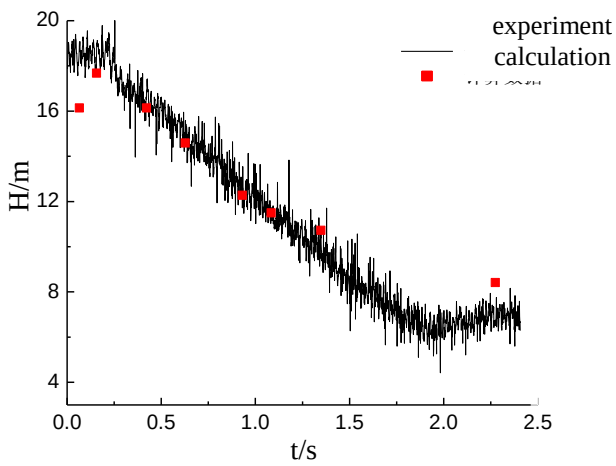

Fig.8 Compare of calculation and experiment results

6. Conclusions

1) Based on the 3D numerical calculation of speed regulating procedure for centrifugal pump model, the initial transient characteristics was achieved, and mainly affected by both the impeller and the fluid acceleration, as the quasi-steady-state numerical method fails to show the effect of two factors.
2) By comparison of numerical results based on quasi-steady-state method with transient state method, it can be concluded that the deviation of the predicted pump head increases with the increase of impeller acceleration and the reduction of flow regulation in its speed regulating process of the centrifugal pump. Furthermore, the influence of both the impeller and flow acceleration can be accurately predicted by the

transient simulation method based on CEL languages function.

3) The precise dynamic speed regulating process was obtained based on the methods of simulation analysis and transient numerical calculation. Again, the transient flow in speed regulating process of the centrifugal pump was achieved by analyzing its flow section, which can help to find generated position and the dynamic root for induced unsteady total pressure. In addition, these can provide certain reference for the centrifugal pump hydraulic design and assessing the rationality of speed regulating scheme.

References

[1] Daigo. H, and ohashi. H. Experimental Study on Transient Characteristics of a Centrifugal Pump during Rapid Acceleration of Rotational Speed, *Proceedings of Second International JSME Symposium, Fluid Machinery and Fluidics*, Vol. 2, pp.175-182, Sept, 1972, Tokyo.

[2] P. J. Lefebvre and W. P. Barker. Centrifugal Pump Performance During Transient Operation, *ASME Journal of Fluid Engineering*, Vol. 117, No. 2, pp. 123-127, 1995.

[3] Tsukamoto H and Ohashi H. Transient Characteristics of a Centrifugal Pump During Starting Period, *ASME Journal of Fluid Engineering*, pp. 6-13, 1982.

[4] Tsukamoto H,et al.Transient Characteristics of a Centrifugal Pump During Stopping Period, *ASME Journal of Fluid Engineering*, pp. 392-399, 1986.

[5] L. Q Wang, D. Z Wu. Study on transient hydrodynamic performance of Mixed-Flow-Pump during starting period, *Journal of Zhejiang University(Engineering Science)*.

[6] L. Q Wang, D. Z Wu. Study on transient characteristics of centrifugal pump, *Journal of Engineering Thermophysics*, Vol. 27, No. 1, pp. 68-70, 2006.

[7] R. J Sui. *Research on Transient Characteristics & Interior Flow of Centrifugal Pump during Starting Period*, Shandong University, 2006.

[8] Z. F Li. *Numerical Simulation and Experimental Study on the Transient Flow in Centrifugal Pump during Starting Period*, Zhejiang University, 2009.

[9] Tramel R Z. A vorticity dynamics theory of three-dimensional flow separation, *Physics of Fluids*, Vol. 12, No. 8, pp.1932-1954, 2002.

Copyright © 2012 DET Corp., Japan All Rights Reserved
International Journal of Comprehensive Engineering
Part C, 1(1), 67-73, 2012
Doi: 10.14270/IJCE2012.1.1.c67
Regular paper

ISSN 2186-2680
e-ISSN 2186-2656
www.iace-journal.org

Mechanism of Characteristic Instability and its Suppression in Mixed Flow Pump

Zhongyong Pan [#], Taotao Wu, Junjie Li and Yanjun Li

Research Center of Fluid Machinery Engineering and Technology, Jiangsu University, Zhenjiang, 212013, China

[#] Corresponding author: pzy@ujs.edu.cn; Tel.: +86-0511-88780281; +086-13815179257

Abstract: It is revealed that positive slope of head-flow performance curves appears when the pump is working at partial flow rates both for experimental and numerical investigations, and characteristics calculated agreed well with experimental ones. CFD was used to study the mechanism of the performance curve instability of a test pump. Because of the existence of high pressure differences at the partial flow rates, the fluid leakage occurred at the tip clearance between the casing and the impeller. Furthermore, pre-rotation generated at the inlet of the impeller. The theoretical head decreased because of the pre-rotation. When the flow rate decreased further, a strong vortex occured at the inlet of the diffuser hub and blocked the discharge of the impeller. Therefore the flow pattern of the impeller tends to a centrifugal type and the head of the mixed flow pump increased, subsequently the positive slope of performance curve occured. Two ways were taken to suppress the performance curve instability, the inadequate of the suppression method of the model and some positive results advices about the performance curve instability suppression are proposed. A swirl-stop and diffuser optimization could somewhat improve the instability but not ideal, while the proper shallow groove is a simple and useful method on suppression of pump performance curve instability.

Keywords: Mixed Flow Pump, Characteristic Instability, Pre-rotation, Groove, CFD.

Received: May 10, 2012 / Accepted: Sept. 12,2012 / Published: Dec. 15,2012

1. Introduction

In recent years, the low specific speed mixed flow pumps have often been applied to the seawater desalination systems to solve the water shortage. From the economic point of view, it is necessary to restrain the total head low at shut off operating point without sacrificing the pump maximum efficiency[1]. The head-flow performance curve often possess positive slope at the low flow rate region, the operating range at that flow rate region is remarkably restricted because of the vibration and noise, so the positive slope region is called as an unstable characteristic[2].

There has been much experimental research associated with unstable characteristics of pumps. Kurokawa et al. measured the flowfield at an impeller inlet and outlet of a mixed flow pump[3]**.** Aoki et al. proposed a method for predicting the inception flow rate of the unstable characteristic, they used the Taylor's pressure coefficient as the index of the stall inception[4]. Masahiro et al. confirmed that a diffuser rotating stall occurs in the original type of a mixed flow pump at about 65% flow rate of best efficiency point (BEP) and it caused the pump characteristic instability[5]. Chisachi et al. reported that the unstable characteristic of an axial pump was caused by reverse flow at the inlet of the impeller[6].

Computation fluid dynamics (CFD) is effective in the analysis of turbomachines, both in design and performance prediction. Some performance predictions of mixed flow pumps have been attempted with Reynolds-averaged Navier-Stokes (RANS) simulation and Large Eddy Simulation (LES)[7]. For example, Chisachi et al. conducted a LES of the internal flow of a mixed flow pump stage and showed a fairly well agreement of the calculation unstable characteristic curve on the impeller with the measured one[6]. However, in every case, the mechanism of characteristic instability of the mixed flow pumps is not clarified clearly. Mixed flow pump performance computed by CFD was compared to the experimental data in this paper. From

comparison it can be concluded that the numerical simulation is credible. Then it explained the mechanism of the performance instability and two methods were proposed to solve the problem. To a certain extent, it provide a reference to solve the positive slope of head-flow performance curve of the mixed flow pump and make it more widespread used in the future projects.

2. Computation Domain and Method

In the present study, the tested pump was BX350-6 (Q_{BEP}=887.76m^3/h, H=5.86m, n=980r/min, n_s=472) and the SST $k-\omega$ turbulence model was adopted because it has a merit for good behavior in adverse static pressure gradient and separated flow. Fig.1 shows the computational model for this study. Full pump geometry was modeled in this calculation, which involved suction casing, impeller, diffuser, and discharge casing. The tip clearance between the impeller and the casing was included. Commercial software, Ansys ICEM CFD, was used to mesh the computational grid. About two million unstructured meshes were used.

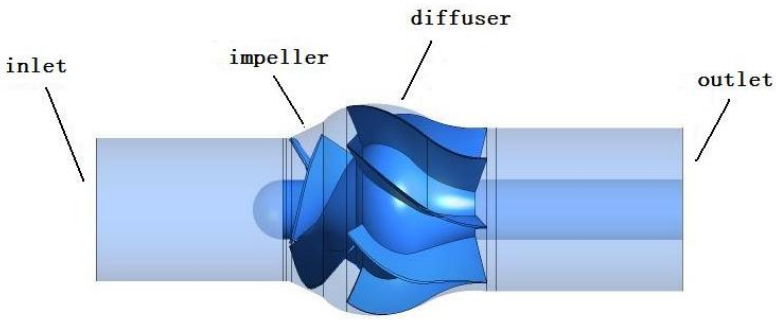

Fig. 1 Computational Model

3. Mechanism of Head-Flow Curve Instability of the Test Pump

Fig. 2 shows comparisons of the head-flow performance curve between the measured and calculated ones. From the figure it is clearly shown that the maximum of the difference value between the two methods was±4.8 percent. So, it can be concluded that the result of the CFD in this paper is reliable. The positive slope appeared between 0.6Q_{BEP}-0.68Q_{BEP}.

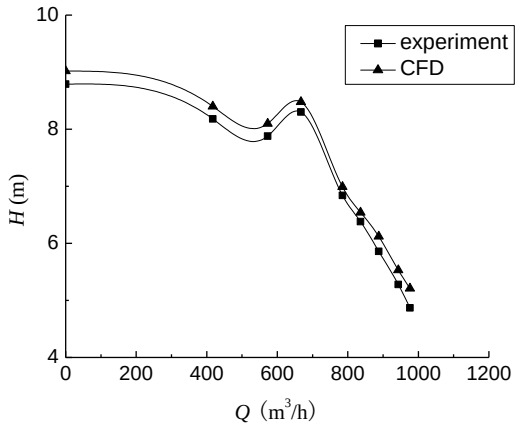

Fig. 2 Performance comparison between CFD and experiment

In order to study the positive slope of the head-flow performance curve, the internal flow of the test mixed flow pump with vane diffuser was investigated. First pressure distributions of the impeller blade were studied. Fig. 3 shows the pressure distributions for both pressure surface and suction surface. From the two pictures it can be seen clearly that there exits pressure differences between the pressure surface (PS) and the suction surface (SS) of the impeller blade and subsequently leakage flow would be formed in the tip clearance from the higher pressure side to the lower one. Some of the leakage flow counteracts the lower pressure region at the inlet of the impeller tip of the suction surface and the load of the suction surface of the impeller increased. Accordingly, it is believed that leakage plays an important role on the head-flow instability. This leakage flow causes to generate vortices and as is known that the flow angle at the impeller inlet is defined as the following equation:

$$\beta_1 = arctan(V_{u1}/V_{m1}) \tag{1}$$

Where β_1 is the flow angle at the impeller inlet, V_{m1} is the meridional velocity and V_{u1} is the circumferential velocity at the impeller eye. When the vortices occurs, V_{m1} increases and the V_{u1} deceases a little, the flow angle at the inlet of the impeller tip decreases and the flow hits the impeller pressure surface. With the decreasing of the flow angle the vortices developed to reverse flow with swirl. The leakage flow has circumferential component of absolute velocity and the swirling energy is continuously supplied by the reverse flow. Therefore, the pre-rotation would occur at the inlet of the impeller.

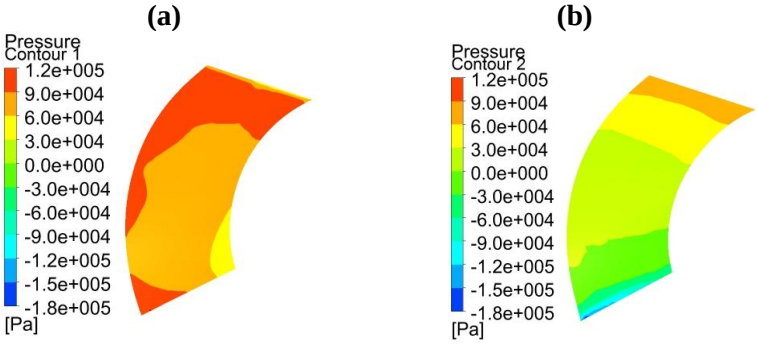

Fig. 3 Pressure distribution. (a) Pressure contour of PS at $0.6Q_{BEP}$. (b) Pressure contour of SS at $0.6Q_{BEP}$

Fig. 4 shows the streamline of inlet flow at $1.0Q_{BEP}$ and $0.6Q_{BEP}$. The streamline of the suction inlet flow keeps initial direction at $1.0Q_{BEP}$, there is no circumference direction streamline at the impeller inlet. But it has circumference direction streamline near the impeller inlet at $0.6Q_{BEP}$. It shows that the fluid has the same rotation direction with impeller before it flows into the impeller which is called pre-rotation. The pre-rotation is probably responsible for the head decrease. The theoretical head of the pump is defined as follows:

$$Ht= (U_2V_{u2} - U_1Vu_1) /g \tag{2}$$

When there is no pre-rotation the V_{u1}=0, so the equation is deduced as:

$$Ht = U_2V_{u2} /g \tag{3}$$

So according to the above results it can be seen that the theoretical head is decreased due to the pre-rotation and the performance curve instability of the pump occured.

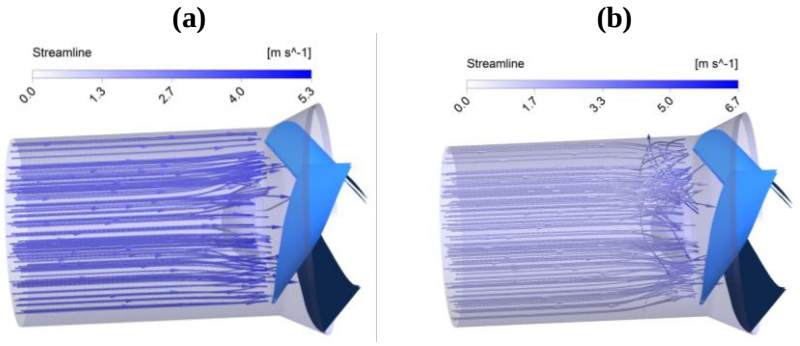

Fig. 4 Streamline at the impeller inlet flow at different flow rates. (a) $1.0Q_{BEP}$ (b) $0.6Q_{BEP}$

However, when the flow rates decrease further, the internal flow structures of the impeller changed, the streamline of impeller passage at different flow rates is shown in Fig. 5, respectively. From Fig. 5a, the internal flow pattern of the mixed flow pump tends to an axial type at high flow rate, while it tends to a centrifugal type at partial flow rate as shown in Fig. 5c. According to the Eq.(2), when the flow pattern tends to a centrifugal type, the component of circumferential velocity U_2 and the circumferential velocity component of absolute velocity V_{u2} became larger and that causes the theoretical head increases.

From the analysis above, the internal flow variation of the mixed flow pump at partial flow is important to investigate the performance curve instability, so more detailed examination about the internal flow at $0.6Q_{BEP}$ was done. Fig. 6 shows the streamline of the meridional plane from impeller to diffuser. It is clearly that a vortex exits at the hub of the diffuser inlet, and it makes flow back into the impeller and block part impeller passage, so

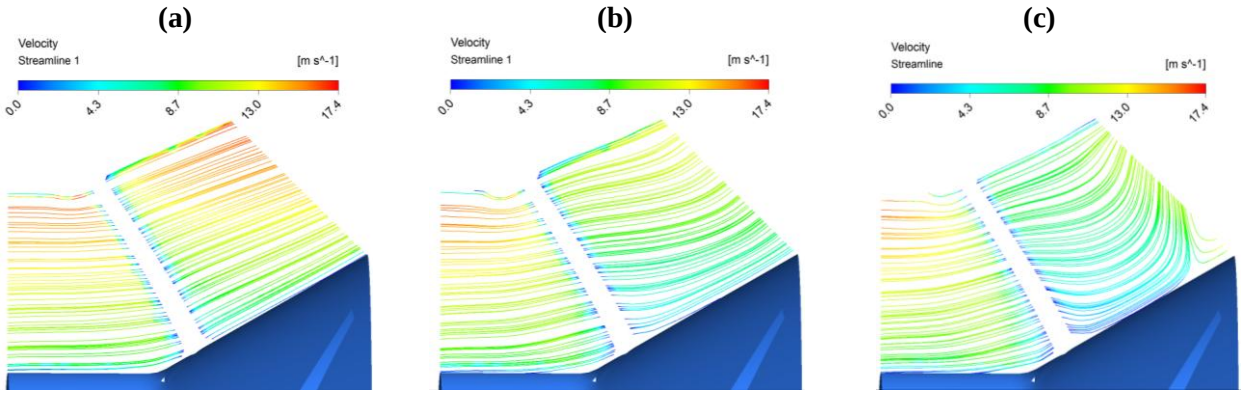

Fig. 5 Streamline of impeller passage at different flow rates. (a) 1.2Q_{BEP} (b) 1.0Q_{BEP} (c) 0.6Q_{BEP}

the diffuser has an important effect on internal flow of the impeller. Fig. 7 shows the streamline of the diffuser and the static pressure on blades and hub. Low pressure region exit alternately in the leading areas of the diffuser flow passages near the hub. Vortices appeared in the low pressure diffuser passages, and what affects the internal flow from impeller passages and makes the flow pattern centrifugal type and therefore total head rised.

According to the analysis discussed above, the mechanism of the head-low curve instability can be concluded as following. Firstly, the flow angle decreased because of the tip leakage developed from pressure surface to suction surface and vortices generated. Then, the pre-rotation occurred at the pump inlet and the theoretical head decreased. However, when the flow rate decreased further, part of the flow fluid at the hub of the diffuser went back to the impeller and blocked the downstream flow from the impeller that the flow pattern tended to a centrifugal type and the total head rised again. Consequently, the positive slope of performance curve occurred.

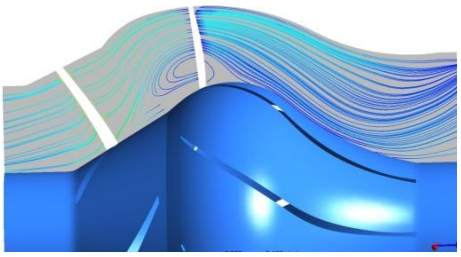

Fig. 6 Streamline of the meridional plane at 0.6QBEP

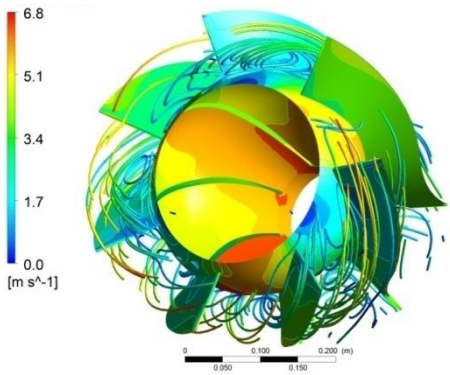

Fig. 7 Streamline of the diffuser passage

4. Two Ways of Characteristic Instability Suppression

When pump is working at partial flow rates conditions its performance curve appears positive slope and the vibration and noise can become serious even cause the resonance of the pump system. Some of researches accelerate the flow velocity at the impeller when performance curve instability happens. For example, to suppress instability of a mixed flow pump, Goto[8] proposed an active method of water jet injection at the impeller inlet, where jet injection in the counter rotating direction of the impeller had been found effective to enlarge the stall margin between the design point and positive slope region of the head-flow characteristic. However, this active control method has some problems, such as it needs complicated mechanisms and utilizes additional machinery that eventually decreases the overall efficiency and reliability. In the present study, the suppression of the head-flow performance curve instability of the mixed flow pump was investigated in two ways.

4.1 With Swirl-stop at the Pump Inlet and Diffuser Optimization

From the analysis above, pre-rotation is an important factor on characteristic instability. Based on this, a swirl–stop is used for suppress the pre-rotation and is presented in Fig. 8. Moreover, the diffuser was modified that the diameter of hub and tip at diffuser inlet was enlarged. Fig. 9 shows the comparison of reverse flow at vane hub inlet between original model and modified one. The reason of this optimization is that when the pump is working at partial flow rates, reverse flow was found near the vane hub inlet, some fluid with low energy was generated. According to the fluid mechanics boundary layer theory, to enlarge the diameter of the hub can

increase the meridional velocity and decrease the component of circumferential velocity that it makes the fluid get high energy, and then eliminate the reverse flow so that the positive slope of head-flow performance curve can be suppressed. Fig. 10 shows comparison of performance between original model and optimized one.

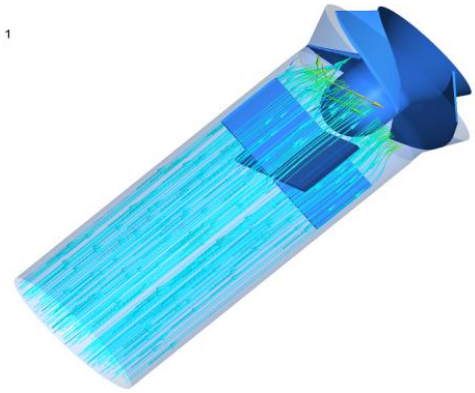

Fig. 8 Streamlie of the impeller inlet with a swirl-stop

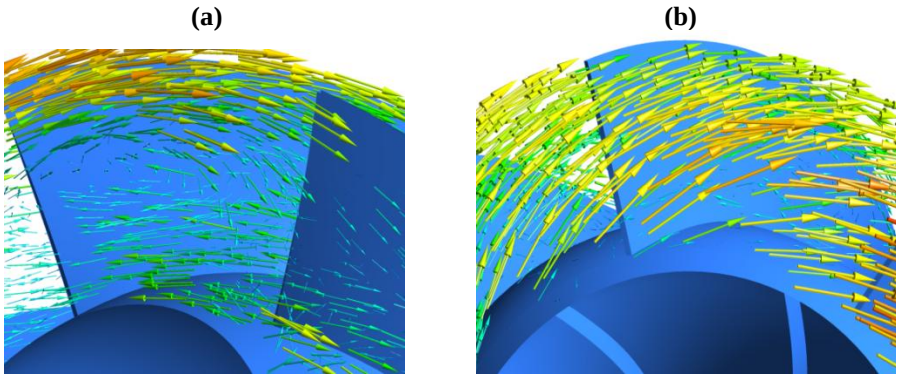

Fig. 9 Comparison of reverse flow at vane hub inlet between modified and not. (a) before modified (b) after modified

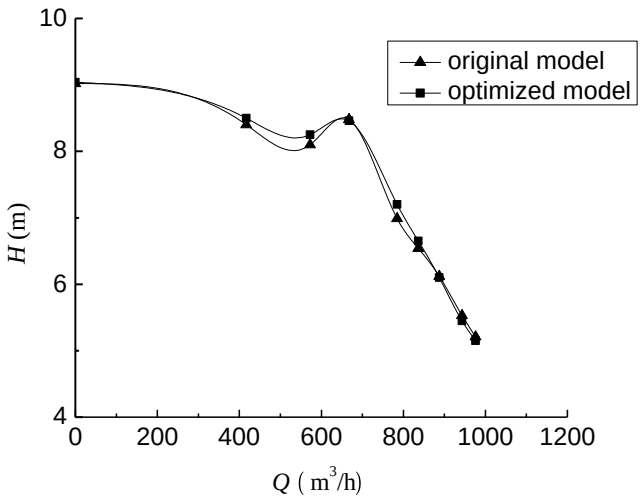

Fig. 10 Comparison of performance between model optimized and not

From pictures above, it worked to some extent with modified model but not ideal, reasons of analysis as follows:

(1) Though the swirl-stop was used but cannot fully suppress the pre-rotation. Accordingly, it cannot increase the head when the head decrease fast. From the mechanism about the positive slope of the performance curve, the effect would be better for restrain the tip leakage and increase flow angle at the impeller inlet.

(2)Enlarging the diffuser inlet diameter of both hub and tip can suppress the vortices at vane hub inlet to some extent, but the internal flow of the diffuser passage is unstable at partial flow rate and it would affect the internal flow of impeller passage. The deficiency of the present study was that the interblade spacing does not consider.

4.2 With Shallow groove on the casing wall

According to the above analysis, we know the decrease of flow angle at the tip of the impeller inlet plays an important role on the head-flow curve instability. In this paper, shallow grooves mounted parallel to the pressure gradient on the casing wall of the mixed flow pump to suppress performance curve instability. Fig. 11 shows the model of mixed flow pump with the shallow grooves.

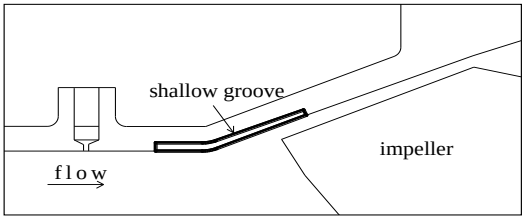

Fig. 11 Shallow groove on the casing wall

The grooves are defined as flowing equation: N × d mm × w mm, where w is the width and d is the depth of a single groove respectively and N is the number of the grooves. Comparisons of the performance curves are shown in Fig. 12.

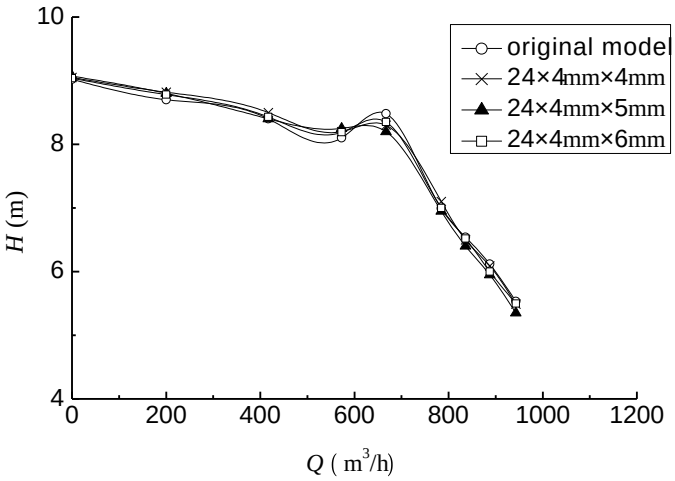

Fig. 12 Comparison of head-flow curve with and without shallow grooves

There are four different cases i.e., no groove, shallow groove of 24×4mm×4mm，24×4mm×5mm and 24×4mm×6mm. Comparing with no groove on the casing, a remarkable improvement could be seen for the groove of 24×4mm×5mm. Almost no positive slope of the head-flow performance curve is seen. However, in case of the other two models only a slight improvement attained. A large instability still remains, although most of the parameters of grooves are same except the width. Therefore, it is clearly that the width of groove is the key factor. However, it is believed that the optimum of groove is related to the parameters of the pump and it is not well known, so, it needs further research.

From the third part of this paper it is revealed that the flow angle and reverse flow are important to the head-flow performance curve. The mechanisms of the shallow groove about the characteristic instability suppression are given. As we know, the width of groove is much smaller than the diameter of the pump and the groove flow has no angular momentum, but the main flow has large angular momentum near the wall when the impeller inlet swirl occurred. Therefore, when the groove flow mixed with the main flow it could decrease the momentum or we can say it could absorb the momentum at the tip of the impeller inlet. Besides, according to Kurokawa and Saha[9-10], the remarkable effects of groove are caused by two mechanisms: one is a remarkable decrease in circumferential velocity, and the other is a remarkable increase in radial velocity due to the groove

reverse flow. According to the Eq.1 we can find that both effects have the same contribution to increase the flow angle.

Consequently, combine the mechanism of characteristic instability with the last paragraph the shallow groove is an effective method to suppress the unstable performance curve and when the pump coupled with proper groove not only can suppress the performance instability but also cannot decrease the pump efficiency. It maybe a simple and useful method on suppression of pump performance curve instability in the future projects.

5. Conclusion

From the present research, the following conclusions can be obtained.

1) CFD could predict the characteristic instability of the mixed flow pumps, its results can be the reference on future pump investigation.

2) The pre-rotation was found at the inlet of the impeller caused by the tip leakage when the pump is working at partial flow rates, it made the theoretical head decrease.

3) The internal flow pattern of the impeller passage tends to a centrifugal type when the flow rates decrease further, it made the theoretical head rise a little. Combine it with conclusion 2, then the positive slope of the performance curve occurred.

4) The swirl-stop was used and the diffuser was optimized for suppression of characteristic instability, it worked to some extent but not ideal.

5) The proper shallow groove on the casing wall was an effective way of positive slope of performance curve suppression.

Acknowledgment

The study was supported by National Science Foundation for Distinguished Young Scholars of China, No.51109096 and the Priority Academic Program Development of Jiangsu Higher Education Institutions (PAPD). These supports are greatly acknowledged.

References

[1] M. Masahiro, F. Akinori and M. Hideaki. On Improvement of Characteristic Instability and Internal Flow in Mixed Flow Pumps, *JSME Journal of Fliud Science and Technology*, Vol. 3, No. 6, pp. 732-743, 2008.

[2] H. Kiyotaka, S. Hayato and N. Yuji. Computational Evaluation Method for Inception Flowrate of Unstable Characteristic in Mixed Flow Pumps, *JSME Journal of Fliud Science and Technology*, Vol. 5, No. 2, pp. 98-110, 2010.

[3] J. Kurokawa, J. Jie and T. Kitahori. Inlet Reverse Flow model and Prediction of Theoretical Head and Water Power of Mixed-Flow Pumps, *JSME International Journal Series B*, Vol. 37, No. 4, pp. 853-860, 1994.

[4] M. Aoki and A. Goto. Positively Sloped Head-Flow Characteristics and inlet Recirculation of a Mixed-Flow Pump, *JSME International Journal*, Vol. 62, No. 596, pp. 162-167, 1996.

[5] M. Masahiro, M. Hideaki and U. Isamu. Unstable Head-Flow Characteristic Generation Mechanism of a Low Specific Speed Mixed Flow Pump, *Journal of Thermal Science* , Vol. 15, No. 2, pp. 115-121, 2006.

[6] K. Chisachi, M. Hiroshi and M. Akira. Large-eddy Simulation of Unsteady Flow in a Mixed-Flow Pump, *International Journal of Rotating Machinery*, Vol. 9, pp. 345-351, 2003.

[7] A. M. Felix, H. Peter and D. Philippe. CFD Caculation of a Mixed Flow Pump Characteristic From Shutoff to Maximum Flow, *ASME Journal of Fluids Engineering*, Vol. 124, No. 3, pp. 798-802, 2002.

[8] A. Goto. Suppression of Mixed-Flow Pump Instability and Surge by the Active Alteration of Impeller Secondary Flows, *ASME Journal of Turbomachinery*, Vol. 116, pp. 621-628, 1994.

[9] J. Kurokawa, S. L. Saha and J. Matsui. Passive Control of Rotating Stall in a Parallel-Wall Vaneless Diffuser by Radial Grooves, *ASME Journal of Fluids Engineering*, Vol. 122, pp. 90-97, 2000.

[10] S. L. Saha, J. Kurokawa, and J. Matsui. Passive Control of Rotating Stall in a Parallel-Wall Vaned Diffuser by J-Grooves, *ASME Journal of Fluids Engineering*, Vol. 123, pp. 507-515, 2001.

Copyright © 2012 DET Corp., Japan All Rights Reserved
International Journal of Comprehensive Engineering
Part C, 1(1), 74-79, 2012
Doi: 10.14270/IJCE2012.1.1.c74
Regular paper

ISSN 2186-2680
e-ISSN 2186-2656
www.iace-journal.org

Study on Autofrettage Design of Composite Natural Gas Vehicle Cylinder

Xiudong Shi [#], Weiwei Zhao, Wanchun Fan

Food Engineering & Machinery Group, School of Mechanical Engineering, Jiangnan University, Wuxi,214122, China

[#] Corresponding author: shixd5718@163.com; Tel.: +86-0510-85910390; Fax.: +86-0510-85910390

Abstract: Based on finite element method, this paper studies the effects of the composite natural gas cylinder of vehicle's autofrettage pressure on bladder's stress as well as the layer number of filament-wound on cylinder's stress. And it further compares the stress of gas cylinder's bladder and the layer of composite without autofrettage and autofrettage. The result shows that the best autofrettage pressure of the composite gas cylinder is 34.3MPa with 10 layers of filament-wound layers while its outer diameter is 356mm, nominal wall thickness 5mm and working pressure 20MPa.

Keywords: Autofrettage, Composite, Cylinder, Natural Gas.

Received: May 20,2012 / Accepted: Sept. 12,2012 / Published: Dec. 15,2012

1. Introduction

In recent years, due to the changes in energy structure and requirements of environmental protection, one of the key developments of the automotive industry is clean energy vehicles. Natural gas as fuel is one of the direction of clean energy vehicles. Conventional steel gas cylinder is heavy, which affects the amount of containers while the use of composite cylinders not only helps to reduce the weight, but also greatly improve their carrying capacity and reliability under high pressure.

Autofrettage design can improve carrying capacity and fatigue life of composite cylinders, which improves the safety of composite cylinders[1-6]. Through finite element analysis, this article studies the effects of the autofrettage pressure on bladder's stress, the layer number of filament-wound on cylinder's stress in order to determine the best autofrettage pressure and filament-wound layers of composite gas cylinder.

2. Principle and Method of Autofrettage

Autofrettage is a fabrication technique, used to introduce pre-compression in a portion of a structure in order to extend the usable strain range of the material and to enhance carrying capacity and fatigue life. The idea of autofrettage is to pressurize cylinder to a proof pressure, which is higher than the operating pressure and lower than the burst pressure. Enough metal plasticity should be achieved during autofrettage so that the liner remains in compression upon unloading.

In order to improve the carrying capacity and fatigue life of composite cylinders, autofrettage processing can be employed. It is achieved by metal yield criterion and pressure-relief principle, that is to say, applying pressure to make metal bladder reaching plastic deformation, forming residual stress after unloading, and bearing more pressure on re-load to offset residual stress. Thus the material mechanical properties are fully played, carrying capacity improved, and fatigue resistance and safety enhance. Autofrettage principle shows in Figure 1.

The method of gas cylinder's autofrettage is that impose autofrettage pressure to gas cylinder in advance after manufacture, under autofrettage pressure, the metal bladder over its yield point, producing permanent plastic deformation and unloading, then composite gas cylinder's bladder has compressive stress, filament-wound has tensile stress. When the gas cylinders work properly, the stress produced by composite cylinder to withstand the

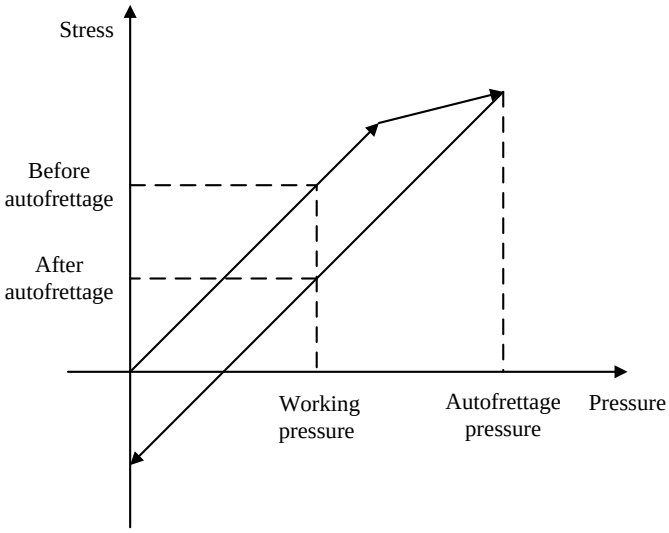

Fig. 1 Processing principle diagram of autofrettage

internal pressure which offset by autofrettage stress, so that the maximum stress value of inner wall decreased and stress value of outer wall increase appropriately, thus make the stress distribution along the wall-thickness direction more uniformly.

3. Model and Calculation

3.1 Mesh Division

First, according to the geometric size of bladder, geometric model of bladder is established, and finite element mesh of bladder divided. The finite element model of the bladder's body is covered by mash of hoop winding composite layer. The thickness of the winding layer is calculated according to winding technology, the composite laminated plate samples of unidirectional ply are composed of multi-layer glass fibers with thickness of 0.469mm. Figure 2 shows the division of finite element mesh model.

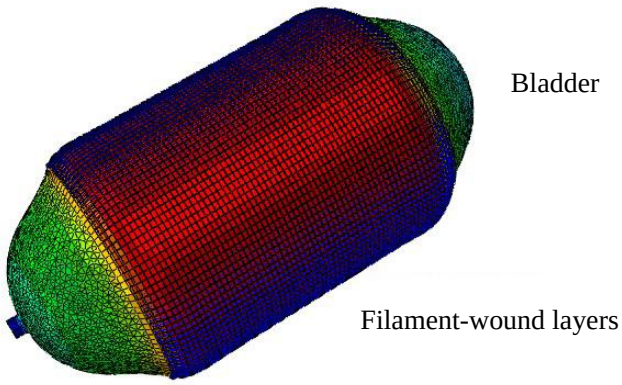

Fig. 2 Finite element mesh model

3.2 Material Model

Composite natural gas vehicle cylinder consists of 30CrMo and ER-2400 glass fiber/epoxy resin composite material with bladder material parameters shown in Table 1 and the composite material parameters in Table 2.

Table 1 Bladder material properties

Grade	Elastic Modulus	Poisson Ratio	Yield Limit	Strength Limit	Elongation
30CrMo	205 GPa	0.29	≥725MPa	≥825MPa	≥14%

Table 2 ER-2400 glass fiber/epoxy resin composite material properties (GPa)

E_x	E_y	E_z	V_{xy}	V_{yz}	V_{xz}	G_{xy}	G_{yz}	G_{xz}
47.33GPa	8.97GPa	8.97GPa	0.26	0.05	0.26	6.2 GPa	2.0 GPa	2.0 GPa

3.3 Load Boundary

According to the design of composite materials and the applying working condition which meet the requirement, the load in accordance with conditions steps is imposed on inner surface of the steel bladder model: imposing autofrettage pressure - unloading to zero pressure after autofrettage - loading to working pressure.

Wound layer method of composite gas cylinders is as follows: 90 degrees of winding angle, 70N/shares of tension, 0.469 mm thickness of each layer with cylinder working pressure of 20MPa.

3.4 Calculation Process

Based on the above finite element model, fractional step loading method is used in finite element calculation process. During the autofrettage pressure applying process, three-step loading inner pressure is applied. The first loading step is for preloading pressure, internal pressure loading gradually from zero until the preloading pressure; the second loading step is unloading, internal pressure unloading to zero gradually; the third loading step is again from zero to the working pressure.

4. Results and Analysis

The purpose of the study on autofrettage design is to research stress distribution of gas cylinder under the working situation, which aims at the adequate and reasonable use of the material with the key on stress distribution and stress changes of gas cylinder's bladder under the working situation. As the gas cylinder working pressure is 20MPa, the research on the changes of autofrettage pressure is studies through the analysis of stress changes of bladder under working pressure, which verifies or helps to find the best autofrettage cylinder pressure.

4.1 Autofrettage pressure effect on bladder's stress

In order to determine the best autofrettage pressure, this paper has calculated the Von Mises stress of bladder under the working pressure 20MPa after different autofrettage pressure with the results shown in Table 3.

Table 3 After different autofrettage pressure, the bladder's Von Mises stress in the working pressure

Autofrettage Pressure（MPa）	22	24	26	28	30	32	34	34.3	36	38
Bladder Von Mises Stress（MPa）	543	512	486	463	440	426	403	395	450	503

Curve diagram 3 of autofrettage pressure effect on bladder's stress is drawn from Table 3.

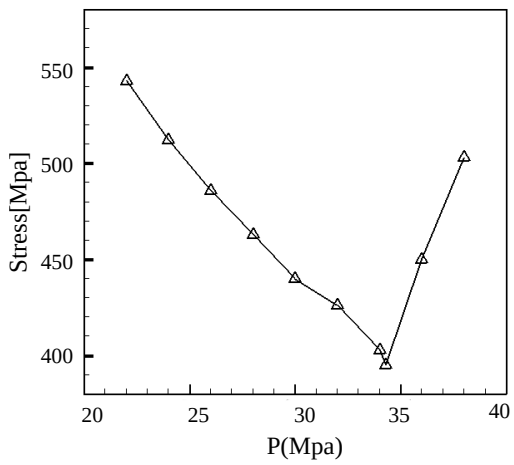

Fig. 3 Curve of autofrettage pressure effect on bladder's stress

It can be seen from Fig. 3, when the autofrettage pressure equals to 34.3MPa, the cylinder's bladder Von Mises stress is minimal under the working pressure. In other words, when the outer diameter of is 356mm, nominal wall thickness 5mm, the best autofrettage pressure of composite gas cylinder is 34.3MPa. And the use of this autofrettage pressure can improve the carrying capacity of cylinder and extend cylinder life effectively.

4.2 The Effect of Fiber Winding Layer Number on Cylinder's Stress

As for composite cylinders, the best autofrettage pressure is 34.3 MPa by autofrettage pressure design. The influence of the numbers of glass fiber's winding layer on stress of the cylinder's bladder and fiber's layer is further researched via finite element analysis. When the best autofrettage pressure is 34.3MPa and working pressure is 20MPa respectively, and the number of glass fiber winding layer is 6,7,8,9,10,12, the Von Mises stress condition of glass fiber layer is calculated. The result is shown in Figure 4.

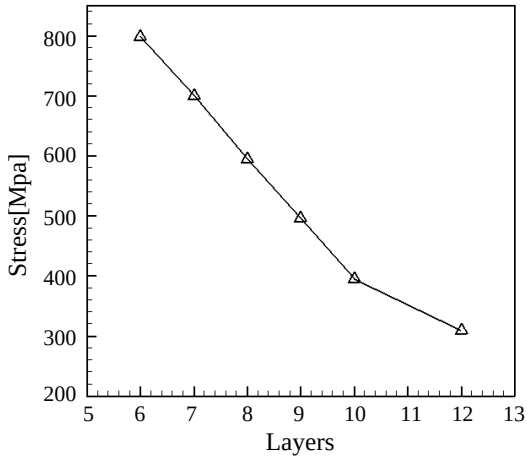

Fig. 4 The stress affect curve of different fiber winding layer to composite layers

Similarly, the Von Mises stress condition of steel bladder can be calculated when the best autofrettage pressure is 34.3MPa and working pressure is 20MPa, and the number of glass fiber winding layer is 6,7,8,9,10,12. The data curve is shown in Figure 5.

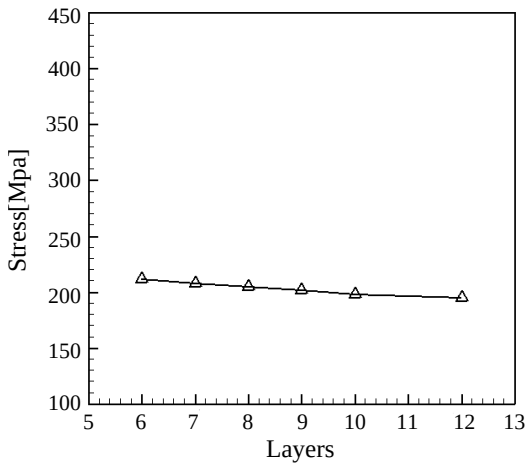

Fig. 5 The relation curve of steel bladder's Von Mises stress and cylinder's fiber layers

Fig. 4 and 5 indicate that in normal working pressure, the influence of different winding layer on the stress of glass fiber layer is greater, while effect on bladder's stress is very small, which is so small that it can be almost neglected. Fig. 4 shows that the increase of the fiber layers means the decrease of the stress of fiber layer, the amount of which is significant. Meanwhile, the smaller the layer number is, the greater the stress of fiber layer is. This implies that the less the winding layers of composite cylinders is, the fuller use of ultimate strength of glass fiber materials is. But in practical production, the safety of gas cylinders should be taken into consideration in order to achieve better integration of security and economy. Thus the final choice of the number of filament winding layer is 10-layer.

4.3 The Stress Value Comparison of Composite Layer and Cylinder Bladder without and with Autofrettage

Fig. 6 and 7 are Von Mises stress distribution figures of cylinder bladder and composite layer under 34.3 MPa autofrettage pressure and 20 MPa working pressure.

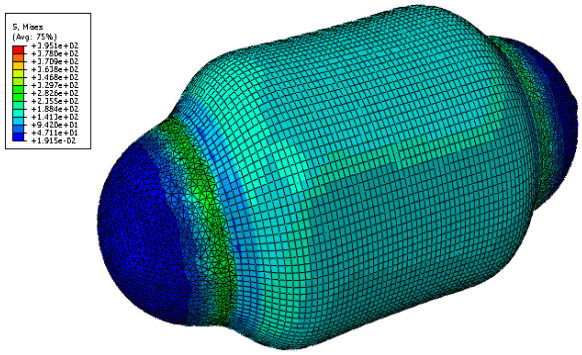

Fig. 6 Stress value of bladder with autofrettage under working pressure

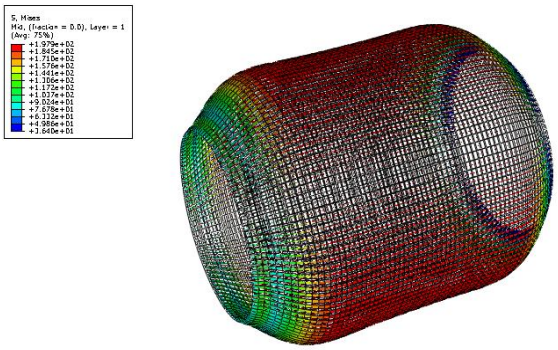

Fig. 7 Stress value of composite layer with autofrettage under working pressure

Fig. 8 and 9 are Von Mises stress distribution figures of the cylinder bladder and composite layer under working pressure of 20MPa without autofrettage.

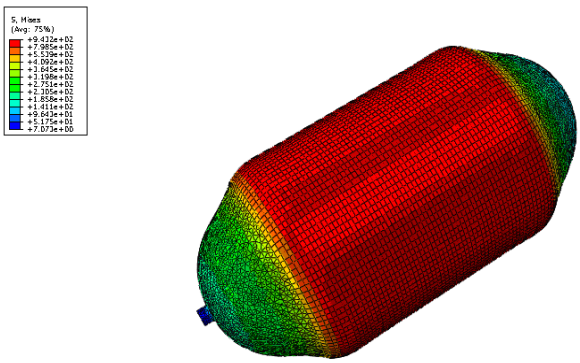

Fig.8 Stress value of bladder without autofrettage under working pressure

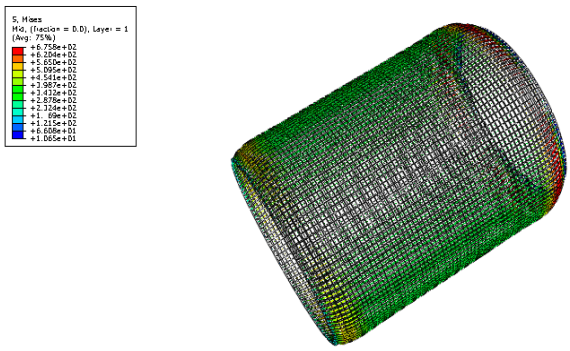

Fig.9 Stress value of composite layer without autofrettage under working pressure

It can be seen from Fig. 6 that secondary stress appears at the junction of cylinder bladder and the head, which means the maximum stress is at the joint which is thickened in manufacturing process. Fig. 6 also shows that the

maximum stress of bladder is 395 MPa at the junction of cylinder body and binding head with autofrettage. Figure 8 shows that the maximum stress of bladder is 943 MPa without autofrettage and the greatest stress is in the cylinder body parts. The maximum stress of cylinders drawn from Fig. 6 and 8 is different, and is the stress distribution in the same position. As in Fig. 6 the maximum stress of 395 MPa is much smaller than 943 MPa in Fig. 8. Fig. 7 and 9 also imply that the compound layer stress distribution of the two cylinders is not the same. The maximum stress of 198 MPa in Fig. 7 is significantly smaller than the maximum stress of 676 MPa in Figure 9. It can be drawn that the autofrettage can effectively reduce the stress and improve the carrying capacity of composite cylinders, and play a significant role in improving the safety and full use of composite materials' property.

5. Conclusions

This paper studies the effect of the specific composites natural gas vehicle cylinders on bladder stress by the employment of finite element method, and then obtains different effect curves of autofrettage pressure on bladder stress. And the curve of bladder's stress and the number of cylinder fiber layer is acquired after the research on the influence of filament-wound layers on cylinders stress, and the stress value of bladder and composite layer without and with autofrettage is then compared respectively. The result shows that when the outer diameter is 356mm, nominal wall thickness 5mm, the composite gas cylinders have best autofrettage pressure 34.3MPa; and when the filament-wound layers is 10, composite gas cylinders enjoy higher security and help to give full play to the composite material performance.

References

[1] X.Y Huang and W.C Cui. Effect of Bauschinger Effect and Yield Criterion on Residual Stress Distribution of Autofrettaged Tube, *Journal of Pressure Vessel Technology*, Vol. 128, No. 3, pp. 212-216, 2006.

[2] J. W Huang, X. M Qian, Y. J Tian, J. Hu, Y. Lv, Z. N Ren, G. C Zhang and W. J Xin. Simulation Experimental Study on Static Intensity of Autofrettage Thick-wall Cylinder, *Ordnance Material Science and Engineering*, Vol. 33, No. 3, pp. 44-45, 2010.

[3] A.A Krikanov. Composite Pressure Vessels with Higher Stiffness, *Composite Structures*, Vol. 48, No. 1-3, pp. 119-127, 2000.

[4] Y. J Liu and Y. J Jin. Design Key Points of Carbon Fiber Full—wrapped with Aluminium Liner Hydrogen Cylinder for Vehicle, *Pressure Vessel*, Vol. 26, No. 12, pp. 28-33, 2009.

[5] X T Zheng and F Z Xuan. Autofrettage and Shakedown Analysis of Strain-Hardening Cylinders under Thermo-mechanical Loadings, *The Journal of Strain Analysis*, Vol. 46, No. 1, pp. 45-55, 2011.

[6] W S Shim, J H Kim, Y S Lee, K U Cha and S K Hong. A Study on Hydraulic Autofrettage of Thick-walled Cylinders Incorporating Bauschinger Effect, *Proceeding of the Society for Experimental Mechanics*, Vol. 67, pp. 621-626, 2011.

[7] Young-Seob Kim, Lae-Hyun Kim and Ji-Sang Park. The Effect of Composite Damage on Fatigue Life of the High Pressure Vessel for Natural Gas Vehicles, *Composite Structures*, Vol. 93, No. 11, pp. 2963-2968, 2011.

[8] B Haghpanah Jahromi, A Ajdari, H Nayeb-Hashemi and A Vaziri. Autofrettage of Layered and Functionally Graded Metaleceramic Composite Vessels, *Composite Structures*, Vol. 92, No. 8, pp. 1813-1822, 2010.

[9] Dae-Sung Son and Seung-Hwan Chang. Evaluation of Modeling Techniques for A Type III Hydrogen Pressure Vessel (70 MPa) Made of An Aluminum Liner and A Thick Carbon/Epoxy Composite for Fuel Cell Vehicles, *International Journal of Hydrogen Energy*, Vol. 37, No. 3, pp. 2353-2369, 2012.

[10] Xu P, Zheng JY and Liu PF. Finite Element Analysis of Burst Pressure of Composite Hydrogen Storage Vessels. *Materials & Design*, Vol. 30, No. 7, pp. 2295-2301, 2009.

[11] Hu J, Chen J, Sundararaman S, Chandrashekhara K and Chernicoff W. Analysis of Composite Hydrogen Storage Cylinders Subjected to Localized Flame Impingements, *Internstional Journal of Hydrogen Energy*, Vol. 33, No. 11, pp. 2738-2746, 2008.

[12] Adibi-Asl R and Livieri P. Analytical Approach in Autofrettaged Spherical Pressure Vessels Considering the Bauschinger Effect, *Journal of Pressure Vessel Technology*, Vol. 129, No. 3, pp. 411-419, 2007.

Copyright © 2012 DET Corp., Japan All Rights Reserved
International Journal of Comprehensive Engineering
Part C, 1(1), 80-86, 2012
Doi: 10.14270/IJCE2012.1.1.c80
Regular paper

ISSN 2186-2680
e-ISSN 2186-2656
www.iace-journal.org

Migration of Lead, Cobalt, Nickel and Zinc from Ceramic Glazes by Acid Food Simulants

Zhanhua Dong [1], Lixin Lu [1, 2, #], Zhigang Liu [1, 2], Yali Tang [1, 2] and Jun Wang [1, 2]

[1] Department of Packaging Engineering, Jiangnan University, 1800 Li Hu Avenue, Wuxi, Jiangsu Province, 214122, China
[2] Key Laboratory of Food Packaging Techniques and Safety of China National Packaging Corporation, Wuxi 214122, China

[#] Corresponding author: lulx@jiangnan.edu.cn; Tel.: +86-0510-85910590;

Abstract: Ceramic food packaging containers with improperly fabricated glazes can release some toxic heavy metals such as lead, cobalt, nickel and zinc into foods, which may contaminate foods and even endanger consumer's health. In order to investigate the safety of ceramic food packaging containers with contact with food and to study the leaching behavior of lead, cobalt, nickel and zinc, long-term contact experiments were carried out on glazed tile specimens with 4% acetic acid solution under different conditions. Results indicate that nickel is the most leachable element among these four heavy metals, and lead is the least leachable one, relatively. The amount of these heavy metals released into the leachate increase with temperature. Similarly, the rates of the release of these heavy metals increase with temperature, too. Parabolic Fit analyses of all the leaching data on the long term yield good correlations (the square of correlation coefficient, R^2 was all above 0.93) which indicate that migration of lead, cobalt, nickel and zinc from the certain glaze into 4% acetic acid were diffusion-controlled process and have a linear dependence on the square root of time for the amount of heavy metals removed from glaze into acid food simulants.

Keywords: Lead, Cobalt, Nickel, Zinc, Ceramic Glazes, Migration.

Received: May 21,2012 / Accepted: Sept. 12,2012 / Published: Dec. 15,2012

1. Introduction

Ceramic food packaging containers are widely used for the storage of a large variety of foodstuffs including the more extractive acidic beverages, such as aromatic vinegar, mature vinegar, lemon juice and other acid foodstuffs. If ceramic food packaging containers decorated with the improperly formulated glazes were inappropriately fired, lead and other heavy metals would not be chemically combined closely in the glass structure[1], which will yield a high release of harmful lead and other heavy metals when contact with foodstuffs mentioned above, and give rise to a high risk to human health.

The toxicity of lead has long been known as its effects are cumulative and systemic. Long-term exposure of lead can harm the kidney and liver seriously, resulting in permanent neurological defects, encephalopathy, and even death, possibly[2]. Cadmium is also a toxic heavy metal and may produce both acute and chronic effects in lungs, kidneys and bones. Itai-itai disease and disorder caused by long-term exposure of cadmium has been reported[3]. Because of their acute toxicity, lead and cadmium are the most widely studied heavy metals on migration from ceramic ware into foodstuffs, and the only metals for which most of the countries and regions have established ceramic ware leaching limits[4-7].

Besides lead and cadmium, however, other harmful heavy metals such as cobalt, nickel and zinc were also detected in many kinds of glazed ceramic ware[8]. They all constitute different hazards to human health. It was reported that cobalt at critical concentration levels could lead to biochemical changes and disrupt the functional state of the body[9]. The toxicity of cobalt mainly embodied in polycythemia and hyperglycemia with transitory

damage to pancreatic alpha-cells[10]. Nickel can also cumulate in all organs, especially in the kidney, spleen and liver. When large amounts of nickel cannot be eliminated in its metabolites, it will affect the function of the kidney, spleen and liver. It has been proven that nickel compounds are carcinogens[11]. Zinc is a trace element essential to human body and generally considered to be relatively nontoxic; however, excessive zinc intake could also lead to poisoning by interfering with the utilization of copper and iron and affecting high-density-lipoprotein HDL cholesterol concentrations. Extremely high zinc intakes could lead to nausea, vomiting, epigastric pain, lethargy, and fatigue[12]. All these metals are trace elements essential to human body and generally considered to be relatively nontoxic, but long-term excessive intake will endanger human's health. However, researchers involving migration or extraction of cobalt, nickel and zinc from ceramic ware into food are rare and national legislations or international standards to monitor and regulate the possible release of these heavy metals with the exception of lead and cadmium are scarce.

Many researchers studied the migration of lead and cadmium from ceramic table wares and their damage to human by repeated leaching from a dish to simulate human's habits of using the ceramic ware[13-16]. Here, this study focused on the safety of the ceramic ware as packaging container and the leaching behavior of these heavy metals existing in the glaze when contacted with acid food over a long period of time. In view of this, the present study on the migration of lead, cobalt, nickel and zinc was carried out to examine the migration of these heavy metals into 4% acetic acid solution under different conditions. Cadmium in ceramic glazes was also an important heavy metal of concern, which is under study now and will be discussed in detail elsewhere.

The purposes of this study were: a) To examine the effect of temperature on the migration of lead, cobalt, nickel and zinc; b) To inquire into whether the ratio of the removal of these metals is coincident or not through the analysis of the amount in the leachates and their ratio in the glaze; c) To study the relationship of the time and the amount of heavy metals released into the food simulants.

2. Materials and methods

2.1 Preparation of Specimens

A number of clay tiles with average of 11.15 by 5.62 by 0.73 cm in volume were manufactured by a ceramic company in Yixing, Jiangsu province, China, fired at a low temperature(about 850℃) in a muffle furnace, glazed with a glaze whose composition is (K_2O 1.89%, Na_2O 0.88%, ZnO 6.07%, PbO 41.47%, Fe_2O_3 0.07%, CoO 4.04%, NiO 4.04%, MgO 0.05%, CaO 0.13%, Al_2O_3 6.69%, SiO_2 34.67%), fired a second time at 1120℃ after they were dry. And the glaze would be fused onto the surface of clay tiles forming a thin layer of glass.

Ceramic specimens were prepared according to the method of ASTM C 738-94(2006), washed with detergent, rinsed with tap water and followed with deionized water, then taken out from an electrically heated drying cabinet standby after they were dry.

2.2 Experiment Design

Each tile specimen was mounted in a Lock＆Lock (HPL812 1.1L), put into the constant temperature box whose temperature was pre-set and its stability was better than ±0.1℃, and allowed to equilibrate before 90 mL of 4% acetic acid solution were added. Five identical tile specimens were used for each test. The temperature was 20 °, 40 °, and 60℃. Leaching tests were continued for 720h, 840h, and 600 h.

10±0.1 mL of Leachate was transferred into a PP centrifuge tube with a pipette for storage before measuring lead, cobalt, nickel and zinc concentrations using Inductively coupled plasma optical emission spectroscopy (ICP-OES), then the volumes of the prepared 4% acetic acid solution were made up to the initial values in order to compensate for evaporation losses and keep a constant pH value.

2.3 Main Instruments and Reagents

The instruments used in this study included Perkin Elmer Optima 5100DV inductively coupled plasma optical emission spectroscopy (ICP-OES) (Perkin Elmer Corporation, USA), Milli-Q Element (Millipore Corporation, USA), THS-AOC-100 constant temperature humidity chamber (KSON Corporation, China), PRX-450C Intelligent Artificial Climate Box (NoKi Corporation, China).

Reagents used in all tests of this study were analytical grade at least.

The calibration curves were obtained by diluting 1000 mg/L standard stock solutions of lead (Pb), cobalt (Co), nickel (Ni) and zinc (Zn) (National Research Center for Certified Reference Materials, China; NRCCRM) with 4% acetic acid. The working standards of final concentrations for lead, cobalt, nickel and zinc were 0.0, 0.2, 1.0, 2.0, 10.0, 20.0, and 100.0, respectively.

The detection limits of the method were 0.03~9.31μg/L for lead, 0.003~0.97μg/L for cobalt, 0.021~1.28μg/L for nickel and 0.192~6.75μg/L for zinc. The mean relative standard deviations (RSD) were 0.1~3.15 % and recovery were 96~105%.

3. Results and Discussion

Results of extraction of lead, cobalt, nickel and zinc with 4% acetic acid solution at 20℃, 40℃ and 60℃ were illustrated in Figs 1 to 4. Concentrations of heavy metals in the leachates were converted to a normalized mass loss in μg/cm2 according to the equation of

$$NM_i = C_i * V / S. \quad (1)$$

Where NMi is the normalized mass loss of element i, Ci represents the concentration of element i in the leachates measured by ICP-OES, V is the volume of the test solution and S is the area of the tile specimen. Each data was the average value of the amount determined from five tiles.

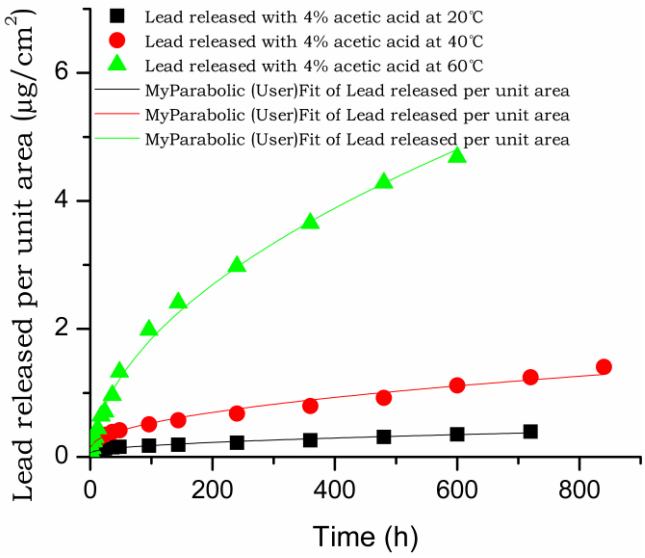

Fig. 1 Lead released per unit area with 4% acetic acid at 20℃, 40℃, 60℃ respectively

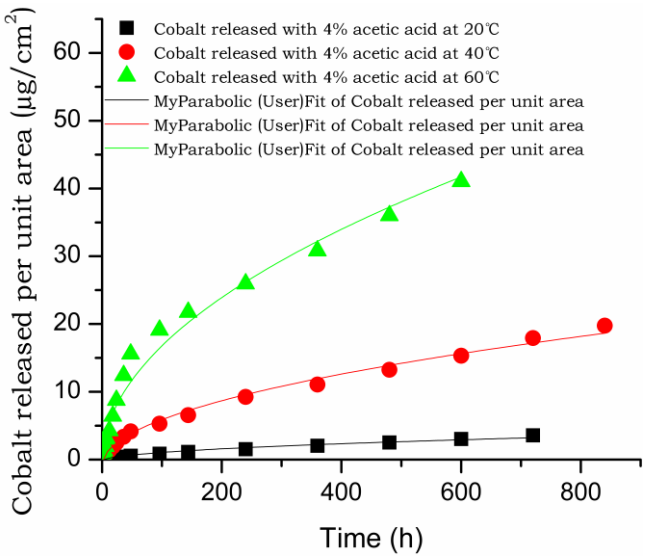

Fig. 2 Cobalt released per unit area with 4% acetic acid at 20℃, 40℃, 60℃ respectively

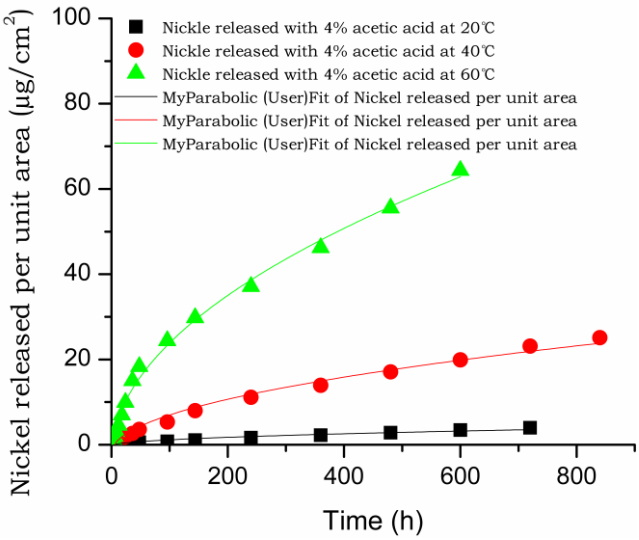

Fig. 3 Nickel released per unit area with 4% acetic acid at 20℃, 40℃, 60℃ respectively

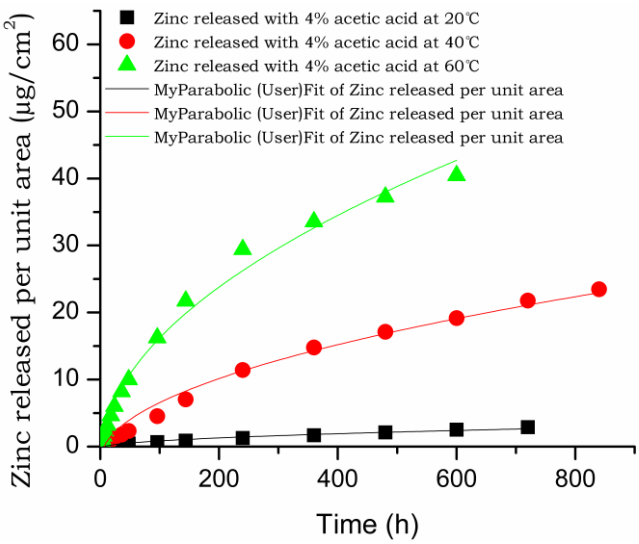

Fig. 4 Zinc released per unit area with 4% acetic acid at 20℃, 40℃, 60℃ respectively

3.1 Effect of Temperature on Migration of Lead, Cobalt, Nickel and Zinc

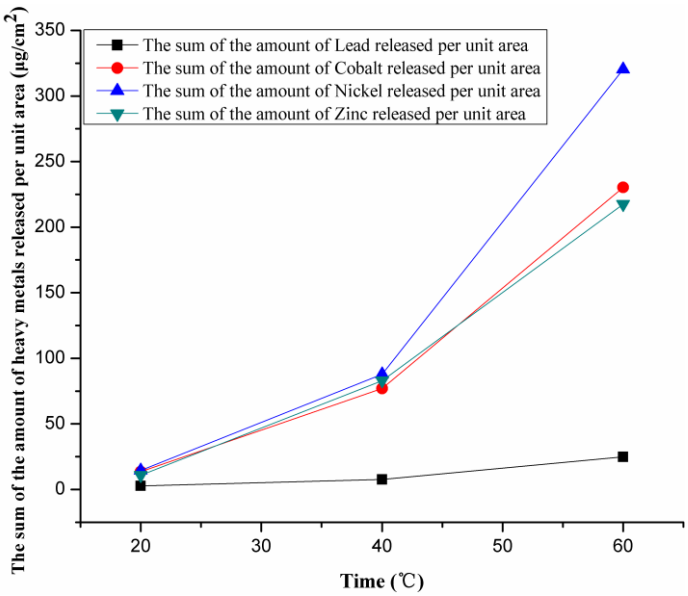

Fig. 5 The rates of removal of Lead, Cobalt, Nickel and Zinc at 20, 40, and 60 ℃

Table 1 The sum of the amount of heavy metals released per unit area

Element	Temperature	4% acetic acid
Lead	20℃	2.629
	40℃	7.59
	60℃	24.85
Cobalt	20℃	13.512
	40℃	77.039
	60℃	230.396
Nickel	20℃	14.573
	40℃	88.01
	60℃	320.237
Zinc	20℃	10.9158
	40℃	82.988
	60℃	217.324

In each plot of Figs. 1 to 4, blank data points, red data points and green data points represent the release of each heavy metal (lead, cobalt, nickel and zinc) at 20℃, 40℃, and 60℃ respectively. It can be seen clearly that the amount of lead, cobalt, nickel and zinc in the leachates all increased with temperature which could be caused by high temperature giving rise to high atomic heat activating energy and migration of these heavy metals occurring more easily. Table 1 shows the sum of the amount of heavy metals released per unit area obtained by calculating summation of mean amounts of heavy metals released per unit area with 4% acetic acid solution at 20℃, 40℃, and 60℃ respectively. Through analysis of the difference of the normalized mass loss of lead, cobalt, nickel and zinc in 4% acetic acid leachates at three temperatures can be obtained that the rates of removal also increase with temperature and the biggest effect of temperature exists in nickel release and the least one in lead release, which can be clearly shown in Fig. 5.

3.2 Relationship between the Amount of Heavy Metals Released and the Ratio of their Oxides in the Glaze

From Figs 1 to 4, it is apparently shown that specimens yield the least amount of lead and the most amount of nickel under all test conditions, the amount of cobalt and zinc are similar to but a bit less than the amount of nickel. Table 2 shows lead: cobalt: nickel: zinc mass ratios in leachates and in glaze which can also describe this phenomenon more clearly. The ratios of the oxide of these heavy metals in the glaze are (PbO 41.47%, CoO 4.04%, NiO 4.04%, ZnO 6.07%). Disagreement between the ratios of the oxide of these heavy metals in the glaze and their release in the leachates suggests that Nickel is most easy to release, next cobalt, then zinc, and lead is the least.

Table 2 Lead: cobalt: nickel: zinc mass ratios in leachates and in glaze

Food simulants	temperature	Lead : cobalt : nickel : zinc ratio in leachates	Lead : cobalt : nickel : zinc ratio in glaze
4% acetic acid	20℃	1 : 5.140 : 5.543 : 4.152	1:0.097:0.097:0.146
	40℃	1 : 10.15 : 11.596 : 10.934	
	60℃	1 : 9.271 : 12.887 : 8.745	

3.3 Relationship of the Time and the Amount of Heavy Metals Released into the Food Simulants

In order to examine the relationship of the time and the amount of heavy metals released into the food simulants, Parabolic Fit analyses were performed on all leaching data for lead, cobalt, nickel and zinc removal from the beginning of the contact till the end of the experiment and also exhibited in Figs 1 to 4. The formula of Parabolic Fit is given by

$$NM_i = a + b * t^{1/2} \tag{2}$$

Where NMi is the normalized mass loss of element i, a, b are the parameters which obtained by calculating the leaching data of the experiment and a chiefly depends on the quality of contact surface and b on the chemical composition of the glaze and on the test solution used[17, 18], t is the contact time.

Results of Parabolic Fit analyses were outlined in Table 3. The square of correlation coefficient (R2) of the leaching data and Parabolic Fit curves are all above 0.97 which indicate that over a long period of the experiment migration of lead, cobalt, nickel and zinc from ceramic glaze into 4% and 10% acetic acid,1% citric acid and 1% lactic acid solution is a process that controlled by diffusion.

Table 3 Results of Parabolic Fit analyses

Food simulants	Element	Temperature	Parameters		R^2
			a	b	
4% acetic acid	Lead	20℃	0.06014	0.01178	0.98126
		40℃	0.13158	0.03992	0.98398
		60℃	-0.19672	0.20413	0.99695
	Cobalt	20℃	-0.22924	0.12868	0.98059
		40℃	-0.81596	0.67164	0.99373
		60℃	-0.41848	1.7196	0.9827
	Nickel	20℃	-0.26866	0.14174	0.97001
		40℃	-1.87178	0.88596	0.98898
		60℃	-2.99818	2.68758	0.99515
	Zinc	20℃	0.97001	0.1071	0.98439
		40℃	0.98898	0.86362	0.98526
		60℃	0.99515	1.8283	0.99127

4. Conclusion

The amount of lead, cobalt, nickel and zinc released into 4% acetic acid under different conditions varied linearly with the square root of time which indicated a diffusion-controlled process that occurred in the contact between the glaze and food simulants. Their release into the food simulants increased with temperature. Disagreement between the ratios of the oxide of these heavy metals in the glaze and their release into the food simulants suggests that dissolution of glaze is not congruent, nickel is the most leachable element, and lead is the least one.

Acknowledgement

This work was financially supported by The National Key Technology R&D Program of China (Grant No. 2009BADB9B04), Ph.D. Students Scientific Research Fund Projects of Jiangnan University (Grant No. JUDCF09011) and Opening Fund of Key Laboratory of Product Packaging and Logistics of Guangdong Higher Education Institutes (Jinan University, Grant No. 2011004).

References

[1] Lehman. Lead Glazes for Ceramic Foodware, *The International Lead Management Center Research Triangle Park*, pp. 98-108, 2002.

[2] Papanikolaou, Hatzidaki, Belivanis, Tzanakakis and Tsatsakis. Lead Toxicity Update. a Brief Review, *Medical science monitor*, Vol. 11, No. 10, pp. A329-A336, 2005.

[3] Godt, Scheidig, Grosse-Siestrup, et al. The toxicity of cadmium and resulting hazards for human health, *Journal of Occupational Medicine and Toxicology*, Vol. 1, No. 22, pp. 1-6, 2006.

[4] 84/500/EEC. Council Directive 84/500/EEC of 15 October 1984 on the approximation of the laws of the Member States relating to ceramic articles intended to come into contact with foodstuffs.

[5] CPG 7117.06. Sec. 545.400 Pottery (Ceramics); Imported and Domestic - Cadmium Contamination.

[6] CPG 7117.07. Sec. 545.450 Pottery (Ceramics); Imported and Domestic - Lead Contamination.

[7] GB 12651-2003. Standard Permissible Limits of Lead and Cadmium Release From Ceramic Ware in Contact with Food.

[8] Sheets. Release of Heavy Metals from European and Asian Porcelain Dinnerware, *Science Of The Total Environment*, Vol. 212, No. 2-3, pp. 107-113, 1998.

[9] Bitel and LevitskiiandZayats. Migration of Harmful Substances From Colored Glazes Into Model Media, *Glass And Ceramics*, Vol. 64, No. 5-6, pp. 201-205, 2007.

[10] Domingo. Cobalt In The Environment and Its Toxicological Implications, *Reviews Of Environmental Contamination And Toxicology*, Vol. 108, pp. 105, 1989.

[11] McCannand Babin. *Health hazards manual for artists*, Lyons Press, 2008.

[12] Fosmire. Zinc Toxicity, *The American journal of clinical nutrition*, Vol. 51, No. 2, pp. 225, 1990.

[13] Sheets. Extraction of Lead, Cadmium and Zinc from Overglaze Decorations on Ceramic Dinner-Ware by Acidic and Basic Food Substances, *Science of Total Environment*, Vol. 197, No. 1-3, pp. 167-175, 1997.

[14] Mohamed and ChinandPok. Leaching of Lead From Local Ceramic Tableware, *Food Chemistry*, Vol. 54, No. 3, pp. 245-249, 1995.

[15] Seth and Sircarand Hasan. Studies on Lead Extraction from Glazed Pottery Under Different Conditions, *Bulletin Of Environmental Contamination And Toxicology*, Vol. 10, No. 1, pp. 51-56, 1973.

[16] Mej ıandCraigmill. Transfer of Lead from Lead-Glazed Ceramics to Food, *Archives Of Environmental Contamination And Toxicology*, Vol. 31, No. 4, pp. 581, 1996.

[17] Hight. Lead Migration from Lead Crystal Wine Glasses, *Food Additives & Contaminants*, Vol. 13, No. 7, pp. 747-765, 1996.

[18] Lehman. Lead-Ion Stability in Soda－Lime Lead Silicate Glasses, *Journal Of The American Ceramic Society*, Vol. 75, No. 8, pp. 2194-2199, 1992.